AD/A-000 476

SEISMIC MASKING OF AN UNDERGROUND NUCLEAR EXPLOSION

Lawrence D. Porter

Northern Illinois University

Prepared for:

Air Force Office of Scientific Research

31 October 1973

UNCLASSIFIED

Security Classification

AD/A-000-476

DOCUMENT CONTROL DATA - R & D

(Security classification of title, body of abstract and indexing annotation must be entered when the overall report is classified)

1. ORIGINATING ACTIVITY (Corporate author) Northern Illinois University Department of Geology DeKalb, Illinois 60115	2a. REPORT SECURITY CLASSIFICATION UNCLASSIFIED 2b. GROUP

3. REPORT TITLE

SEISMIC MASKING OF AN UNDERGROUND NUCLEAR EXPLOSION

4. DESCRIPTIVE NOTES (Type of report and inclusive dates)

Scientific - Final

5. AUTHOR(S) (First name, middle initial, last name)

Porter, Lawrence D.

6. REPORT DATE 31 October 1973	7a. TOTAL NO. OF PAGES 128	7b. NO. OF REFS 28
8a. CONTRACT OR GRANT NO. AFOSR-73-2522 b. PROJECT NO. AO 2468 c. 62701E d.	9a. ORIGINATOR'S REPORT NUMBER(S) Final Technical Report, 73-12-2 9b. OTHER REPORT NO(S) (Any other numbers that may be assigned this report) AFOSR - TR - 74 - 1583	

10. DISTRIBUTION STATEMENT

Approved for public release; distribution unlimited.

11. SUPPLEMENTARY NOTES	12. SPONSORING MILITARY ACTIVITY AF Office of Scientific Research/NPG 1400 Wilson Boulevard Arlington, VA 22209

13. ABSTRACT

This study examines the accidental interference of a teleseism from an earthquake with the seismic signals from an underground nuclear explosion by presenting a compilation of seismograms from thirty-two near-regional stations associated with the explosion. The explosion was detonated by the U.S. on 14 August 1969 at the Nevada Test Site. It had a yield of 3 kt (seismic estimate) and a depth of burial of 784 feet in alluvium. The interfering earthquake was a principal aftershock of a Kurile Island earthquake sequence, with a magnitude of 6.2 and a distance of 70° from explosion. The explosion waveform was embedded completely in the teleseismic P-wave at all near-regional stations. The data for the distance range 144-975 km show that the seismic waveform characteristic of this explosion remains clearly visible out to 288 km. The study also analyzes the quantitative aspects of the masking by measuring the reduction in the relative duration of the explosion waveform caused by the interference. The duration without masking is determined from the traces of events similar to the masked explosion. Forty-two traces of comparison events are presented in juxtaposition with sixty-one traces of the masked explosion in order to determine the duration with interference. The masking increases with distance, but shows marked irregularities from a smooth trend which may be due to regional effects. The masking also exhibits secondary dependences on the azimuth and the differences in arrival times.

DD FORM 1 NOV 65 1473

UNCLASSIFIED

Security Classification

14 KEY WORDS	LINK A		LINK B		LINK C	
	ROLE	WT	ROLE	WT	ROLE	WT
seismology						
underground nuclear explosions						
hiding of an explosion in an earthquake						
comprehensive test ban treaty						
masking						
seismic masking						
seismic interference						
masked explosion						
explosion waveforms						
duration of explosion waveforms						
reduction in explosion waveform duration due to interference						
regional variations						
Nevada Test Site						
earthquake						
teleseism						
superposition of two signals						
degradation of explosion waveform						
instrumentation						
seismograph						

73-12-2

SEISMIC MASKING OF AN UNDERGROUND NUCLEAR EXPLOSION

FINAL TECHNICAL REPORT

Prepared for

AIR FORCE OFFICE OF SCIENTIFIC RESEARCH
ARLINGTON, VIRGINIA 22209

Sponsored by

ADVANCED RESEARCH PROJECTS AGENCY
ARPA ORDER No. 2468

by

Lawrence D. Porter

Department of Geology
Northern Illinois University
DeKalb, Illinois 60115

Phone: (815) 753-1778

GRANT:

No. AFOSR-73-2522
Effective date: 1 May 1973
Expiration date: 31 October 1973
Amount: $12,435

PROGRAM:

Code 3F10
Manager:
William J. Best
Phone: (202) 694-5456

ii

This document was prepared under the sponsorship of the Air Force. Neither the U. S. Government nor any person acting on behalf of the U. S. Government assumes any liability resulting from the use of the information contained in this document or warrants that such use will be free from privately owned rights.

ii

PREFACE

The driving force behind this investigation has been the pertinence of this unique example of seismic masking to the one aspect of the broad problem of seismic evasion which has yet to be examined experimentally, namely the question of hiding a nuclear explosion in an earthquake. When one realizes the extent of the masking in terms of its widespread nature and timing, particularly the closeness of the near coincidence and the total embedding of the explosion waveforms in the teleseism, as well as the quantity of the comparison data available, the desire to proceed further with the study becomes all the more compelling.

The investigation has been guided by the fundamental decision to present the data in a form as complete as possible. The reasons for documenting the data in their entirety are threefold: 1) the extremely low probability of another accidental incident with as widespread a pattern of near-coincident arrivals for the competing signals ever happening again, 2) the extraordinary difficulty of executing a similar experiment in a planned manner, and 3) the need to give a realistic picture of both the quantity and quality of the data available.

The prospect of acquiring another data set like this one with such an extensive near-coincidence would be rare: Of the more than 300 U. S. underground nuclear explosions which have been detonated since the resumption of testing in 1961, this is the only case known in which severe earthquake interference at a large number of stations has been recorded. When the shortness of the time difference (attaining a minimum of 12 seconds at the point of nearest coincidence) between the arrivals for the teleseism and those from the underground nuclear explosion is taken into account the probability of a repeat performance, planned or unintentional, with timing even nearly as close, let alone equal or better, would indeed be remote.

In a report of this type one could always cite only the most striking examples to illustrate the effects. However, such an approach might easily give the reader the impression that the omitted data are of the same quality. Furthermore, redundancy is not a critical problem. The spacing of the instruments with respect to range and azimuth from the explosion epicenter has no points of particular concentration. The types of instruments are also sufficiently varied as to require samples of each of their responses, even for those sites with multiple seismographs.

The pressures of expediancy have forced only one temporary concession: I have recognized the natural division in the documentation of any experiment by reporting the data separately from their analysis. The contents of the present compilation have been extended considerably beyond those normally associated with a typical data report by including the interpretation of the seismograms as well as the preliminary analysis involved in the selection of the comparison events, the last step being required by the accidental nature of the incident. The perspective and implications of the present data with respect to seismic evasion and the theory of masking have been placed in a separate document which is to appear later.

Since this study was conducted under University auspices it has remained unclassified, even though nuclear seismology, like all topics connected with nuclear test activities, is weighed down by a huge, unpublished literature, partly restricted in accessibility. I have avoided reference to any material which has not been published in either book form or commercially available journals. In a few cases where important data are not accessible elsewhere, I have cited the pertinent unpublished reports which have open distributions.

I am indebted to many of my colleagues for their helpful remarks and ideas, and in particular to Dr. Jack Evernden for his comments on the presentation of the seismograms and to Mr. Fred Raab for his critical suggestions regarding the text and questions of style.

The assistance received in the technical production of this manuscript is also to be acknowledged. The text and captions for the seismograms were typed by Mrs. Janet Jenswold. Certain tables and listings were prepared by Mrs. Mayme Matsumoto. The report was printed by Zandonella Automated Printing.

I am grateful for the financial assistance which made this study possible and especially the printing of this report without which the data could appear only in a much more abbreviated form. This research was supported by the Advanced Research Projects Agency under Air Force Grant No. AFOSR-73-2522 monitored by the U. S. Air Force Office of Scientific Research and by a grant from the Council of Academic Deans of Northern Illinois University.

L.D.P.

SUMMARY

This study examines the accidental interference of a teleseism from an earthquake with the seismic signals from an underground nuclear explosion by presenting a compilation of seismograms from thirty-two near-regional stations associated with the explosion. On 14 August 1969 the United States, without any prior knowledge of the earthquake, detonated an explosion at the Nevada Test Site almost simultaneously with the passage of the teleseism over the western United States. The timing of the earthquake and the explosion produced an unusual pattern of arrivals at all principal stations surrounding the explosion. Even though the explosion was detonated 12 seconds before the passage of the teleseism over its epicenter a review of the station records shows that the teleseism always preceded the explosion waveforms. At the point of closest near-coincidence the separation between the arrivals reached a minimum of 12 seconds, with the explosion waveform still embedded completely in the teleseism. This set of records, which so far is unique in the history of seismology, provides an unusual opportunity to examine the question of hiding a nuclear explosion in an earthquake by supplying data about the one problem of seismic evasion which has not yet been examined with the aid of a planned experiment.

The nuclear explosion had a yield of approximately 3 kt (determined seismically) and a depth of burial of 784 feet in alluvium. The interfering earthquake was a principal after shock of a major earthquake sequence in the Kurile Islands, with a magnitude of 6.2, a depth of 46 km, and an unusually large worldwide station registration of 400 observations. An analysis of the data for the distance range 144-975 km shows that the seismic waveform characteristic of this explosion remains clearly visible out to 288 km. Beyond this critical distance, defined here as the maximum range of domination for the masked explosion, the role of the dominant wave is taken over by the teleseism, although instances of partial visibility occur at further distances.

As the distance from the masked explosion increases the teleseismic interference first degrades the fine structure of the tail of the explosion waveform; then it obliterates the sharp onset of the waveform, and finally it destroys the principal portions which are the Pg and Sg phases. Because the amplitude of the Sg phase is frequently the largest, it is generally more persistent than the Pg phase.

As a further step the study analyzes the quantitative features of the masking by measuring the reduction in the relative duration of the explosion waveform caused by the interference. The duration without masking is determined with the aid of traces from events with source characteristics similar to those of the masked explosion. The masked explosion is located fortuitously in a cluster of fifteen closely-spaced explosions and the most appropriate comparison event is selected by reviewing this catalogue of candidates with respect to geology and seismic waveforms. By a circumstance even more unusual an explosion with a yield and depth of burial almost identical to that of the masked explosion is available to serve as a primary comparison event. The terminations of the waveforms for the masked explosion are identified by visual inspection of its records in juxtaposition with those from the comparison event. Forty-two of the sixty-one traces from the masked explosion are presented in this manner. The masking exhibits marked deviations from the correlation with the logarithm of distance that would be expected for masking in the presence of interference of constant amplitude. These variations may be due to regional effects. The masking also shows secondary dependences on the azimuth and the differences in arrival times.

In addition to the need to bring these specific results into the full context of the general subject of seismic evasion and detection, and place them in their proper perspective, this study suggests three problems which should be examined first: 1) the projection from this incident of masking up to the level of extreme worldwide seismic interference that follows any major complex release of tectonic energy, by making use of the records of 11 August 1969 for the main event of the earthquake sequence; 2) the extension from the yield of the masked explosion up to that for the largest explosion (38 kt) in the catalogue of comparison events, by reviewing the records for the explosion of 9 October 1964 (PAR); 3) an examination of the probability for positive identification of a masked explosion as a function of the ratio of the amplitude between the explosion and the interference.

CONTENTS

TABLES

FIGURES

SEISMOGRAMS

(arranged in the order of increasing epicentral distance from the Masked Explosion)

Key to abbreviations

CE = Comparison Event
ME = Masked Explosion

The symbols in parentheses to the right of each station and instrument refer to the designations by which the records are identified; they follow the date on the label which appears in the upper right-hand corner of each record.

The range in parenthesis to the right of each station is the distance in kilometers to the epicenter of the Masked Explosion.

*Seismograph located at Boulder City, Nevada (BCN)

GLOSSARY

AEC	Atomic Energy Commission
AFOSR	Air Force Office of Scientific Research
AFTAC	Air Force Technical Applications Center
ARPA	Advanced Research Projects Agency
CIT	California Institute of Technology (Pasadena)
ESSA	Environmental Science Services Administration (replaced by NOAA)
ISC	International Seismological Center (Edinburgh)
LASA	Large Aperture Seismic Array
LASL	Los Alamos Scientific Laboratory
LLL	Lawrence Livermore Laboratory
LRSM	Long Range Seismic Measurements Program (AFTAC)
NCER	National Center for Earthquake Research (USGS)
NOAA	National Oceanic and Atmospheric Administration
NOS	National Ocean Survey (NOAA)
NSF	National Science Foundation
NTS	Nevada Test Site (AEC)
SL	Sandia Laboratories (Albuquerque, New Mexico)
UCB	University of California, Berkeley
USAF	United States Air Force
USC&GS	United States Coast and Geodetic Survey (replaced by NOS)
USGS	United States Geological Survey
WWSSN	World-Wide Standard Seismograph Network

I. INTRODUCTION

The hiding of underground nuclear explosions in earthquakes is one of the major areas of interest in the general problem of seismic detection and evasion. Despite its importance as a primary consideration in treaty negotiations for a comprehensive test ban, the seismic masking of underground explosions prior to 1969 could be discussed only in speculative terms because there were no data. In August of that year teleseisms from a strong earthquake in the Kurile Islands interfered with the signals from an underground nuclear explosion in Nevada. Even though the incident was purely accidental the data set generated by it can be applied to the problem of hiding in an earthquake in a manner that is much more direct than one might surmise just from the source locations and their magnitudes.

A closer examination of the incident shows that 1) the masked explosion is embedded in a group of closely-spaced seismic events from which one can extract not only another explosion with nearly identical source characteristics to serve as a comparison event, but also several other explosions which permit yield scaling to levels possibly significant to nuclear testing, and 2) the interfering earthquake is a member of a well-recorded earthquake sequence which allows projection from this accidental occurrence to the conditions of extreme worldwide interference that follow any major release of tectonic energy. The investigator thus has at his disposal from nearly the same configuration of sources and stations data sufficient to synthesize the case for the masking of a nuclear explosion with a yield likely to be meaningful under the worst possible signal conditions.

The present study documents the interference observed for the masked explosion by placing seismograms from it side-by-side with those of appropriate comparison events. By confronting the viewer directly with the data in a highly compressed format of seismogram pairs his capability for pattern recognition is enhanced far beyond the level normally associated with the use of only single traces. A perspective on the necessity for this approach can be gained by noting that the data are machine-readible at only one-third of the stations. The instruments at the remaining stations generate only photographic records and any manipulation of this data by signal-processing techniques (for example, spectral analysis, etc.) would require hand digitization of each trace to convert the analogue record into its corresponding time series. As a final comment it should be pointed out that this data set was produced by methods which are the least sophisticated of those currently in use: the networks involved are only partially coordinated with the aid of telemetry, master time signals and magnetic recording systems, while the remaining stations are operated remotely in isolation. Since no data from dedicated arrays are included the quality of the masking measurements obtained here can serve as a lower bound for that which could be acquired with more advanced systems.

Since this document is basically a data report for the explosion of 14 August 1969 its contents are divided into three chapters dealing with the introduction, data and conclusions. The discussions devoted to the more detailed interpretation of the data as well as the theory of seismic masking and the implications of this incident to seismic detection and evasion are presented separately in a supplementary report.

Chapter II presents the seismograms for the masked explosion and its comparison events together with introductory sections describing the interfering earthquake and the selection of the comparison events. The analysis needed for the last task is carried out by applying a series of increasingly restrictive limitations to a catalogue of nuclear test events located in the immediate vicinity of the masked explosion. The catalogue is partitioned with the aid of geological considerations and then reduced by ordering the explosions in terms of their seismic amplitudes and scaled depths of burial. Finally, a review of these sorted parameters yields one explosion with source characteristics nearly identical to those of the masked explosion. Alternate comparison events are used in those cases where traces from the primary comparison event are unavailable or the stations are of relatively recent installation. The seismograms are presented in the order of increasing distance from the masked explosion with captions containing short tabulations of the readings from the records which include onset and termination times for the signals, values of the masking as well as distance and range calculations for all events involved.

Chapter III contains the conclusions of the analysis. The values of masking obtained from the sequence of seismograms in Chapter II are condensed into a single tabulation. A second table presents the qualitative characterization of the masking effects by listing the dominant wave and its level of domination. Since the primary objective of this document is to present the data for the masked explosion, the accompanying analysis is directed almost exclusively towards the interpretation of the seismograms.

II. DATA

2.1 THE INTERFERING EARTHQUAKE

During August 1969 the Kurile Islands were the location of a major earthquake sequence (Fig. 1). The main event occurred on 11 August with a magnitude of 6.5. It produced a tsunami and it was felt at least as far as Tokyo, 1100 km away. It was preceded by a series of at least eight foreshocks that began the day before and followed by a sequence of more than 230 aftershocks that lasted until the end of the month.

In the period immediately following the main event there was a relatively large number of aftershocks, some of which were quite strong and produced signals clearly separated from those of other events in the sequence. As a consequence they were well recorded worldwide. Several of the principal aftershocks were of sufficient magnitude and isolation from interference that they could be identified distinctly at far more seismic stations than the main event. Thus, in spite of the larger magnitude of the main event, the masking of its arrivals by its immediate foreshocks caused a severe decrease in worldwide station registration for it (Porter, 1974a).

On 14 August an aftershock of magnitude 6.2 took place. Almost 11 minutes later, without any prior knowledge of or planning with respect to the earthquake, the United States Atomic Energy Commission detonated an underground nuclear explosion at the Nevada Test Site (NTS) (Fig. 2). On a seismic scale the timing can only be regarded as that approaching the incredible: the detonation occurred less than 12 seconds before the teleseism from the aftershock passed over the explosion epicenter. This timing can be deduced from the travel time curve (Fig. 3) for P-wave arrivals at the principal seismic stations in the western United States (Fig. 4)[1]. Despite the fact that the P-wave from the teleseism arrived at the explosion epicenter after the detonation took place its effective surface velocity (18.1 km/sec at NTS) so greatly exceeded the total velocity (5.8 km/sec, NTS to NEL[2]) for the near-regional P-waves from the explosion, that it arrived before the P-waves from the explosion at all of the principal stations in the western United States shown in Figure 4.

The closeness of the near-coincidence is most easily explained by reviewing the locations of the seismic stations with respect to NTS. On the earthquake side of NTS, no station was close enough to the explosion epicenter for the waves from it to arrive before the teleseism. The same was also true for the stations located in the directions lateral with respect to the lines from the earthquake epicenter to NTS (an azimuth of 310° at NTS). On the side away from the earthquake the case of closest near-simultaneity took place at Nelson, Nevada, where the difference reached its minimum of 12 seconds. All of the succeeding stations on the travel time curve for the teleseism (Fig. 3) recorded greater separations in time between the two signals.

The next item of importance is the structure of the teleseismic waveform because it determines the nature of the interference through which the signals from the masked explosion must be observed. The description given here is limited by

1. The symbols for the seismic stations and their corresponding locations are given in Appendix A.
2. Nelson, Nevada, the station of closest near-coincidence.

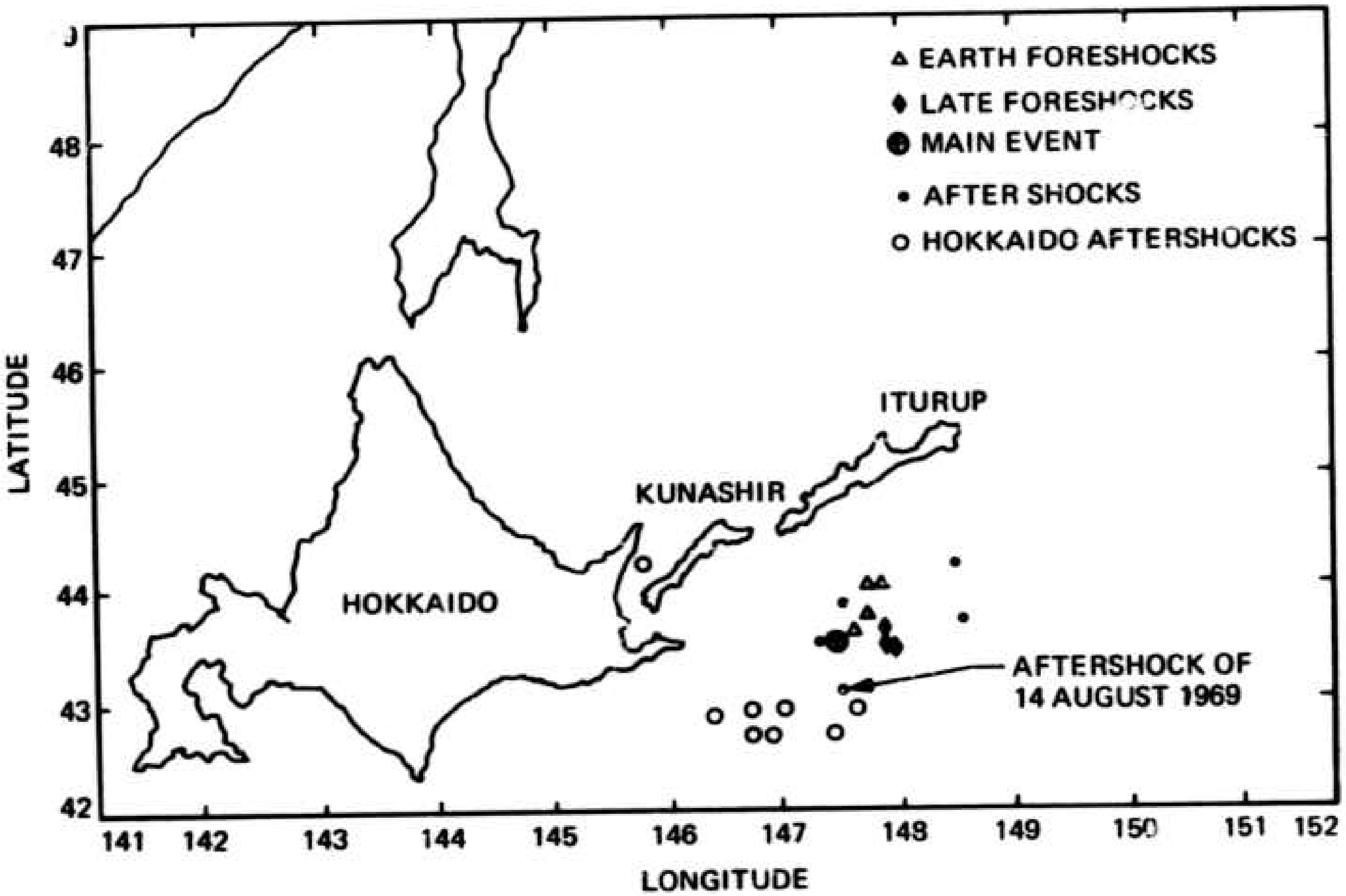

Figure 1. Location of the main event and principal aftershocks for the earthquake sequence in the Kurile Islands during August 1969. Locations are shown for the early and late foreshocks as well as the Hokkaido aftershocks.

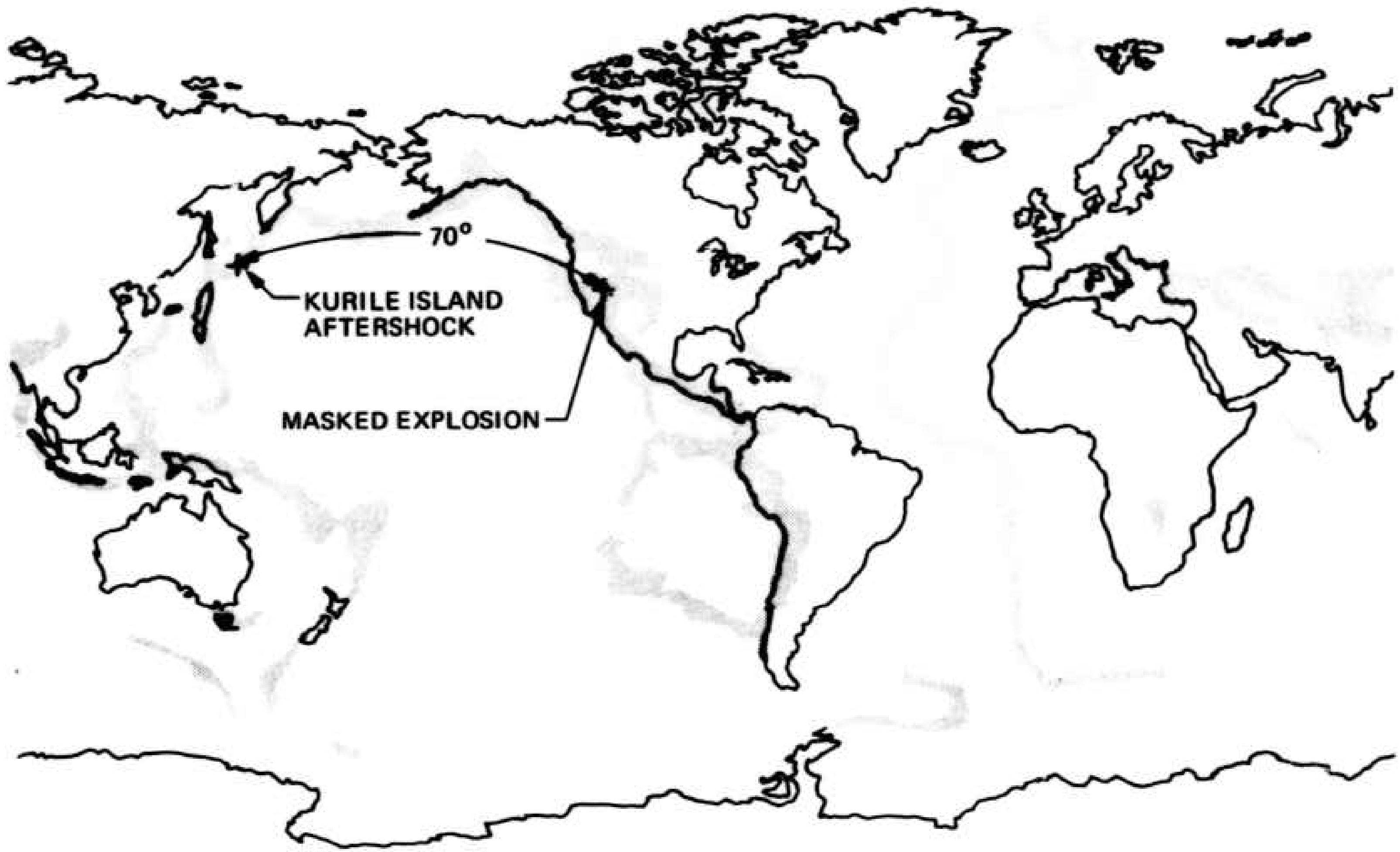

Figure 2. Location of the epicenters for the interfering earthquake (Kurile Islands) and the Masked Explosion (Nevada Test Site) of 14 August 1969. The seismically active zones of the world for 1969 are shown by the cross-hatched areas.

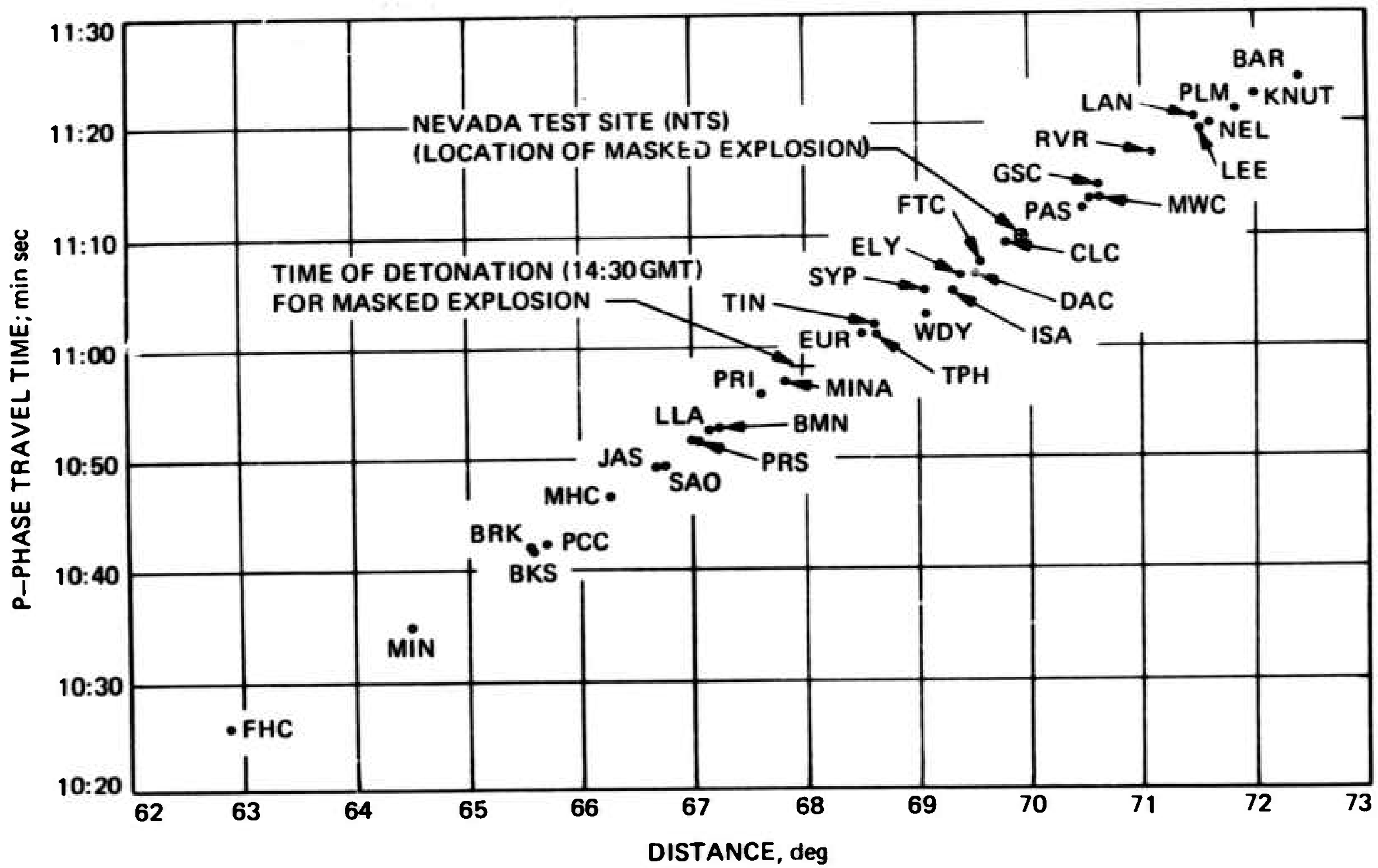

Figure 3. Travel times to seismographs located in the Western United States for P-waves from the earthquake in the Kurile Islands of 14 August 1969.

Figure 4. Location of the principal seismic stations at near-regional distances from the Nevada Test Site which were in operation during 1969.

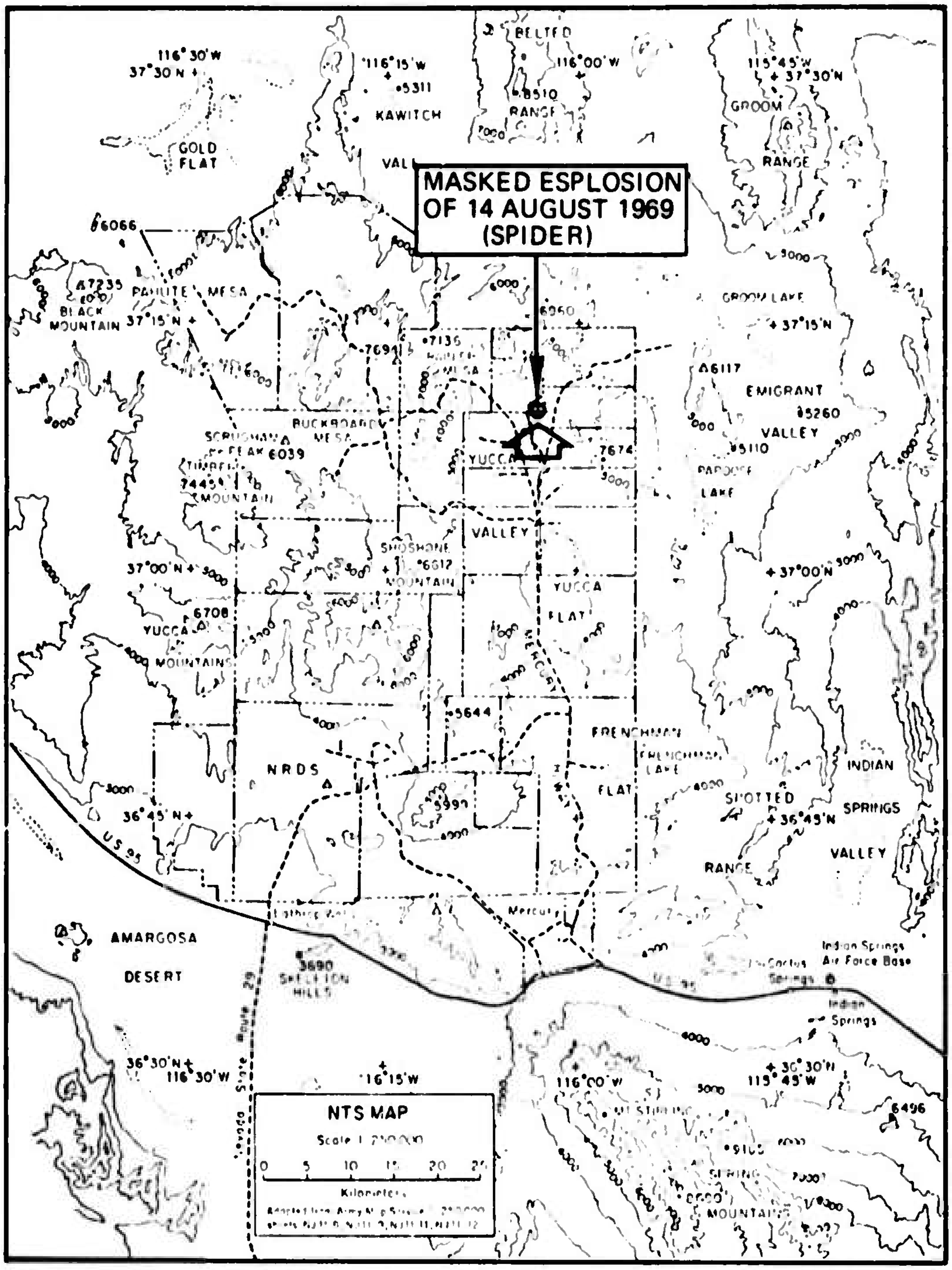

Figure 5. Location of the Nevada Test Site (NTS) and the Masked Explosion of 14 August 1969 (SPIDER).

SEISMIC MASKING OF AN UNDERGROUND NUCLEAR EXPLOSION
Final Technical Report to Grant No. AFOSR-73-2522
by Lawrence D. Porter

CORRECTION

Page 9, line 12 from the bottom should read "7820 feet"
instead of "720 feet"

definition to this specific aftershock, even though the epicenters of all members of the earthquake sequence are located relatively near each other. At most stations, for this particular teleseism, there were usually three quite well defined arrivals with delays of 7, 19 and 60 seconds after the P-wave arrival. Since all of these delays were constant with respect to range, they had travel paths similar to those for the P-wave and hence must have been generated by mechanisms in the near vicinity of the source.

For western United States stations in these range and azimuthal intervals the first two delayed arrivals are identified as pP and sP, respectively, by the International Seismological Center (ISC). This selection is open to a possible review because a check of the travel time tables gives 13 and 18.5 seconds for the delays pP-P and sP-P at the source depth (ISC) of 46 km. This implies that pP arrived about 5-6 seconds early with respect to the table values. Albuquerque has the only core reflection (PcP) listed for the stations used in this study. The identity of the third delayed arrival is not given by the ISC, but it could be associated with the abbreviated curve one minute behind the initial P-wave that appears on the Pasadena travel time chart of 1934 (Richter, 1958, Curve No. 8, Figure 17-6, p. 262).

2.2 THE MASKED EXPLOSION AND ITS COMPARISON EVENTS

In order to generate a catalogue of appropriate comparison events we review the listing of data for U. S. underground nuclear explosions (Springer and Kinnaman, 1971) with respect to the source parameters for the masked explosion. The primary comparison event (the one most closely resembling the masked explosion seismically) then is selected by applying a series of limitations with increasing restrictions to this group of sources with similar seismic waveforms.

The masked explosion of 14 August 1969 took place in the Yucca Valley portion of NTS (Fig. 5). The device was detonated at a depth of 784 feet in alluvium, 1141 feet above the water table and 916 feet above the paleozoic layer. (App. B, C).

Starting with the fact that shot medium is weak (alluvium) and dry (well above the water table) we restrict our attention to those explosions which are located not only in the same medium with approximately the same water content, but also in the immediate vicinity of the masked explosion. A search of the compilation by Springer and Kinnaman (1971) under these conditions yields a group of 15 events, the farthest of which, the explosion of 27 April 1967 (EFFENDI), is located 7[illegible]20 feet away from the masked explosion (Fig. 6, App. D).

The great variability in seismic waveforms often exhibited, however, even for shots closely adjacent to each other in the same medium and with approximately equal yields and depths of burial prompts us to make a restriction in the geological as well as the geographical sense. The map (Fig. 6) of the subarea of NTS containing the masked explosion shows that the Yucca Fault (Hinrichs, 1968) divides the event catalogue into two subgroups: 1) the 13 events (including the masked explosion) to the west of the fault, and 2) the remaining three events to the east. We assign highest priority to the first subgroup as candidates for comparison because of its position with respect to the fault and its proximity to the masked explosion. The partitioning of this subarea into microzones is based on the observation (Hays and Murphy, 1971) that the Yucca Fault can cause significant variations in travel times for seismic waves propagating across it. The measurements were made in conjunction with the explosion of 26 March 1965 (CUP) which was detonated 7622 feet to the southeast of the masked explosion.

To rate the explosions in terms of their dynamic responses we select one or two stations with instruments that discriminate well against the spectra of the teleseism and which are at ranges where the explosion waveforms can compete effectively in amplitude against the interference from the earthquake. Furthermore, we choose those instruments that have been in service at constant levels of magnification for the entire period of the event catalogue. Even though the sequence of explosions as a function of their amplitudes is not necessarily unique for all stations and in fact may vary slightly from site to site or even between the different components of the same type of instrument (as shown, for example, by the measurements in Table I), this method of selected stations is much more efficient than attempting to analyze all available records. Such a straightforward, brute-force approach would require an inordinate amount of analysis because the instrument-event matrix would have at least 480 entries (30 sensors, 16 events), if one assumes a loss factor of almost 70% in reducing the number of instruments from a maximum (80) for all stations and components to be considered to a realistic estimate (30) which incorporates the operational features and histories of the equipment involved.

The most logical choices are the Wood-Anderson seismographs at Tinemaha, California. The design of this sensor (Anderson and Wood, 1925) consists of horizontal torsion pendulum suspended by gold filament. A small mirror is mounted directly on the filament and the recording is accomplished by reflecting light from the mirror onto moving photographic paper placed on a rotating drum. The gain (2800) is relatively low and fixed. The frequency response is of a high-pass type which records explosion spectra well.

Table I lists the explosions shown in Figure 6 in the order of increasing trace amplitude for the Sg phase from these instruments. A missing value precludes use of the North-South component. The shots are grouped as dictated by Figure 6; those in Section A are examined first, while those in Section B are used as candidates for comparison only at Jamestown, California, and Golden, Colorado.

The Sg phase is selected because it quite frequently dominates explosion seismograms beginning at this range (193 km) and thus in those instances of domination it would have the largest ratio of signal to noise. As a crustal wave it exhibits much less of the structure intimate to the immediate source region than in the case of any single direct wave.

At this point in the analysis the existence of the Lgl phase (Ewing, Jardetzky, and Press, 1957, p.219; Richter, 1958, p. 267; Båth, 1973, p. 76) should be mentioned because it occurs frequently on near-regional records. Its velocity (3.54 km/sec) is nearly that for the Sg phase (3.37 km/sec) and on vertical records at distances less than 5° it is virtually impossible to distinguish between them without the aid of additional components. These velocities are taken from the discussion by Båth who goes on to say that the Lgl phase in the records of continental earthquakes at short distances frequently has larger amplitudes than the Sg phase and often is mistaken for it. He comments further that attention must be paid to both phases and that they should not be mixed under the false assumption that they are only different observations of the same wave. The present study makes no attempt to resolve this dilemma because most of the data are from vertical instruments. The short-period horizontal records which are available (Tonopah, Nevada; Darwin, California; and Golden, Colorado) are too few to permit any conclusion about the existence of Lg1 and furthermore they do not show any appreciable amplitudes transverse to the direction of propagation, except for the moderate values at Darwin.

As a final comment on the value of crustal waves and in particular of the Sg and Lg phases we note the results of Baker (1970) who shows that the near-regional and regional magnitudes determined from the Lg phase have less scatter than those from body waves. Baker bases his magnitudes on the ratios of amplitude to period for this phase and compares them directly with body-wave magnitudes (derived in the conventional manner) for the same set of 78 seismic events (73 explosions, 5 collapses, all at NTS). These results are obtained despite the fact that the Lg phase may be distorted by previous arrivals from the same event. On the other hand, the first body-wave arrival, although by definition free from same-source interference, has a relatively weak amplitude and exhibits a waveform highly dependent on local structure.

The yield estimates quoted in Table I are determined from the amplitudes for the Sg phase as recorded by the Wood-Anderson seismograph (East-West direction) at Tinemaha, California. The logarithms of amplitude and yield are assumed to correlate in a linear fashion and the exact nature of the relationship is specified with the aid of the yields (25 and 38 kt) listed by Springer and Kinnaman for two of the explosions (25 June 1966 (VULCAN) and 9 October 1964 (PAR), respectively). The yields for the remaining explosions are projections onto the yield axis from the intersections of the Sg amplitudes with this linear relationship. It should be emphasized that our interest here is to generate working estimates only of the yields; more accurate values would require the use of data from additional stations. These estimates are examined more fully in a separate study (Porter, 1973) which also confirms their reasonableness with the aid of a second calculation performed in the same manner with data from Mount Hamilton, California at a range of 495 km from NTS.

The final step in the selection of the primary comparison event is to examine the scaled depths of burial for the candidates in Table I. The scaled depth is defined by the equation:

$$\text{Scaled depth of burial} = \text{depth of burial (ft)}/[\text{yield (kt)}]^{1/3} \qquad (1)$$

It serves a source parameter particularly useful in determining the interaction of an underground explosion with the free surface above. The values to be expected are shown by two different examples. For contained explosions at NTS 350-400 is considered nominal; a value over 400 (8 events in Table I) generally means an overburied shot. On the other hand, excavation experiments require explosions with much smaller scaled depths: the cratering shot of 6 July 1962 (SEDAN), for example, with a depth of 635 feet and a yield of 100 kt has a scaled depth of 137.

A review of the yields and scaled depths for the events in Table I shows that the parameters for the masked explosion most closely resemble those for the explosion of 13 September 1963 (AHTANUM) and therefore we select this explosion as the primary comparison event. Both explosions have seismic yield estimates of approximately 3 kt and are overburied with scaled depths of 521 for AHTANUM and 552 for SPIDER. The epicenter for AHTANUM lies 5090 feet N77°W from that for SPIDER.

TABLE I

UNDERGROUND NUCLEAR EXPLOSIONS LOCATED IN THE VICINITY OF THE MASKED EXPLOSION OF 14 AUGUST 1969 (listed in the order of increasing seismic trace amplitude[1] at Tinemaha, California)

No.	Date	Name[2]	Device depth[2] (ft)	Trace amplitude Tinemaha, CA (mm) WA NS	WA EW	Seismic yield[3] (kt)	Scaled depth of burial ($ft/kt^{1/3}$)
A.	**Explosions located in the microzone of the masked explosion**						
1.	11 June 1964	ACE	862	2.2	3.5	2.0	684
2.	14 August 1969	SPIDER	784	4.0	4.5	2.9	552
3.	13 September 1963	AHTANUM	740	4.5	4.5	2.9	521
4.	19 August 1964	ALVA	545	4.9	4.6	3.0	378
5.	27 April 1967	EFFENDI	719	5.0	4.6	3.0	499
6.	15 January 1969	PACKARD	810	-	8.6	7.3	418
7.	15 August 1963	SATSOP	738	7.0	8.7	7.4	378
8.	18 January 1968	HUPMOBILE	810	10.0	13.0	13	347
9.	25 June 1966	VULCAN	1057	14.8	20.2	(25)[4]	372
10.	10 April 1968	NOOR	1250	25.0	24.0	32	393
11.	9 October 1964	PAR	1325	16.2	27.2	(38)[4]	394
B.	**Explosions located outside of the microzone of the masked explosion**						
1.	5 November 1966	SIMMS	650	1.6	2.0	0.9	672
2.	10 August 1966	ROVENA	635	1.7	2.2	0.95	642
3.	29 September 1966	NEWARK	750	4.0	4.7	3.1	514

C. Explosions located in the microzone of the masked explosion, but excluded from further study

No.	Date	Name	Depth (ft)	Reason for exclusion
1.	21 February 1963	CARMEL	536	signal is contaminated by the explosio KAWEAH which was detonated 8 seconds earlier at NTS.
2.	12 February 1965	ALPACA	737	signal is too weak to be recorded well at near-regional stations.

---

1. amplitude as measured by the Wood-Anderson seismograph (East-West direction).
2. Springer and Kinnaman (1971).
3. yield as determined by inverse estimation from the amplitudes measured by the Wood-Anderson seismograph (East-West direction) at Tinemaha, California.
4. announced values, determined by radiochemical and other means (Springer and Kinnaman, 1971).

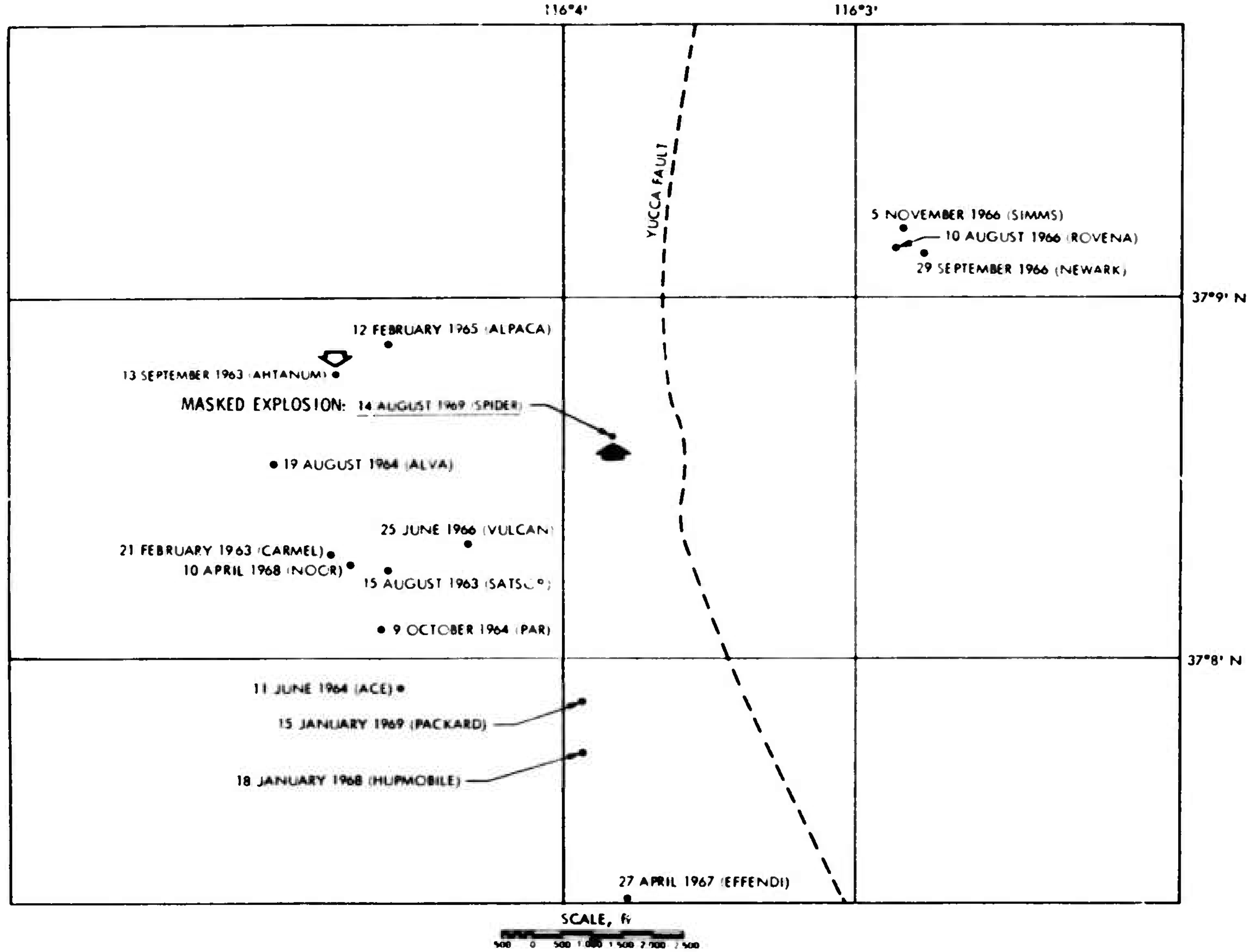

Figure 6. Location of the underground nuclear explosions in the immediate vicinity of the Masked Explosion of 14 August 1969 (solid arrow). This subarea is located in Yucca Valley at the Nevada Test Site. The hollow arrow denotes the primary comparison event.

So far the discussion deals almost exclusively with the determination of the source parameters for the masked explosion and the selection of appropriate comparison events. There remains, however, another complex task of obtaining as many stations and instruments as possible with records of both the masked explosion and a comparison event. Because of the uniqueness to date of this masking incident considerable effort is made to generate this data set in a manner as complete as possible within the limits of time and support, even to the extent of using substitute comparison events at three stations as well as extensive photographic manipulation (Sect. 2.6) of many of the traces.

In the case of the closest of these stations (Eureka, Nevada) the record of another overburied explosion, that of 11 June 1964 (ACE), is available. At the remaining two stations (Jamestown, California, and Golden, Colorado) it is necessary to go outside of the microzone containing the masked explosion. Even though the explosion of 29 September 1966 (NEWARK) listed in Section B of Table I appears to have source parameters qualifying it as a substitute comparison event, an examination of its amplitudes at Jamestown shows a disparity so large with respect to the waveform of the masked explosion that the explosion catalogue in Table I must be abandoned. As a last resort we turn our attention to other seismic events in southern Nevada as possible candidates for comparison. This category includes unidentified seismic events with explosion-like signals (McEvilly and Peppin, 1972, p. 69) as well as earthquakes. The resemblance of the latter to the former for these two possibly different kinds of sources can be exceedingly close in certain cases, even to the point of misidentification (for example, the Colorado earthquake of 4 April 1967 that was mistaken as an NTS event, Krivoy and Mears, 1969, p. B119). An examination (Porter, 1973) of southern Nevada earthquakes and NTS explosions as recorded by Jamestown also confirms this close resemblance. Southern Nevada is a relatively aseismic region and a limited search of the ISC and NOAA catalogues yields only five events with appropriate epicenters for the period 1969-73 (App. E).

As in the case of any study involving data collected from a large number of sensors at different sites there are some locations which produced unusable traces or for which no suitable records could be found. Plate 31 gives an example typical of the search conducted in the case of a telemetered network using multiple-channel recording methods. Of the original set of fifty-two locations, thirty-two have records suitable for inclusion in this study; the remaining stations and the reasons for the exclusion of their records are listed in App. F.

2.3 ARRANGEMENT OF THE DATA

The seismograms in this compilation are arranged in the order of increasing epicentral distance from the masked explosion. The traces are assembled into groups with the trace for the comparison event (if present) always being placed directly above that for the earthquake and masked explosion. Each pair of traces is assigned a group number in which the suffix a always denotes the comparison event and suffix b the masked explosion. The distribution of the instruments with respect to the stations associated with the masked explosion and its comparison events is given in Table II. The map in Figure 7 shows the approximate locations of the seismometers.

At any given station with multiple instrumentation the data are presented in the following sequence: short-period, high-pass (Wood-Anderson), wide-band and long-period. Within each class of instruments the vertical component is presented first followed by the horizontals. For the latter the sequence of orientations is radial, transverse or North-South, East-West. An effort is made to place as many seismograms as feasible on each plate, consistent with the widths of the records. As a result of this procedure it is possible to condense the data compilation from 66 to 31 plates.

The conventional time scale of drum records of 1 mm/sec is maintained as much as possible throughout the compilation. All data recorded at other time scales are converted photographically to this nominal standard so that a direct comparison between all seismograms is possible. Only in the case of the long-period data is the original time scale of 0.5 mm/sec retained. Special care was exercised during the assembly of the seismogram pairs to insure consistency of the time scales between members even though some recopying of the data was necessary.

2.4 CAPTION FORMAT AND NOMENCLATURE

The captions are designed to minimize the need for reference to external tables. The upper portion of each caption gives tabular information about the range, azimuths, origin time and readings of the seismograms, while the lower portion is devoted to a corresponding written comment. These remarks are divided into two paragraphs. The first paragraph describes the seismic features of the traces, while the second deals with the preparation of the data.

The table headings for the captions are defined as follows:

Event — Directly below this heading are listed three abbreviations:

- CE — Comparison Event. The primary Comparison Event for this study is the underground nuclear explosion of 13 September 1963 (AHTANUM). The substitute Comparison Events are the underground nuclear explosion of 11 June 1964 (ACE) and the seismic event in southern Nevada of 18 March 1969.
- EQ — Earthquake. The earthquake which generated the teleseisms that masked the nuclear explosion of 14 August 1969.
- ME — Masked Explosion. The underground nuclear explosion (SPIDER) of the same date.

Date — The date (GMT) of the event in question.

Δ — The range in degrees between the event epicenter and the station. This quantity is defined formally as the angle subtended at the earth's center by the arc connecting the station and epicenter (Bullen, 1963, Chapter 10).

Range — The range on the surface of the earth in kilometers as computed according to Rudoe's formulae for the normal section distance on the surface of a spheroid (Bomford, 1962, pp. 108-110).

Azm — The azimuth in degrees which is the angle (measured from north through east) between the meridian line through the epicenter and the normal section line connecting the epicenter with the station. The azimuth is determined from Rudoe's formulae.

B Azm — The back azimuth in degrees which is defined in the same manner as above, except for the interchange of epicenter and station.

Origin	The origin time (GMT) of the event in hours, minutes and seconds.
T C	The time correction in seconds for the trace. For example, a positive value indicates that the station clock was slow and the correction should be added to the station timing marks by translating the trace to the left of the reference mark for true time. The time corrections were taken into account during the mounting and annotation of the seismograms.
Onset	The first appearance for the signal from the event in question. For the CE or ME the value is the time in seconds after the origin time. In the case of the EQ it is the actual arrival time of the first phase in minutes and seconds after 14:00:00 GMT.
Dif	The difference in seconds between the onset for the EQ and that for the CE or ME. The values given in the CE row are the differences between the observed first arrivals for the CE and EQ and hence measure the extent to which the explosion waveform is embedded in the teleseism without any masking. Values in the ME row (when given) indicate the extent of embedding in the teleseism with masking effects included.
Term	The termination of the explosion waveform, in seconds after the origin time. In some instances two values are given. Those with the suffix a denote the end of the principal portion of the explosion waveform, or in other words, the end of the motion characteristic of the explosion. The suffix b signifies the values for the complete cessation of the signal. No readings for the termination of the earthquake are attempted.
Dur	The duration in seconds of the explosion waveform. This value is computed by subtracting the onset time from the termination. Two durations are quoted for those cases where two terminations are listed.
Mask	The relative masking in percent which describes the relative loss of duration of the ME when compared to that for the CE. It is given by the formula $$\text{Masking } (\%) = \frac{\text{Duration (CE)} - \text{Duration (ME)}}{\text{Duration (CE)}} \times 100 \qquad (2)$$ The relative masking is given only if the durations of both the CE and ME are known or can be estimated. A value is given for each duration of the CE quoted.
Mask F	The masking factor which is the reciprocal of the relative masking (the ratio given above without multiplication by 100). This factor is included because a separate study (Porter, 1973) shows that the masking factor for an explosion waveform with exponential time decay observed in the presence of a teleseism of constant amplitude has a linear relationship with the logarithm of the distance from the explosion. A masking factor is given for each value of the relative masking.

2.5 ANNOTATION OF THE SEISMOGRAMS

The upper right-hand corner of each seismogram contains a label showing the date, station symbol and instrument abbreviation. In some instances the gain of the instrument or the vertical scale is also given. To insure a consistent method of annotation each seismogram is marked in the following manner: The origin time for the CE or ME is indicated by a solid arrow (⬆). The origin time (GMT) is inscribed directly above or below this arrow. In addition, as an aid to the reader, the time elapsed after the origin time of the explosion is marked off in minutes.

To further the interpretation the phases of the CE, EQ and ME are identified whenever possible and their corresponding arrival times tabulated. To insure consistency in the identifications of the phases, those made in this study are compared against the ones given by Båth (1973), Richter (1958) and Simon (1972, pp. 32-35). The records of three larger NTS explosions from Golden, Colorado by Simon are of particular interest because the phases are annotated and the traces can be compared directly with those on Plate 29. The present study lists table values for the arrival times (Table III) in those cases where the explosion does not have a distinct onset or its waveform is masked or missing. These calculated values, denoted by Pcal or Scal, are the first arriving phases of the two shown for each type of wave in Table III. Table III is constructed in a composite manner: The P-wave travel times are from Herrin (1968), while the S-wave times are from Jeffreys and Bullen (1940).

2.6 PHOTOGRAPHIC PREPARATION

Because of the importance attached in this study to the direct visual comparison of seismograms, significant attention is devoted to the photographic reproduction of the data in the forms with the greatest possible resolution and contrast. The complete avoidance of half-tone prints is accomplished through the use exclusively of film processes with lithographic-like features. Although the variety of recording methods,

1) mechanical:
   - inked pen
   - hot-wire stylus

2) photographic:
   - paper
   - film (16 and 35 mm),

3) electronic:
   - magnetic tape,

used by the seven reporting networks permits us to compare one technique against another, this diversity at the same time requires much more photographic experimentation in order to achieve results of uniformly high quality, than normally would be necessary in a report dealing with only one type of record. As a consequence, several different methods of photography are employed (Table IV). Original records are used whenever possible to minimize any degradation or loss of detail in the appearance of the waveforms; the best copies available from archives are employed only as a last resort.

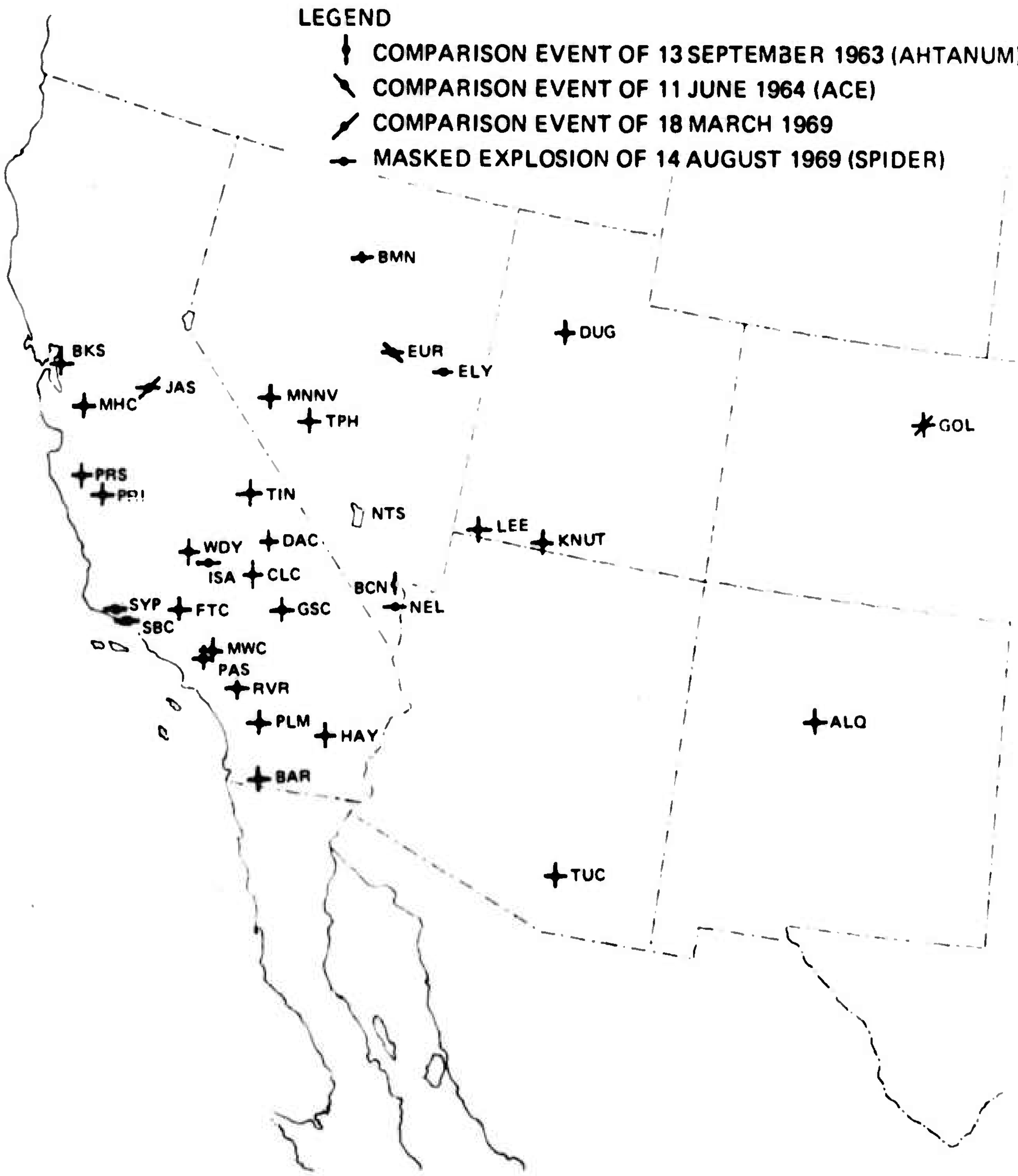

Figure 7. Location of the seismographs in the Western United States which recorded the Masked Explosion of 14 August 1969.

THE DISTRIBUTION OF INSTRUMENTS FOR NEAR-REGIONAL STATIONS ASSOCIATED WITH THE MASKED EXPLOSION AND ITS COMPARISON EVENTS

(listed in the order of increasing epicentral distance from the explosion)

No.	Station Symbol	Range (km)	Instruments													Plate
			Short-period						High-pass[2]		Wide-band		Long-period			
			18-300[1]	Z	R	T	NS	EW	NS	EW	Z	R	Z	NS	EW	
1	TPH	144		C, M	C, M	C, M					M	M	M			1,2
2	DAC	168		C, M	C, M	C, M					M[3]	M[3]				3,4
3	TIN	193		C, M					C, M	C, M			C, M	C, M	C, M	5,6,7
4	NEL	194	M	C[4], M	C[4]	C[4], M					M[3]	M[3]				8,9
5	CLC	203		C, M												10
6	GSC	217		C, M[5]												11
7	MN-NV	232		C, M[6]												12
8	LEE	239	M	C, M	C	C, M						M				13,14
9	ELY	242	M								M	M				15
10	EUR	258		C, M[7]												16
11	ISA	273		M												17
12	KN-UT	288		C, M												18
13	WDY	297		C, M												19
14	FTC	360		C, M												20
15	RVR	371		C, M												20
16	MWC	373		C, M												20
17	BMN	377	M								M	M				21
18	PAS	385		C, M										M	M	22
19	HAY	385		C, M												22
20	JAS	396		C, M[8]												23
21	PRI	427		C, M												24
22	PLM	429		C, M												24
23	DUG	440		C, M												25
24	SBC	447		M												26
25	SYP	459		M												26
26	PRS	483		C, M[9]												26
27	MHC	495		C, M												27
28	BAR	500		C, M												27
29	BKS	551		C, M												27
30	TUC	723		C, M												28
31	ALQ	899		C, M												28
32	GOL	975		C, M[10]			C, M[10]	C, M[10]								29,30
Total Records			4	27 30	4 2	4 4	1 1	1 1	1 1	1 1	5	6	1 2	1 2	1 2	

(see following page for notes)

Key to abbreviations

Instrument orientations

Z vertical

R radial (parallel to the direction from the station to NTS)

T transverse (perpendicular to the direction from the station to NTS)

NS North-South (although some of the individual traces show SN to indicate that the instrument has been positioned in the exact opposite sense)

EW East-West (the same comment as above applies)

Events

C Comparison Event: underground nuclear explosion of 13 September 1963 (AHTANUM)

M Masked Explosion: underground nuclear explosion of 14 August 1969 (SPIDER)

---

1. A short-period vertical seismograph with a response very close to that of the Benioff.
2. Wood-Anderson horizontal torsion seismograph with a magnification of 2800 and a pendulum of period 0.8 second.
3. Traces are given for both high and low gain levels.
4. The data for the CE were recorded at the station BCN in Boulder City, Nevada. The station NEL replaced BCN prior to the ME and the traces used in this report are expanded in time scale by photographic enlargement to match the Pg arrival times at Nelson, Nevada.
5. A second record transcribed by telemetry at Pasadena is given for the ME.
6. The station MN-NV was withdrawn from service prior to the ME. The trace used in this report was recorded at the adjacent station MINA and transcribed by telemetry at Berkeley.
7. The record for 13 September 1963 was unavailable. The trace from the underground nuclear explosion of 11 June 1964 (ACE) is used for the CE.
8. The station JAS was installed after 13 September 1963. The trace from the seismic event of southern Nevada of 18 March 1969 is used for the CE.
9. The short-period vertical instrument was replaced by a horizontal Willmore with an orientation of N45°E prior to the ME. The record used in this report is a photoreduction of a hand tracing that was obtained from a projection of the 16 mm film original.
10. The traces for the explosion of 13 September 1963 are too heavily embedded in the noise to be useful as waveforms for the CE. Instead, they are replaced by traces from the seismic event of southern Nevada of 18 March 1969.

TABLE III

TRAVEL TIMES TO NEAR-REGIONAL STATIONS FOR THE PRINCIPAL SEISMIC PHASES FROM THE MASKED EXPLOSION

Station No.	Symbol	Δ (°)	Range (km)	P Arrivals[1] Pn (sec)	Pg (sec)	S Arrivals[2] Sn (sec)	Sg (sec)
1	TPH	1.30	144	25.3	24.1	43.8	43.0
2	DAC	1.51	168	28.1	27.1	49.1	49.9
3	TIN	1.73	193	31.2	30.7	54.6	57.2
4	NEL	1.75	194	31.4	31.1	55.1	57.9
5	CLC	1.82	203	32.2	33.7	56.9	60.2
6	GSC	1.95	217	34.2	36.1	60.2	64.5
7	MN-NV	2.09	232	36.2	38.7	63.8	69.1
8	LEE	2.15	239	36.9	39.8	65.3	71.1
9	ELY	2.17	242	37.2	40.2	65.8	71.7
10	EUR	2.32	258	38.7	43.0	69.7	76.7
11	ISA	2.45	273	41.0	45.4	73.0	81.0
12	KN-UT	2.59	288	43.0	48.0	76.5	85.6
13	WDY	2.67	297	44.1	49.5	78.4	88.2
14	FTC	3.24	360	52.0	60.0	93.0	107.0
15	RVR	3.34	371	53.2	61.9	95.6	110.3
16	MWC	3.35	373	53.4	62.1	95.8	110.7
17	BMN	3.39	377	53.9	62.8	97.0	112.0
18	PAS	3.46	385	54.9	64.1	98.6	114.3
19	HAY	3.46	385	54.9	64.1	98.6	114.3
20	JAS	3.56	396	56.3	66.0	101.1	117.6
21	PRI	3.84	427	60.1	71.2	108.2	126.9
22	PLM	3.85	429	60.2	71.3	108.5	127.3
23	DUG	3.95	440	61.6	73.2	111.0	130.6
24	SBC	4.02	447	62.3	74.5	112.7	132.9
25	SYP	4.13	459	63.9	76.2	115.5	136.5
26	PRS	4.34	483	67.0	80.4	120.7	143.4
27	MHC	4.45	495	68.5	82.5	123.7	147.1
28	BAR	4.50	500	69.1	83.4	124.9	148.7
29	BKS	4.96	551	75.4	91.9	136.5	163.9
30	TUC	6.50	723	96.5	120.4	175.1	214.8
31	ALQ	8.09	899	118.2		214.8	267.3
32	GOL	8.77	975	127.5		231.8	289.8

[1]Herrin, E. (Chairman) (1968).

[2]Jeffreys, H. and K. E. Bullen (1940).

TABLE IV

NOTES ON PHOTOGRAPHIC PREPARATION
(listed in alphabetical order by reporting network)

		Original Record		Photographic Preparation		
Note	Reporting Network	Material	Time Scale (mm/sec)	Process/Film	Scale Factor (%)	Comments
1.	California Institute of Technology (Pasadena)	photographic paper	1	PMT[1]	100	
2.			0.5			
3.		inked-pen paper	1			
4.	Long-Range Seismic Measurements Program, U.S. Air Force (LRSM)	35 mm film	0.25		402	Only best copy from archives is available; direct contact with original is not possible.
5.	Sandia Laboratories Albuquerque, NM	oscillograph playout reproduced from magnetic tape	0.4064 (.16 in/sec)	Ortho[2]	24.6	Oscillograph playout is light sensitive and has very low contrast.
6.		Sanborn recorder playout reproduced from magnetic tape	1	Ortho[2]	100	Requires use of filters to suppress grid of chart paper.
7.	University of California, Berkeley	hot-wire stylus paper	1	double photostat	100	
8.		16 mm film Develocorder	0.467	Panchromatic (continuous contrast film)	218	
9.					707	
10.		hand tracing of projected image from 16 mm film	10	Ortho[2]	10	
11.	World-Wide Standard Seismograph Network (WWSSN)	photographic paper	1	PMT[1]	100	Best copy available from archives.
12.						Original record.

[1] Photo-Mechanical Transfer (a film process with lithographic-like features, by Kodak).
[2] Ortho (a lithographic film by Kodak).

2.7 Seismograms of the masked explosion and its comparison events

Event	Date (GMT)	Δ (°)	Range (km)	Azm (°)	B Azm (°)	Origin (h m s)	T C (s)	Onset (s)	Dif (s)	Term (s)	Dur (s)	Mask (%)	Mask F (1/M)
Group 1	Tonopah, Nevada (TPH)			Short-period vertical (SPZ)									
a) CE	13 SEP 63	1.28	143	315.4	134.8	13:53:00.15	0	25.2		145a 352b	120a 327b		
b) EQ	14 AUG 69	68.6	7622	57.5	308.5	14:19:01.6	0	30:03.7					
ME	..do..	1.30	144	315.1	134.4	14:30:00.04		25.3	21.6	75	50	58.3a 84.7b	1.72a 1.18b
Group 2	..do..			Short-period radial (SPR)									
a) CE							0	25.2		175a 350b	150a 325b		
b) EQ	..do..						0	30:03.7					
ME								25.5	21.8	90	65	56.7a 80.0b	1.75a 1.25b
Group 3	..do..			Short-period transverse (SPT)									
a) CE							0	26.2		125a 308b	100a 282b		
b) EQ	..do..						0	30:04.9					
ME								26.5	21.6	80	54	46.0a 80.9b	2.28a 1.24b

The Pg and Sg phases of the ME completely dominate the EQ for all three short-period components, although the profiles are somewhat dissimilar with respect to those of the CE.

The data for the CE are reproduced from oscillograph playouts at a scale factor of 24.6%; those for the ME are reproduced from Sanborn recorder transcriptions at a scale factor of 100%. The disparity in amplitudes between the CE and ME is due to differences in gain and recording methods. (See Notes 5 & 6, Table IV).

---

a. End of the motion characteristic of the explosion.
b. End of the signal.

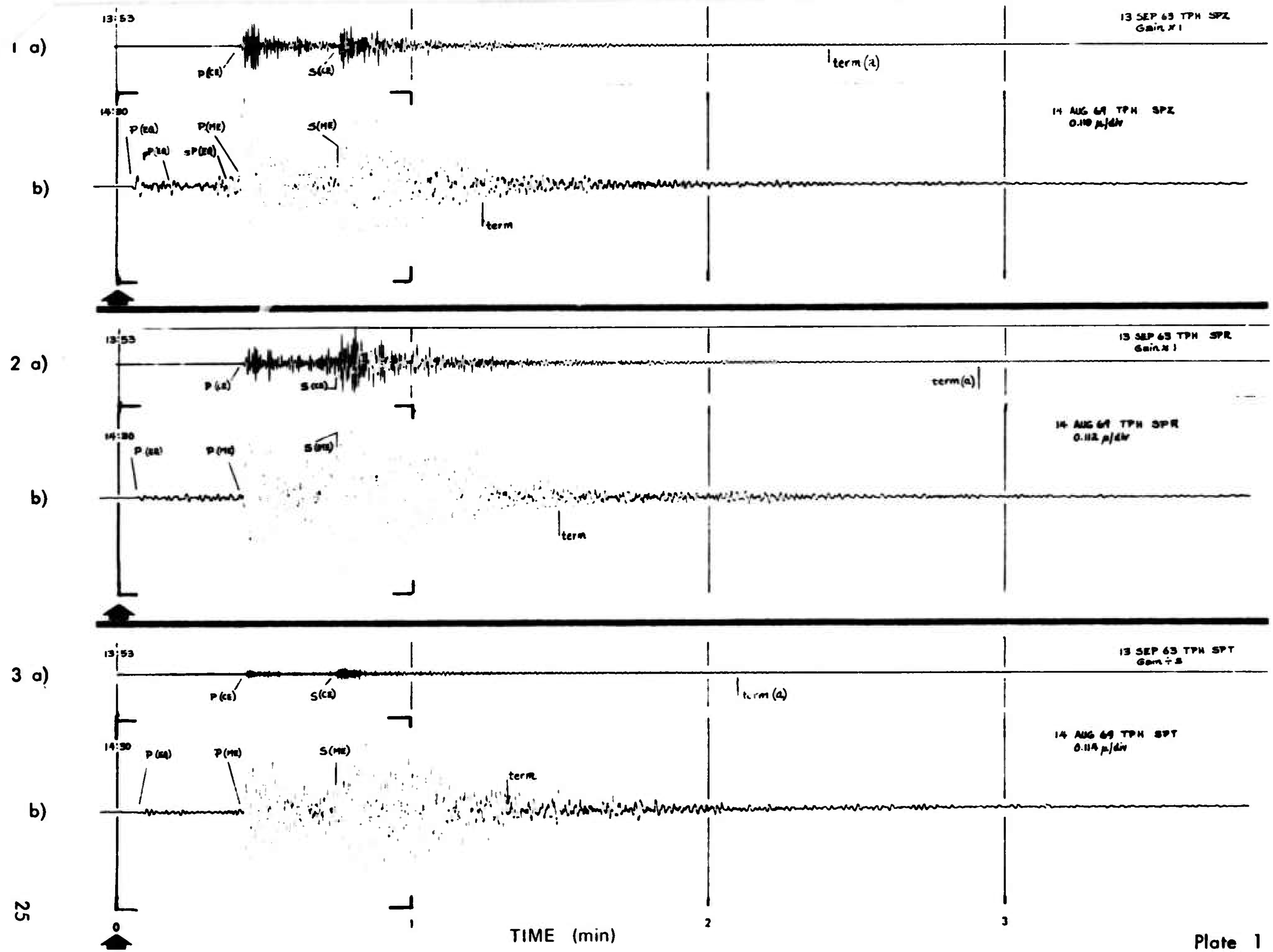
1 a)
13:53
13 SEP 63 TPH SPZ
Gain x 1
P(CE)
S(CE)
term (a)
b)
14:30
14 AUG 69 TPH SPZ
0.110 μ/div
P(EA)
pP(EA)
sP(EA)
P(ME)
S(ME)
term
2 a)
13:53
13 SEP 63 TPH SPR
Gain x 1
P(CE)
S(CE)
term(a)
b)
14:30
14 AUG 69 TPH SPR
0.112 μ/div
P(EA)
P(ME)
S(ME)
term
3 a)
13:53
13 SEP 63 TPH SPT
Gain ÷ 2
P(CE)
S(CE)
term (a)
b)
14:30
14 AUG 69 TPH SPT
0.114 μ/div
P(EA)
P(ME)
S(ME)
term
0
1
2
3
TIME (min)

Plate 1

Event	Date (GMT)	Δ (°)	Range (km)	Azm (°)	B Azm (°)	Origin (h m s)	T C (s)	Onset (s)	Dif (s)	Term (s)	Dur (s)	Mask (%)	Mask F (1/M)
Group 4	Tonopah, Nevada (TPH)			Wide-band vertical (WBZ)									
a) CE	none										150*		
b) EQ	14 AUG 69	68.6	7622	57.5	308.5	14:19:01.6	0	30:03.0					
ME	..do..	1.30	144	315.1	134.4	14:30:00.04		25	22	82	57	60*	1.67*
Group 5	..do..			Wide-band radial (WBR)									
a) CE											150*		
b) EQ	..do..						0	30:03.4					
ME								25	21.6	80	55	60*	1.67*
Group 6	..do..			Long-period vertical (LPZ)									
a) CE											150*		
b) EQ	..do..						0	30:03.5					
ME								25.6	22.1	94	68	55*	1.83*

These instruments were installed relatively recently; no traces from suitable CE's are available. The Pg and Sg phases of the ME completely dominate the EQ on all traces.

The data are reproduced from Sanborn recorder transcriptions at a scale factor of 100%. (see Note 6, Table IV).

*Estimated from the short-period data given on Plate No. 1.

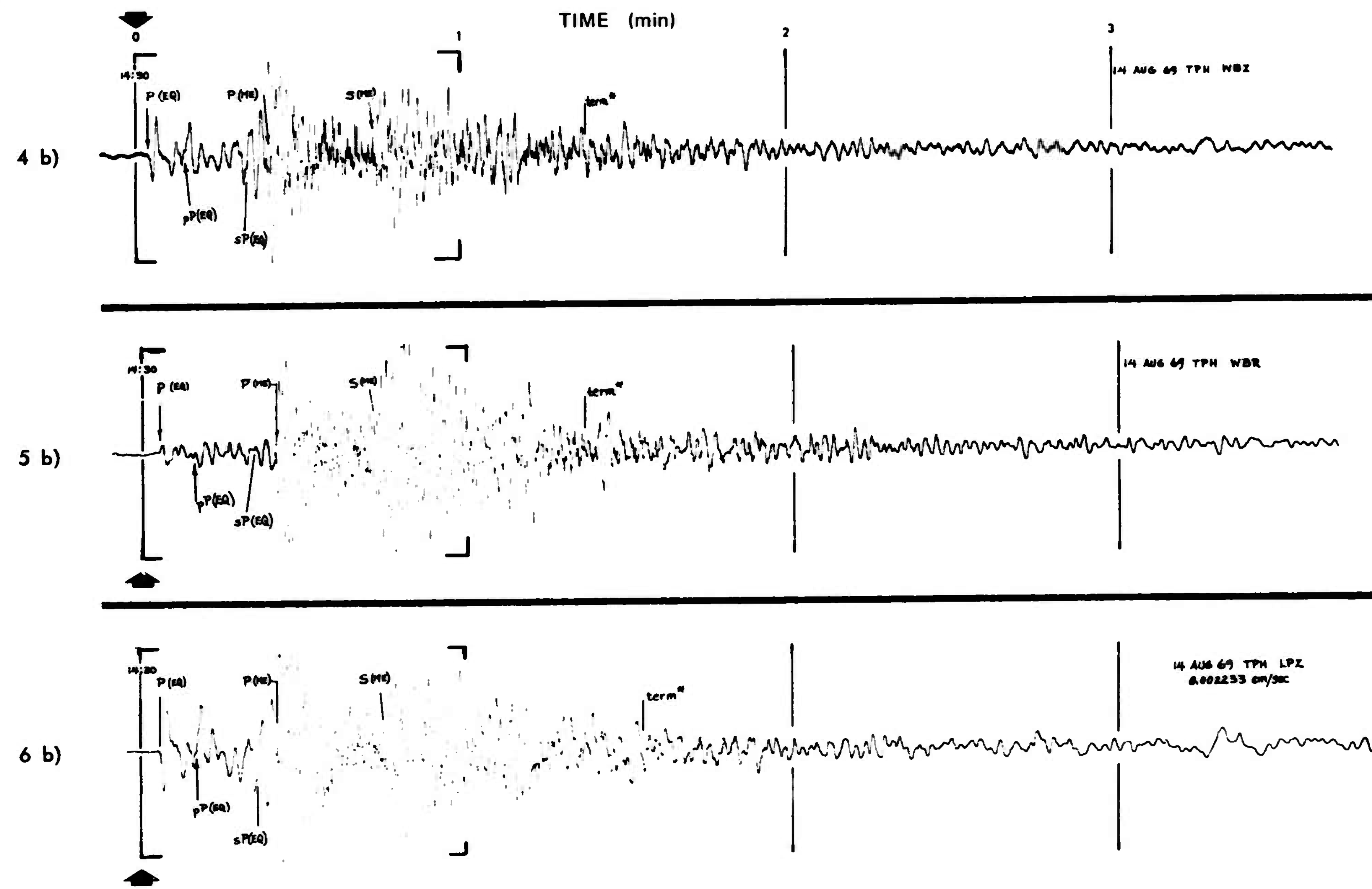

TIME (min)
0
1
2
3
4 b)
5 b)
6 b)
14:30
P (EQ)
pP(EQ)
sP(EQ)
P (ME)
S (ME)
term*
14 AUG 69 TPH WBZ
14 AUG 69 TPH WBR
14 AUG 69 TPH LPZ
0.002233 cm/sec

Plate 2

Event	Date (GMT)	Δ (°)	Range (km)	Azm (°)	B Azm (°)	Origin (h m s)	T C (s)	Onset (s)	Dif (s)	Term (s)	Dur (s)	Mask (%)	Mask F (1/M)
Group 7	Darwin, California (DAC)			Short-period vertical (SPZ)						115a	87a		
a) CE	13 SEP 63	1.50	167	234.4	53.5	13:53:00.15	0	28		183b	155b		
b) EQ	14 AUG 69	69.5	7722	59.2	308.9	14:19:01.6	0	30:08					
ME	..do..	1.51	168	234.8	53.9	14:30:00.04		29	21	91	62	28.7a	3.48a
												60.0b	1.67b
Group 8	..do..			Short-period radial (SPR)						131a	103a		
a) CE							0	28		177b	149b		
b) EQ	..do..						0	30:08					
ME								28	20	94	66	35.9a	2.73a
												55.7b	1.80b
Group 9	..do..			Short-period transverse (SPT)						138a	110a		
a) CE							0	28		335b	307b		
b) EQ	..do..						0	30:09					
ME								31	22	87	56	49.1a	2.04a
												81.8b	1.22b

The EQ is dominated completely by the Sg and only partially by the Pg phases of the ME on all three short-period components. The profiles of the ME differ somewhat from those of the CE.

The data for the CE are reproduced from oscillograph playouts at a scale factor of 24.6%; those for the ME are reproduced from Sanborn recorder transcriptions at a scale factor of 100%. The disparity in amplitudes between the CE and ME is due to differences in gain and recording methods. (see Notes 5 & 6, Table IV).

a. End of the motion characteristic of the explosion.
b. End of the signal.

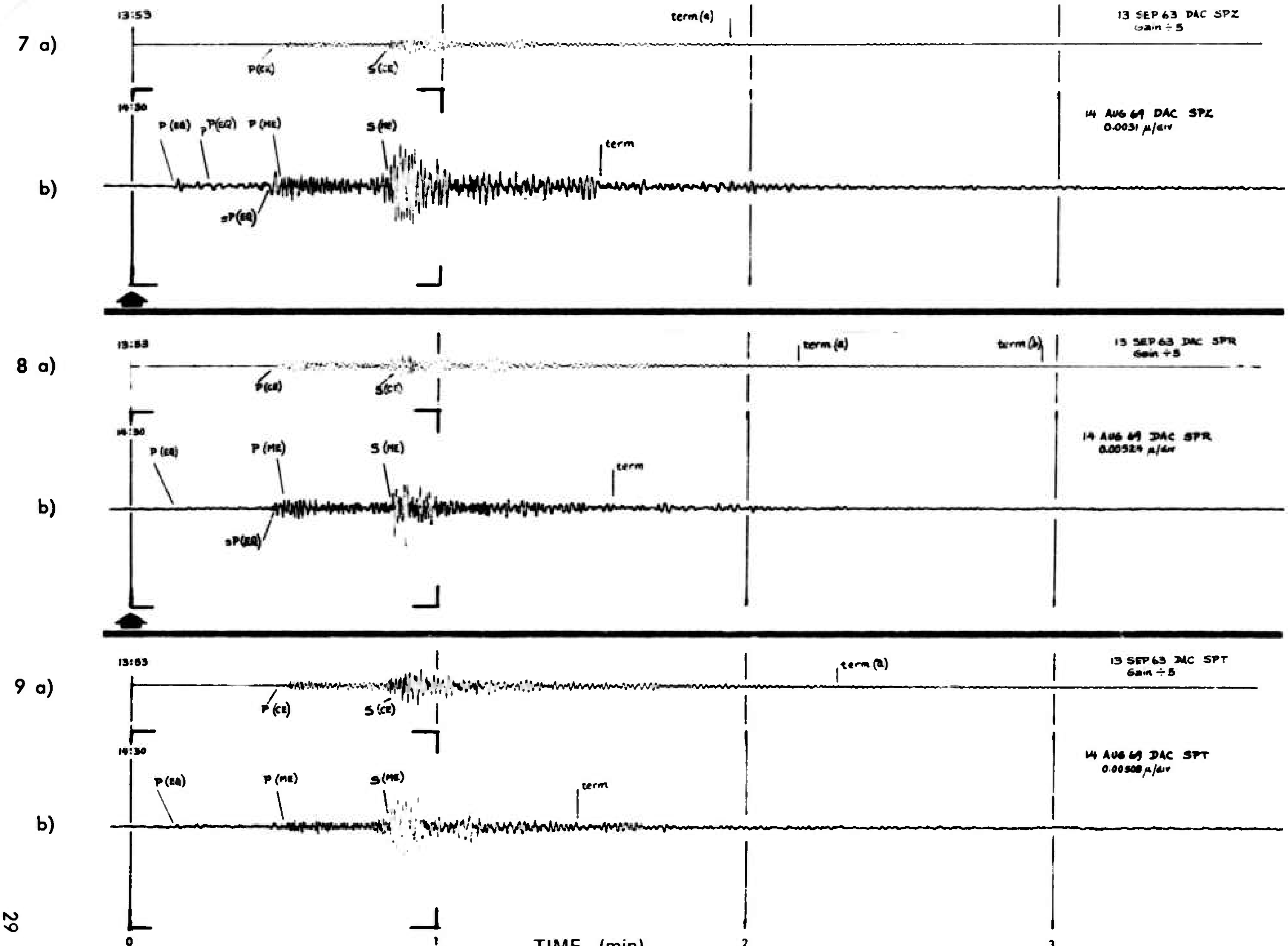

7 a)
b)
8 a)
b)
9 a)
b)
13:53
14:30
13 SEP 63 DAC SPZ
Gain ÷ 5
14 AUG 69 DAC SPZ
0.0031 μ/div
P(CE)
S(CE)
P (EB)
P(EQ)
P (ME)
S (ME)
sP(EB)
term
term (a)
13 SEP 63 DAC SPR
Gain ÷ 5
14 AUG 69 DAC SPR
0.00524 μ/div
term (b)
13 SEP 63 DAC SPT
Gain ÷ 5
14 AUG 69 DAC SPT
0.00508 μ/div
0
1
2
3
TIME (min)

Plate 3

Event	Date (GMT)	Δ (°)	Range (km)	Azm (°)	B Azm (°)	Origin (h m s)	T C (s)	Onset (s)	Dif (s)	Term (s)	Dur (s)	Mask (%)	Mask F (1/M)
Group 10	Darwin, California (DAC) Wide-band vertical (WBZ), two gain levels												
a) CE	none										105*		
b) EQ	14 AUG 69	69.5	7722	59.2	308.9	14:19:01.6	0	30:09					
ME	..do..	1.51	168	234.8	53.9	14:30:00.04		29	20	92	63	30*	3.33*
Group 11	..do.. Wide-band radial (WBR), two gain levels												
a) CE											130*		
b) EQ	..do..						0	30:09					
ME								29	20	96	67	35*	2.86*

The wide-band instruments were installed relatively recently; no traces from suitable CE's are available. The EQ is dominated completely by the Sg phase and only partially by the Pg phase of the ME on both components of the wide-band traces.

The data are reproduced from Sanborn recorder playouts at a scale factor of 100%. (see Note 6, Table IV).

*Estimated from the short-period data given on Plate No. 3.

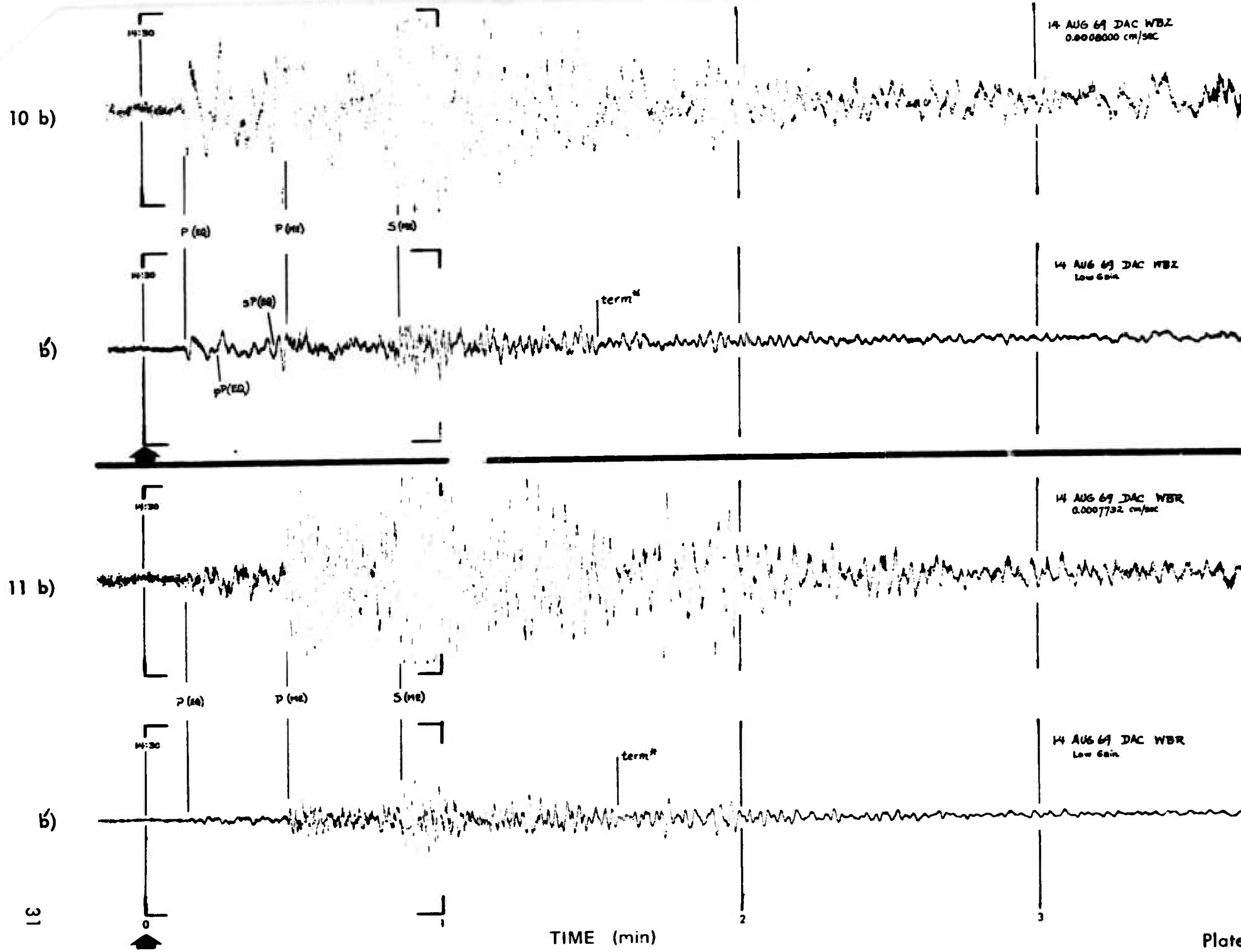
10 b)
b')
11 b)
b')
14 AUG 69 DAC WBZ
0.0008000 cm/sec
14 AUG 69 DAC WBZ
Low Gain
14 AUG 69 DAC WBR
0.0007732 cm/sec
14 AUG 69 DAC WBR
Low Gain
14:30
P (EQ)
P (ME)
S (ME)
sP(EQ)
pP(EQ)
term*
0
1
2
3
TIME (min)

Plate 4

Event	Date (GMT)	Δ (°)	Range (km)	Azm (°)	B Azm (°)	Origin (h m s)	T C (s)	Onset (s)	Dif (s)	Term (s)	Dur (s)	Mask (%)	Mask F (1/M)
Group 12	Tinemaha, California (TIN) Short-period vertical (SPZ)												
a) CE	13 SEP 63	1.72	191	267.0	85.8	13:53:00.15	0	32	28	147a 269b	115a 237b		
b) EQ	14 AUG 69	68.6	7623	58.9	308.4	14:19:01.6	05	30:04					
ME	..do..	1.73	193	267.2	85.9	14:30:00.04		33		148	115	0a 51.5b	∞a 1.94b

The Pg and Sg phases of the ME dominate the EQ. There is almost no masking of the signal characteristic of the explosion.

The data are reproduced from photographic paper originals at a scale factor of 100%. The gain of the instrument is assumed to be constant. (see Note 1, Table IV).

a. End of the motion characteristic of the explosion.
b. End of the signal.

12 a)

b)

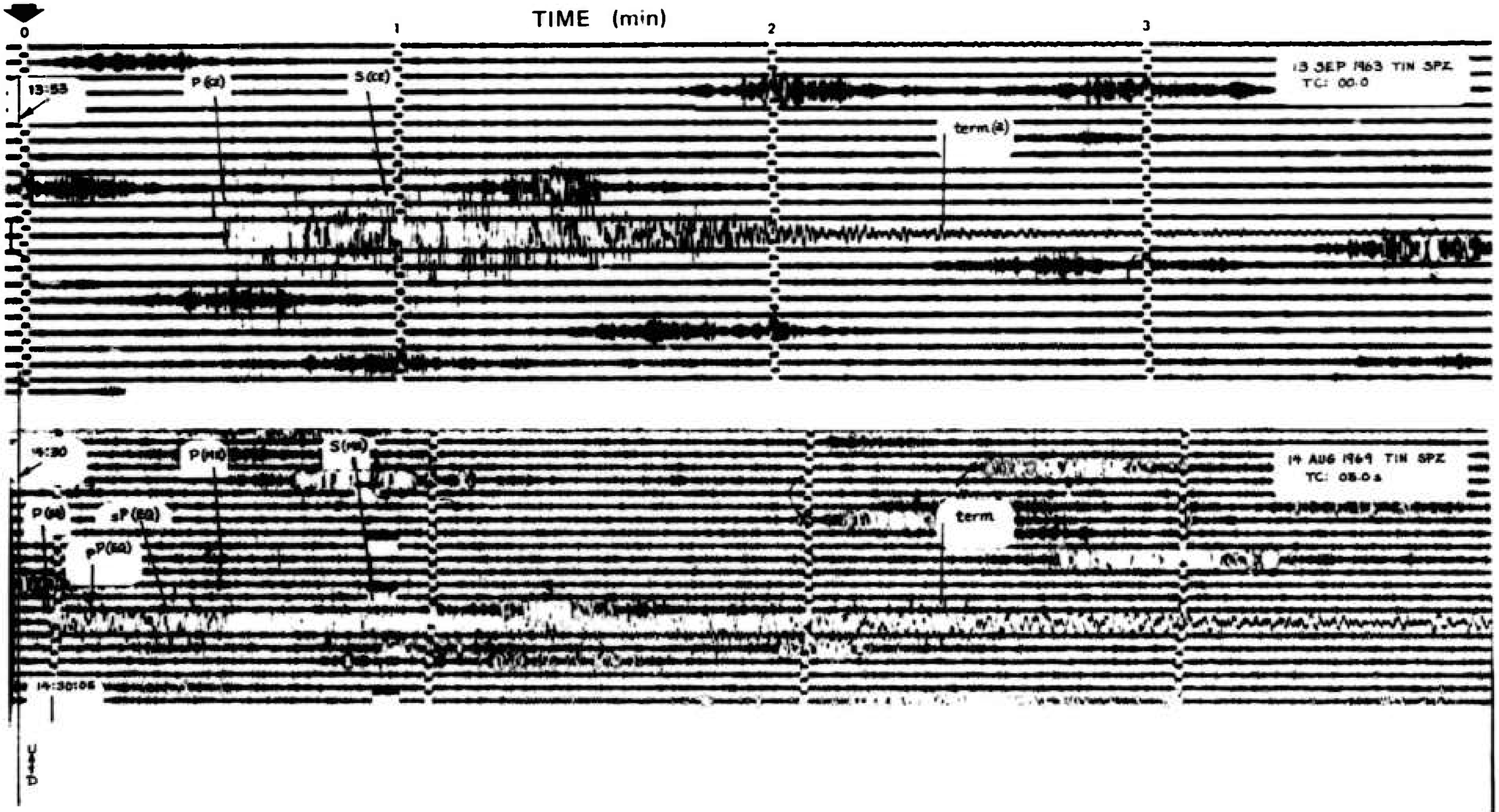
TIME (min)
0
1
2
3
13 SEP 1963 TIN SPZ
TC: 00.0
13:53
P(ct)
S(ct)
term(a)
14 AUG 1969 TIN SPZ
TC: 05.0 s
14:30
P(BB)
sP(BB)
pP(BB)
P(MD)
S(MD)
term
14:30:05
U
D

Event	Date (GMT)	Δ (°)	Range (km)	Azm (°)	B Azm (°)	Origin (h m s)	T C (s)	Onset (s)	Dif (s)	Term (s)	Dur (s)	Mask (%)	Mask F (1/M)
Group 13	Tinemaha, California (TIN)				Wood-Anderson North-South (WA NS)								
a) CE	13 SEP 63	1.72	191	267.0	85.8	13:53:00.15	0	33		128a 208b	95a 175b		
b) EQ	14 AUG 69	68.6	7623	58.9	308.4	14:19:01.6	05	30:06					
ME	..do..	1.73	193	267.2	85.9	14:30:00.04		34	28	117	83	12.6a 52.6b	7.92a 1.90b
Group 14	..do..				Wood-Anderson West-East (WA WE)								
a) CE							0	33		131a 225b	98a 192b		
b) EQ	..do..						05	30:06					
ME								34	28	118	84	14.3a 56.3b	7.00a 1.78b

The Pg and Sg phases for the ME dominate the EQ. There is only a slight masking of the signal characteristic of the explosion.

The data are reproduced from photographic paper originals at a scale factor of 100%. The magnifications of the instruments are assumed to be constant. (See Note 1, Table IV).

a. End of the motion characteristic of the explosion.
b. End of the signal.

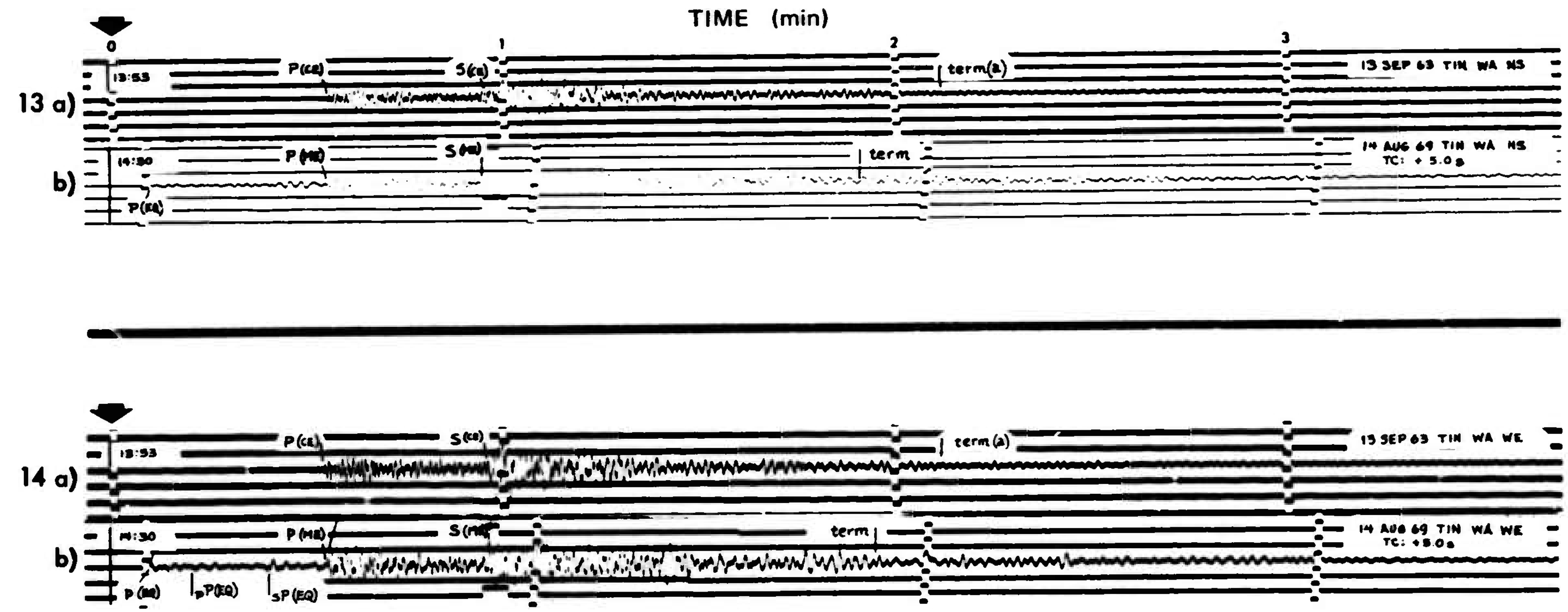
TIME (min)
0
1
2
3
13 a)
b)
14 a)
b)
13:53
14:30
P(CE)
S(CE)
term(a)
P(ME)
S(ME)
term
P(EQ)
P(ME)
pP(EQ)
sP(EQ)
13 SEP 63 TIN WA NS
14 AUG 69 TIN WA NS
TC: + 5.0 s
13 SEP 63 TIN WA WE
14 AUG 69 TIN WA WE
TC: +5.0 s

Plate 6

Plate 7

Event	Date (GMT)	Δ (°)	Range (km)	Azm (°)	B Azm (°)	Origin (h m s)	T C (s)	Onset (s)	Dif (s)	Term (s)	Dur (s)	Mask (%)	Mask F (1/M)
Group 15	Tinemaha, California (TIN)				Long-period vertical (LPZ)					142a	110a		
a) CE	13 SEP 63	1.72	191	267.0	85.8	13:53:00.15	0	32		218b	186b		
b) EQ	14 AUG 69	68.6	7623	58.9	308.4	14:19:01.6	05	30:05					
ME	..do..	1.73	193	267.2	85.9	14:30:00.04		33	28	96	63	42.7a 66.1b	2.34a 1.51b
Group 16	..do..				Long-period South-North (LP SN)					118a	84a		
a) CE							0	34		230b	196b		
b) EQ	..do..						05	30:05					
ME								37	32	73	44	47.6a 77.6b	2.10a 1.29b
Group 17	..do..				Long-period West-East (LP WE)					128a	94a		
a) CE							0	34		226b	192b		
b) EQ	..do..						05	30:05					
ME								37	32	77	48	48.9a 75.0b	2.04a 1.33b

The Pg and Sg phases of the ME are less visible than in the case of the short-period records. There is considerable masking of the tail of the explosion waveform.

The data are reproduced from photographic paper originals at a scale factor of 100%. The gains of the instruments are assumed to be constant. (See Note 2, Table IV).

a. End of the motion characteristic of the explosion.
b. End of the signal.

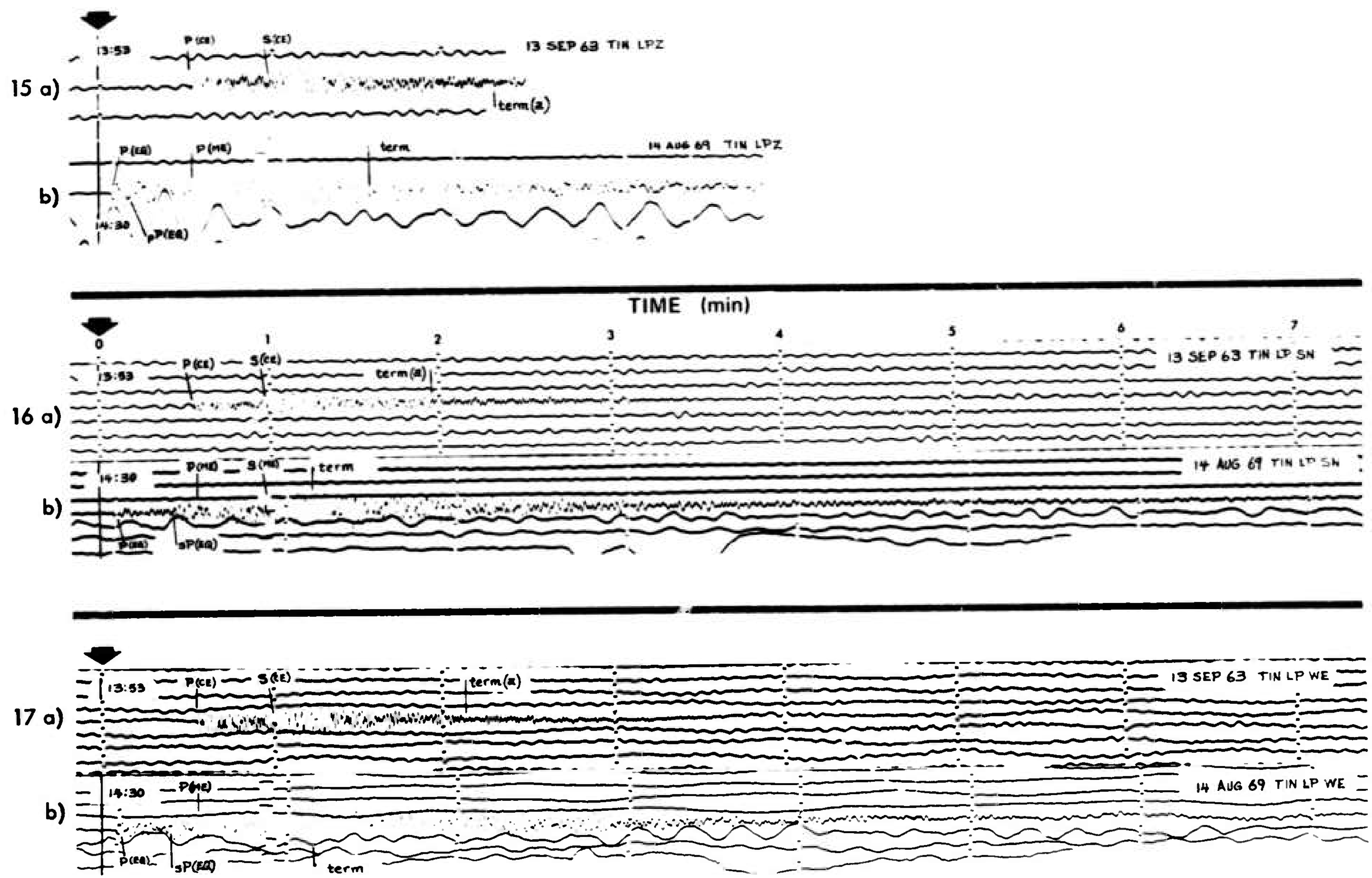
15 a)
b)
16 a)
b)
17 a)
b)
13:53
P(EE)
S(EE)
13 SEP 63 TIN LPZ
term(a)
P(EE)
P(ME)
term
14 AUG 69 TIN LPZ
14:30
pP(EQ)
TIME (min)
0
1
2
3
4
5
6
7
13 SEP 63 TIN LP SN
term(a)
14 AUG 69 TIN LP SN
sP(EQ)
13 SEP 63 TIN LP WE
14 AUG 69 TIN LP WE

Plate 7

Event	Date (GMT)	Δ (°)	Range (km)	Azm (°)	B Azm (°)	Origin (h m s)	T C (s)	Onset (s)	Dif (s)	Term (s)	Dur (s)	Mask (%)	Mask F (1/M)
Group 18	Nelson, Nevada (NEL[c]) Short-period vertical (18-300)												
b) EQ	14 AUG 69	71.6	7953	58.1	310.2	14:19:01.6	0	30:21.5					
ME	..do..	1.75	194	145.4	326.1	14:30:00.04		34	13	93	59	34*	2.90*
	*assuming CE duration of 90 s estimated from Group Nos. 19-20.												
Group 19	..do..			Short-period vertical (SPZ)						122a	88a		
a) CE	13 SEP 63	1.54	171	139.6	320.3	13:53:00.15	0	34		202b	168b		
b) EQ	14 AUG 69	71.6	7953	58.1	310.2	14:19:01.6	0	30:21.5					
	..do..	1.75	194	145.4	326.1	14:30:00.04		33.5	12	90	56	36.3a 66.7b	2.75a 1.50b
Group 19A	..do..			Short-period radial (SPR)						125a	91a		
a) CE	13 SEP 63	1.54	171	139.6	320.3	13:53:00.15	0	34		234b	200b		
Group 20	..do..			Short-period transverse (SPT)						130a	96a		
a) CE	13 SEP 63	1.54	171	139.6	320.3	13:53:00.15	0	34		203b	169b		
b) EQ	14 AUG 69	71.6	7953	58.1	310.2	14:19:01.6	0	30:23.5					
ME	..do..	1.75	194	145.4	326.1	14:30:00.04		35	12	90	55	42.7a 67.5b	2.34a 1.48b

The data for the CE were recorded at the C&GS station BCN, Boulder City, Nevada. Prior to the ME the instruments were relocated to NEL[c]; to provide comparison data the times and traces shown here have been expanded by the ratio of the distances (194 km/171 km = 1.14).

The Pg and Sg phases are visible, but there is some masking of the tail of the explosion waveform.

The data for the CE are reproduced from oscillograph playouts at a scale factor of 27.9%; those for the ME are photographed from Sanborn recorder transcriptions at a scale factor of 100%. The disparity in amplitudes between the CE and ME is due to differences in gain and recording methods. (see Notes 5 & 6, Table IV).

---

a. End of the motion characteristic of the explosion.

b. End of the signal.

c. The SPR was replaced by the 18-300

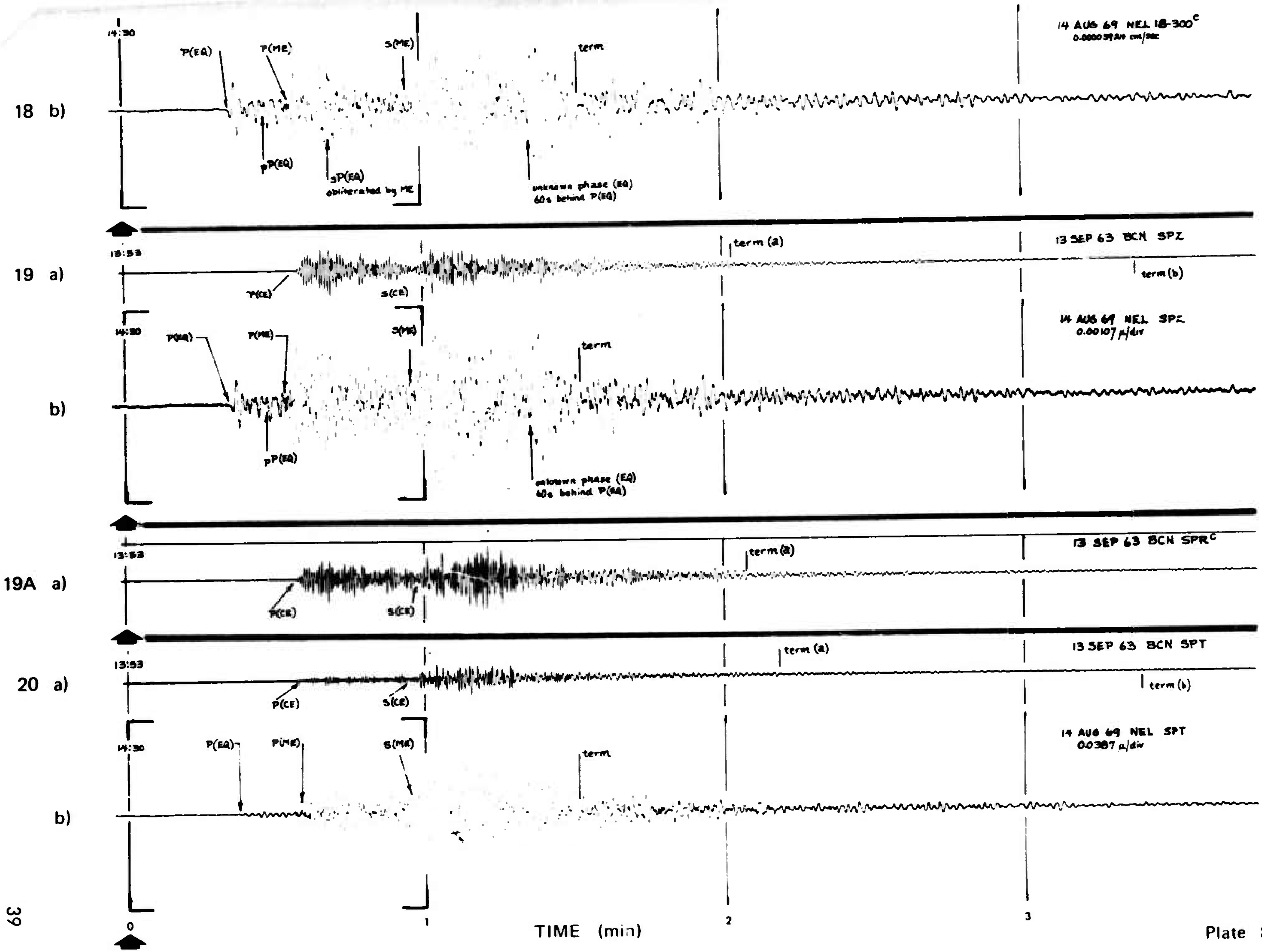

18 b)
19 a)
b)
19A a)
20 a)
b)
14:30
13:53
14 AUG 69 NEL 18-300^c
13 SEP 63 BCN SPZ
14 AUG 69 NEL SPZ
0.00107 μ/div
13 SEP 63 BCN SPR^c
13 SEP 63 BCN SPT
14 AUG 69 NEL SPT
0.0387 μ/div
P(EQ)
P(ME)
S(ME)
pP(EQ)
sP(EQ)
obliterated by ME
unknown phase (EQ)
60s behind P(EQ)
term
term (a)
term (b)
P(CE)
S(CE)
0
1
2
3
TIME (min)

Plate 8

Event	Date (GMT)	Δ (°)	Range (km)	Azm (°)	B Azm (°)	Origin (h m s)	T C (s)	Onset (s)	Dif (s)	Term (s)	Dur (s)	Mask (%)	Mask F (1/M)
Group 21	Nelson, Nevada (NEL) Wide-band vertical (WBZ), two gain levels												
a) CE	none												
b) EQ	14 AUG 69	71.6	7953	58.1	310.2	14:19:01.6	0	30:21.5					
ME	..do..	1.75	194	145.4	326.1	14:30:00.04		33.5	12	87	55	40*	2.5*
Group 22	..do.. Wide-band radial (WBR), two gain levels												
a) CE													
b) EQ	..do..						0	30:21.5					
ME								33.5	12	90	56	40*	2.5*

The Pg and Sg phases of the ME are much less visible than those for the short-period data. Only in the case of the radial instrument can one clearly recognize the explosion wave form.

The data are reproduced from Sanborn recorder playouts at a scale factor of 100%. (See Note 6, Table IV).

*estimated from the short-period data given on Plate No. 8

These wide-band instruments were installed relatively recently; no traces from suitable CE's are available.

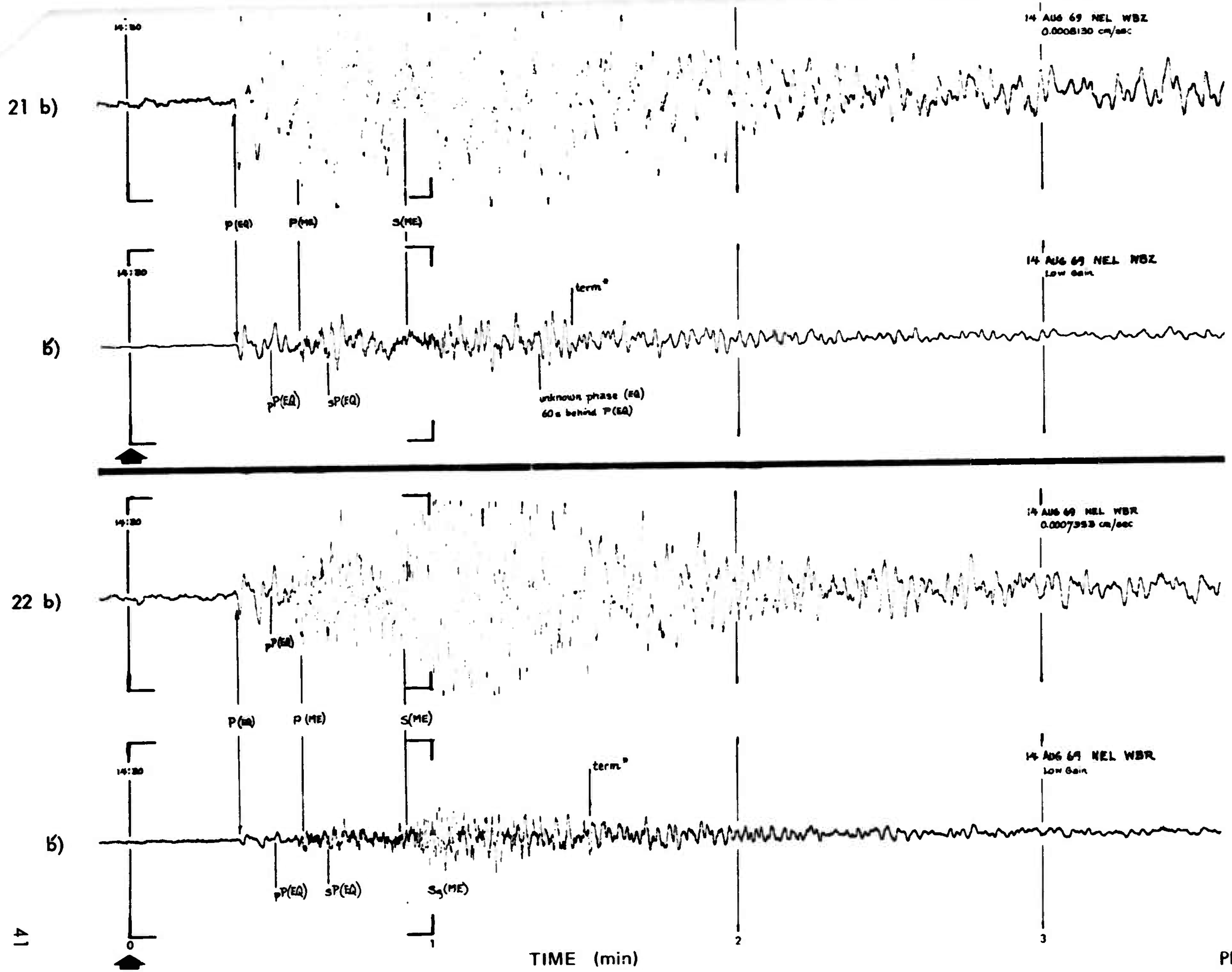
21 b)
14:30
14 AUG 69 NEL WBZ
0.0008130 cm/sec
P(EQ)
P(ME)
S(ME)
b)
14:30
14 AUG 69 NEL WBZ
Low Gain
term*
pP(EQ)
sP(EQ)
unknown phase (EQ)
60s behind P(EQ)
22 b)
14:30
14 AUG 69 NEL WBR
0.0007353 cm/sec
pP(EQ)
P(EQ)
P (ME)
S(ME)
b)
14:30
14 AUG 69 NEL WBR
Low Gain
term*
pP(EQ)
sP(EQ)
S_g(ME)
0
1
2
3
TIME (min)

Plate 9

Event	Date (GMT)	Δ (°)	Range (km)	Azm (°)	B Azm (°)	Origin (h m s)	T C (s)	Onset (s)	Dif (s)	Term (s)	Dur (s)	Mask (%)	Mask F (1/M)
Group 23	China Lake, California (CLC) Short-period vertical (SPZ)												
a) CE	13 SEP 63	1.82	202	222.7	41.8	13:53:00.15	-24.6	32.4		129a 275b	96a 242b		
b) EQ	14 AUG 69	69.8	7754	59.5	309.0	14:19:01.6	08.1	30:11					
ME	..do..	1.82	203	223.1	42.2	14:30:00.04		33	22	123	90	6.3a 62.8b	16a 1.59b

The Pg and Sg phases for the ME are clearly recognizable. There is a slight masking of the latter portion of the explosion waveform.

The data are reproduced from photographic paper originals at a scale factor of 100%. The magnification of the instrument is assumed to be constant. (See Note 1, Table IV).

---

a. End of the motion characteristic of the explosion.
b. End of the signal.

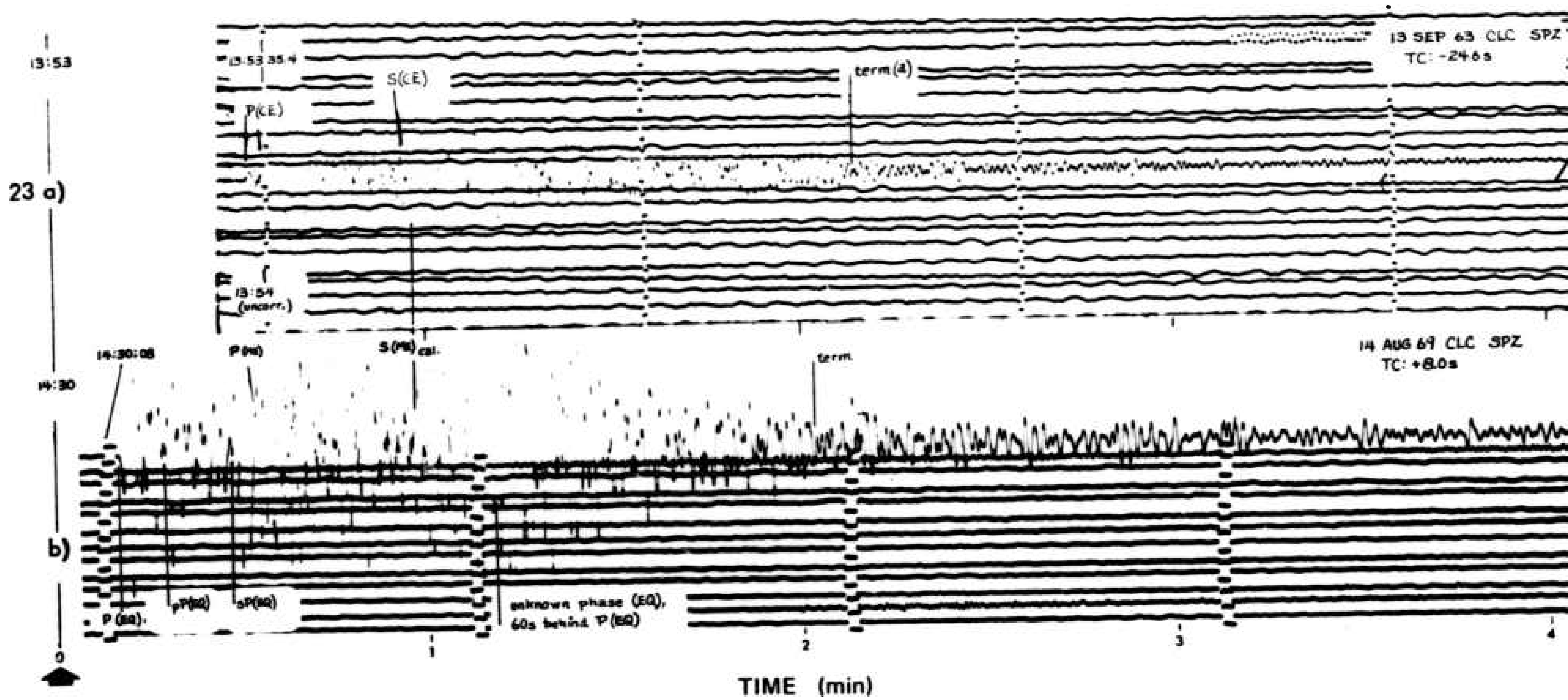
13:53
23 a)
13:53:35.4
P(CE)
S(CE)
term(d)
13 SEP 63 CLC SPZ
TC: -24.6s
13:54
(uncorr.)
14:30
14:30:08
P (MI)
S (MI)
cal.
term.
14 AUG 69 CLC SPZ
TC: +8.0s
b)
P (EQ).
pP(EQ)
sP(EQ)
unknown phase (EQ),
60s behind P(EQ)
0
1
2
3
4
TIME (min)

Plate 10

Event	Date (GMT)	Δ (°)	Range (km)	Azm (°)	B Azm (°)	Origin (h m s)	T C (s)	Onset (s)	Dif (s)	Term (s)	Dur (s)	Mask (%)	Mask F (1/M)
Group 24	Goldstone, California (GSC)				Short-period vertical (SPZ)								
a) CE	13 SEP 63	1.95	217	197.7	17.3	13:53:00.15	0	35		205a 287b	170a 252b		
b) EQ +, *	14 AUG 69	70.6	7845	59.5	309.5	14:19:01.6	0	30:16					
ME	..do..	1.95	217	198.1	17.7	14:30:00.04		35	19	160	125	26.5a 50.4b	3.77a 1.98b

The Pg and Sg phases are visible for the ME, but at this range the masking of the tail of the explosion waveform begins to appear as a high frequency modulation of the teleseism.

The trace b+ for the ME is reproduced from the original inked pen record. The remaining two traces are reproduced from the best archive copies available. The scale factor in all cases is 100%.

The 90-second portion of the CE trace beginning at 13:53 contains the ends of the record; the best copy available from archives is light-damaged for this interval and a hand tracing has been inserted in the print used in this report. The magnification of the instrument is assumed to be constant. (see Notes 1 & 4, Table IV).

\+ Recorded by telemetry at Pasadena, California, using an inked pen.
* Recorded photographically at Goldstone, California.

a. End of the motion characteristic of the explosion.
b. End of the signal.

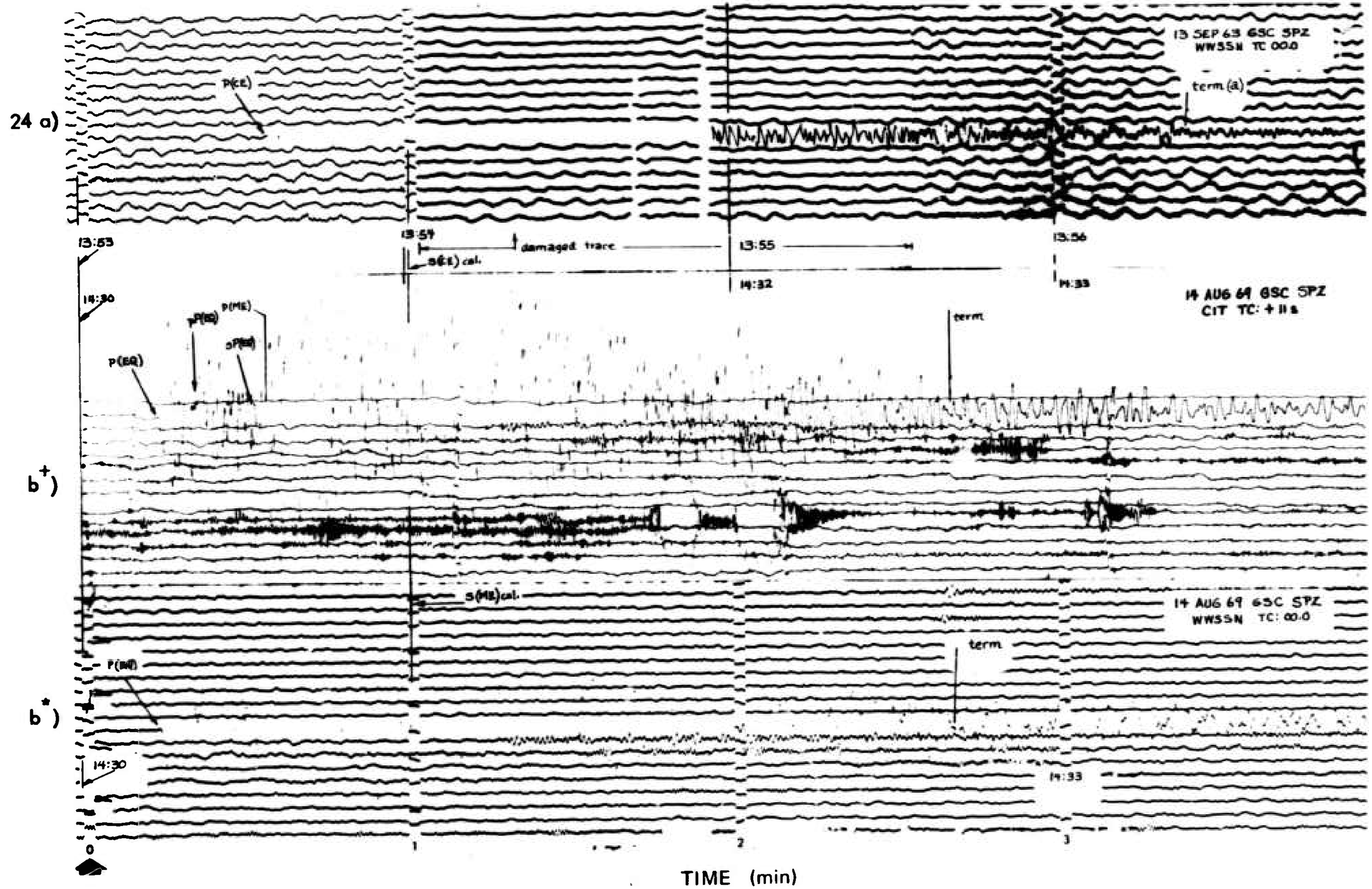

24 a)
b⁺)
b*)
13 SEP 63 GSC SPZ
WWSSN TC 00.0
term (a)
P(CE)
13:53
13:54
13:55
13:56
damaged trace
S(CE) cal.
14:30
14:32
14:33
14 AUG 69 GSC SPZ
CIT TC: + 11 s
term
P(EQ)
pP(EQ)
P(ME)
sP(EQ)
S(ME) cal.
14 AUG 69 GSC SPZ
WWSSN TC: 00.0
P(ME)
0
1
2
3
TIME (min)

Plate 11

Event	Date (GMT)	Δ (°)	Range (km)	Azm (°)	B Azm (°)	Origin (h m s)	T C (s)	Onset (s)	Dif (s)	Term (s)	Dur (s)	Mask (%)	Mask F (1/M)
Group 25	Mina, Nevada (MN-NV)			Short-period vertical (SPZ)									
a) CE	13 SEP 63	2.07	230	308.4	127.2	13:53:00.15	0	37		177a 440b	140a 403b		
b) EQ	14 AUG 69	67.8	7534	57.7	308.0	14:19:01.6	0	29:58.4					
ME	..do..	2.09	232	308.1	126.8	14:30:00.04		37	38.6	137	100	28.6a 75.2b	3.5a 1.33b

Prior to the ME the station MN-NV was withdrawn from service. The trace shown here was recorded by telemetry at the University of California, Berkeley, from a wide-band seismograph located at the adjacent station MINA. The signal has been filtered electronically to simulate the short-period response of the Benioff instrument.

The Pg and Sg phases for the ME are still visible even though the record is clipped. The record for the CE is also clipped.

The trace for the CE is reproduced from the best archive copy available of the 35 mm film original at a scale factor of 402%: that for the ME is reproduced from the original hot-wire stylus record at a scale factor of 100%. The disparity in amplitudes between the CE and ME is due to differences in gain and instruments. (see Notes 4 & 7, Table IV).

a. End of the motion characteristic of the explosion.
b. End of the signal.

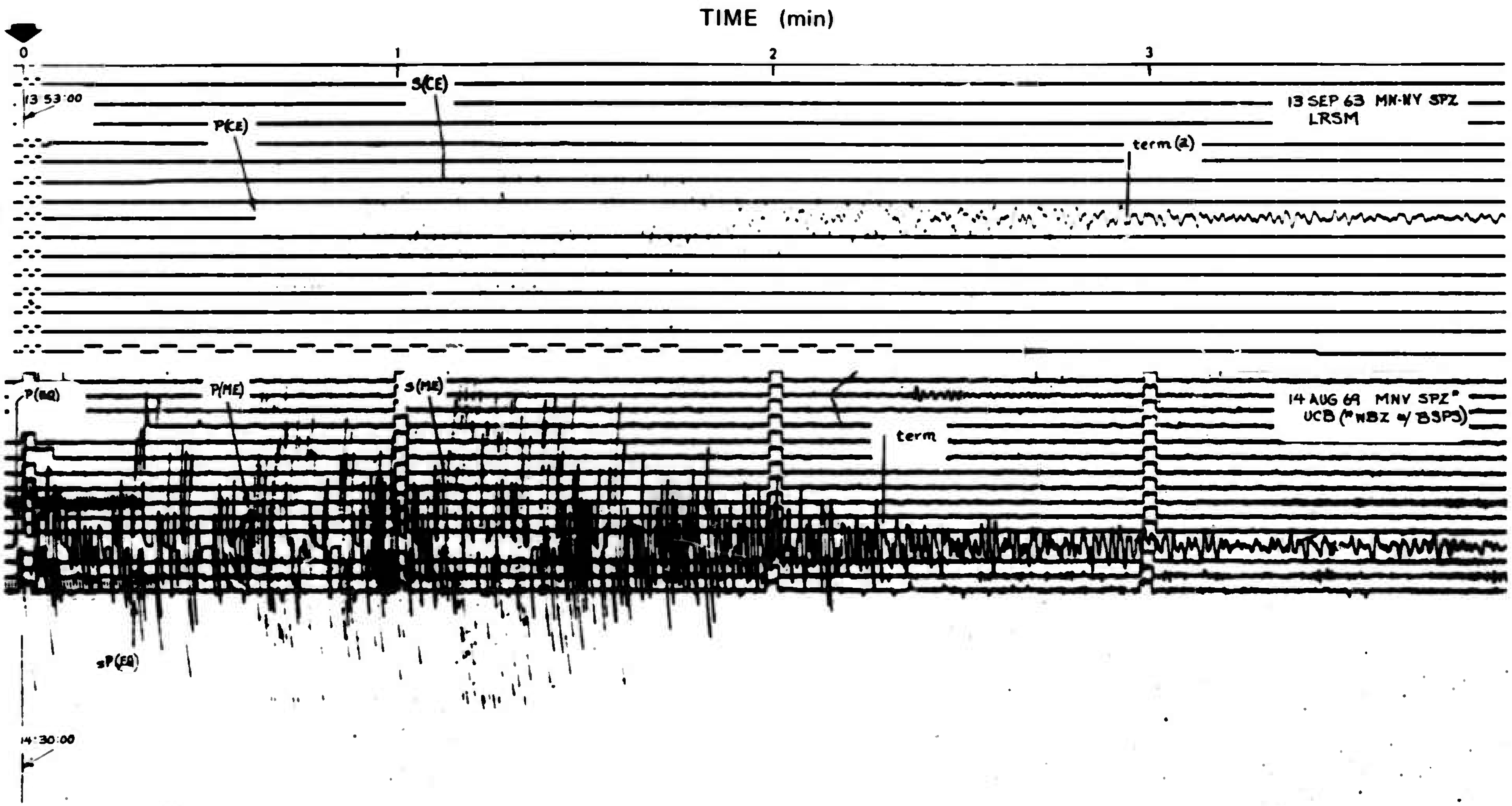

25 a)
b)

Plate 12

Event	Date (GMT)	Δ (°)	Range (km)	Azm (°)	B Azm (°)	Origin (h m s)	T C (s)	Onset (s)	Dif (s)	Term (s)	Dur (s)	Mask (%)	Mask F (1/M)
Group 26	Leeds, Utah (LEE)			Short-period vertical (SPZ)						170a	133a		
a) CE	13 SEP 63	2.16	240	87.1	268.7	13:53:00.15	0	37.2		257b	220b		
b) EQ	14 AUG 69	71.5	7943	56.1	310.4	14:19:01.6	0	30:21.5					
ME	..do..	2.15	239	87.0	268.6	14:30:00.04		37.6	16	138	100	24.8a 54.5b	4.03a 1.83b
Group 27	..do..			Short-period radial (SPR)						170a	133a		
a) CE	13 SEP 63	2.16	240	87.1	268.7	13:53:00.15	0	37.2		250b	213b		
b) EQ	none[c]												
ME	..do..												
Group 28	..do..			Short-period transverse (SPT)						170a	133a		
a) CE	13 SEP 63	2.16	240	87.1	268.7	13:53:00.15	0	37.2		314b	277b		
b) EQ	14 AUG 69	71.5	7943	56.1	310.4	14:19:01.1	0	30:22					
ME	..do..	2.15	239	87.0	268.6	14:30:00.04		38	16	128	90	32.3a 67.5b	3.09a 1.48b

The Pg and Sg phases for the ME are visible, but the later portions of the explosion waveforms are masked. The radial and transverse for the CE components (Traces 27a and 28a) are clipped.

The data for the CE are reproduced from oscillograph playouts at a scale factor of 24.6%; those for the ME are reproduced from Sanborn recorder transcriptions at a scale factor of 100%. The disparities in amplitudes between the CE and ME are due to the changes in recording methods. (see Notes 5 & 6, Table IV).

a. End of the motion characteristic of the explosion.
b. End of the signal.
c. Withdrawn from service prior to the ME.

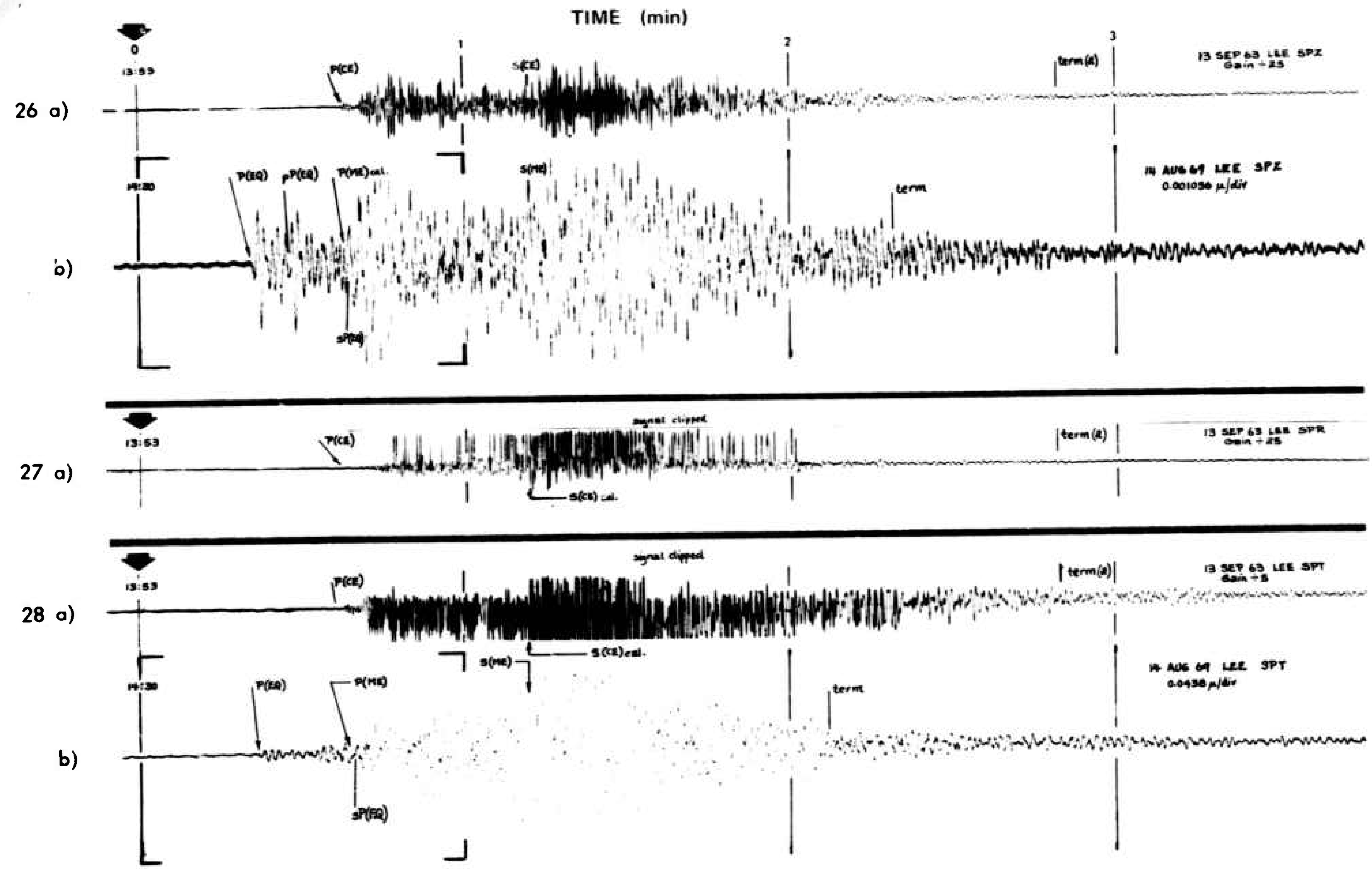
TIME (min)
0
1
2
3
13:53
P(CE)
S(CE)
term(d)
13 SEP 63 LEE SPZ
Gain ÷ 25
26 a)
14:30
P(EQ)
pP(EQ)
P(ME)cal.
sP(EQ)
S(ME)
term
14 AUG 69 LEE SPZ
0.001036 μ/div
b)
13:53
P(CE)
signal clipped
S(CE) cal.
term(d)
13 SEP 63 LEE SPR
Gain ÷ 25
27 a)
13:53
P(CE)
signal clipped
S(CE) cal.
term(d)
13 SEP 63 LEE SPT
Gain ÷ 5
28 a)
14:30
P(EQ)
P(ME)
sP(EQ)
S(ME)
term
14 AUG 69 LEE SPT
0.0438 μ/div
b)

Plate 13

Event	Date (GMT)	Δ (°)	Range (km)	Azm (°)	B Azm (°)	Origin (h m s)	T C (s)	Onset (s)	Dif (s)	Term (s)	Dur (s)	Mask (%)	Mask F (1/M)
Group 29	Leeds, Utah (LEE)		Short-period vertical (18-300)										
a) CE	none									130*	130*		
b) EQ	14 AUG 69	71.5	7943	56.1	310.4	14:19:01.6	0	30:21					
ME	..do..	2.15	239	87.0	268.6	14:30:00.04		38	17	130	92	30*	3.33*
Group 30	..do..		Wide-band radial (WBR)										
a) CE													
b) EQ	..do..							30:21					
ME								38	17	130	92		

The Pg and Sg phases are visible for the short-period record (Trace 29b) which should be compared with the short-period vertical record (Trace 26b) from the Benioff seismograph. In contrast, the wide-band radial record (Trace 30b) does not show the peak Pg and Sg phases well and there is only slight evidence of the high-frequency signal due to the ME.

The data are reproduced from Sanborn recorder playouts at a scale factor of 100%. (see Note 6, Table IV).

* Estimated from the short-period data given on Plate No. 13.

These instruments were installed relatively recently; no traces from suitable CE's are available.

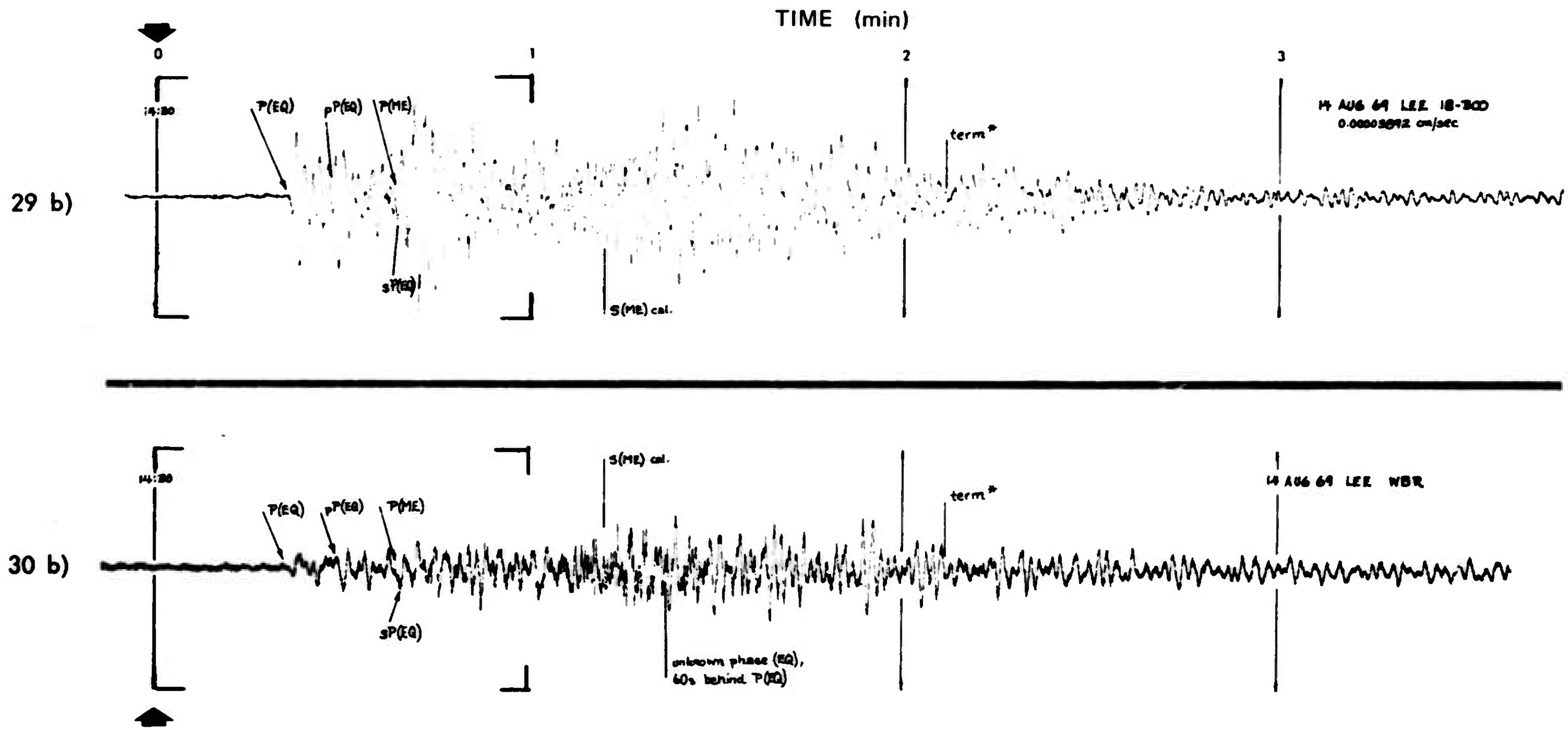
TIME (min)
0
1
2
3
29 b)
14:20
P(EQ)
pP(EQ)
P(ME)
sP(EQ)
S(ME) cal.
term*
14 AUG 69 LEE 18-300
30 b)
14:20
P(EQ)
pP(EQ)
P(ME)
sP(EQ)
S(ME) cal.
unknown phase (EQ),
60s behind P(EQ)
term*
14 AUG 69 LEE WBR

Plate 14

Event	Date (GMT)	Δ (°)	Range (km)	Azm (°)	B Azm (°)	Origin (h m s)	T C (s)	Onset (s)	Dif (s)	Term (s)	Dur (s)	Mask (%)	Mask F (1/M)
Group 31	Ely, Nevada (ELY) Short-period vertical (18-300)												
a) CE	none												
b) EQ	14 AUG 69	69.4	7707	55.4	309.2	14:19:01.6	0	30:08					
ME	..do..	2.17	242	24.8	205.5	14:30:00.04		40.5	32	93	52		
Group 32	..do.. Wide-band vertical (WBZ)												
a) CE													
b) EQ	..do..						0	30:08					
ME								41	33	123	82		
Group 33	..do.. Wide-band radial (WBR)												
a) CE													
b) EQ	..do..						0	30:08					
ME								41	33	128	87		

This station was installed relatively recently; no traces from suitable CE's are available.

The short-period record (Trace 31b) does not show clearly the Pg and Sg phases, although some high-frequency signal is present at the times of their peak amplitudes. In the case of the wide-band data, the radial record (Trace 33b) shows the Pg and Sg phases more clearly than the vertical record (Trace 32b).

The data are reproduced from Sanborn recorder playouts at a scale factor of 100%. (see Note 6, Table IV).

31 b)

32 b)

33 b)

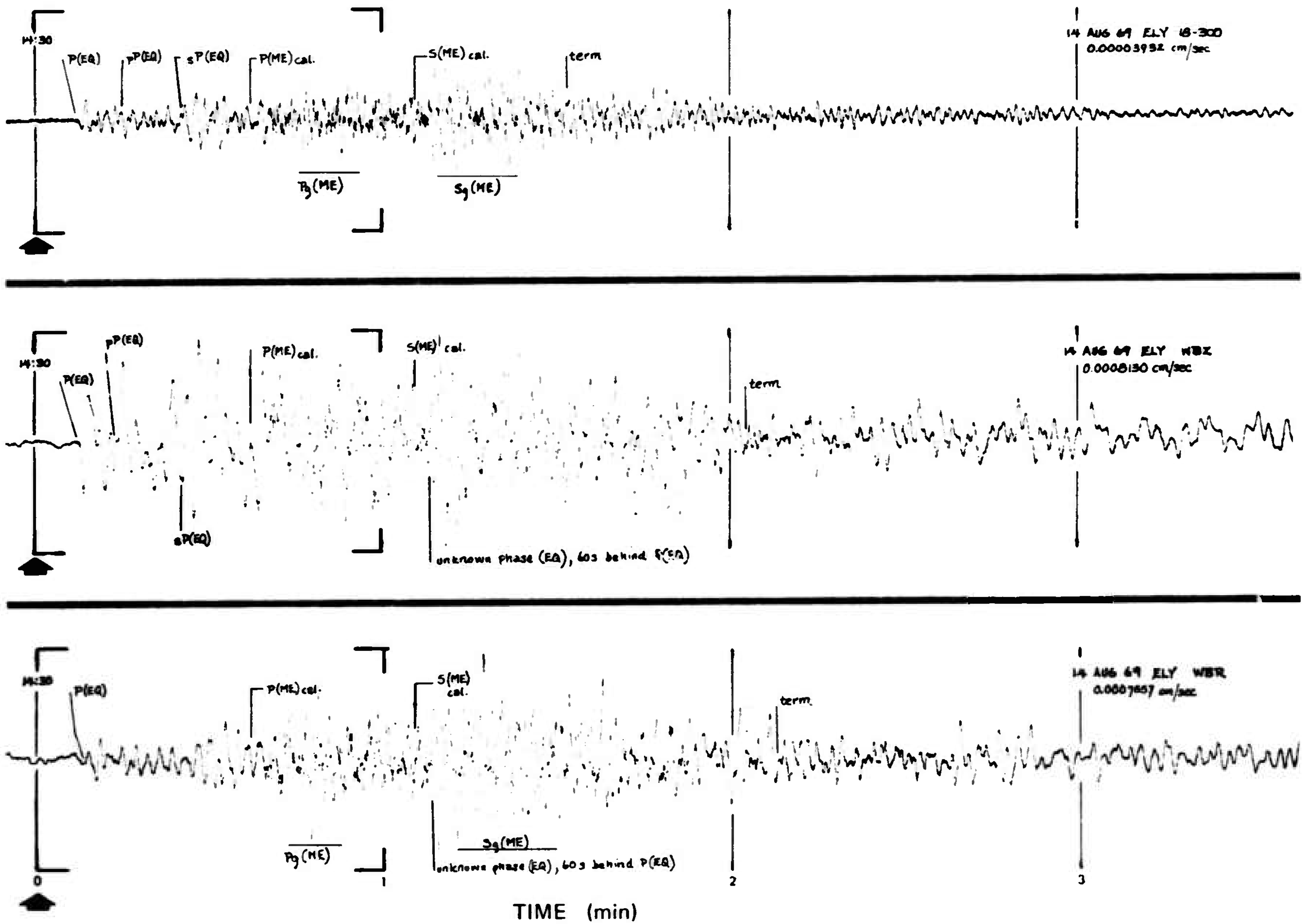

Plate 15

Event	Date (GMT)	Δ (°)	Range (km)	Azm (°)	B Azm (°)	Origin (h m s)	T C (s)	Onset (s)	Dif (s)	Term (s)	Dur (s)	Mask (%)	Mask F (1/M)
Group 34	Eureka, Nevada (EUR) Short-period vertical (SPZ)												
a) CE	11 JUN 64	2.33	259	2.0	182.1	16:45:00.15	-27.5	40	37	277	237		
b) EQ	14 AUG 69	68.5	7610	55.6	308.6	14:19:01.6	0	30:03					
ME	..do..	2.32	258	1.8	181.9	14:30:00.04		*	37**	*	*		

Due to the poor quality of the copy available, only the onset times and the later portion of the waveform for the CE are discernible. Although some peaks are visible for the ME (Trace 34b), their relation to the signal cannot be determined clearly.

The data are reproduced from the best archive copies available at a scale factor of 100%. The magnification of the instrument is assumed to be constant for both records. (see Note 11, Table IV).

The trace from the primary CE of 13 September 1963 is unavailable; it is replaced by the record from the explosion of 11 June 1964 (ACE).

* Not visible.
** Estimated value.

34 a)

b)

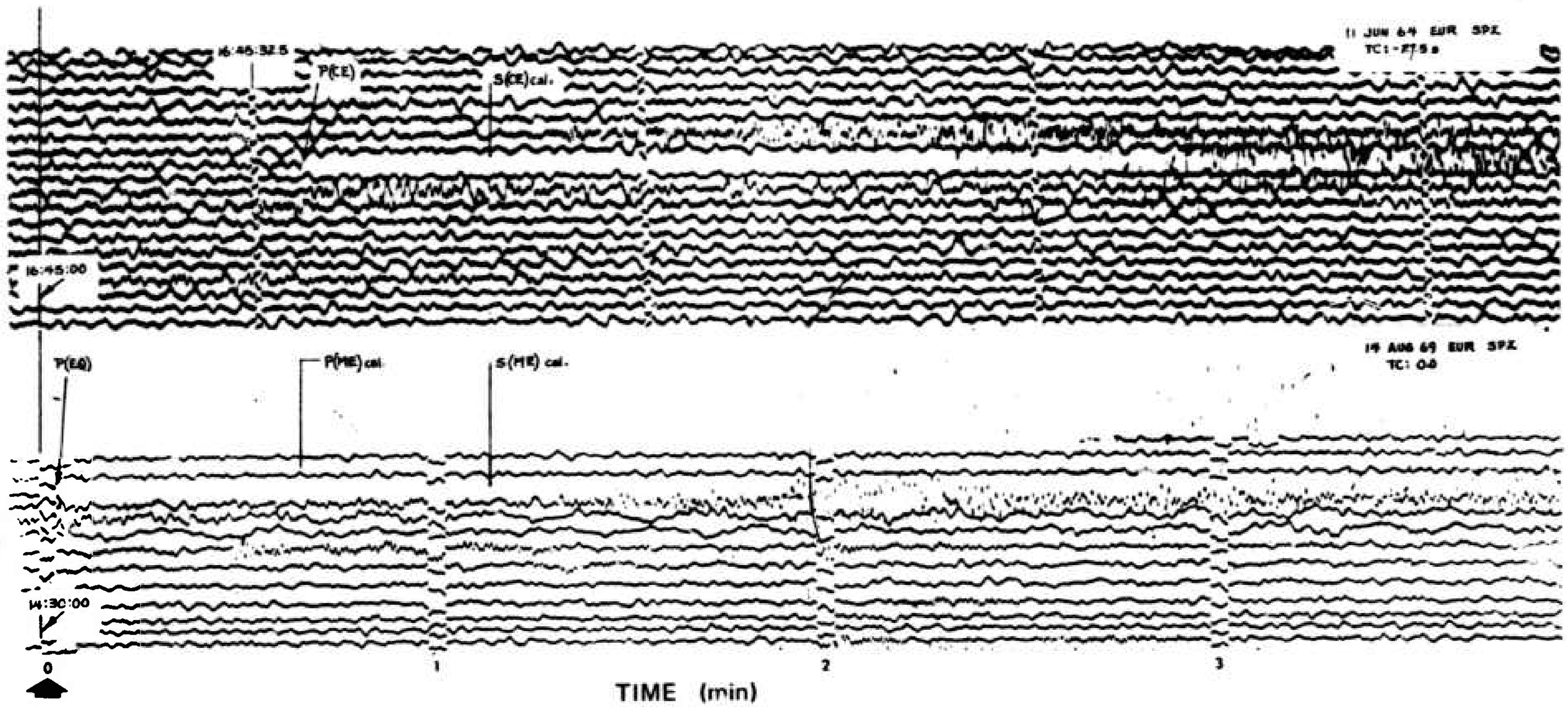

Plate 16

Event	Date (GMT)	Δ (°)	Range (km)	Azm (°)	B Azm (°)	Origin (h m s)	T C (s)	Onset (s)	Dif (s)	Term (s)	Dur (s)	Mask (%)	Mask F (1/M)
Group 35	Isabella, California (ISA) Short-period vertical (SPZ)												
a) CE	none												
b) EQ	14 AUG 69	69.3	7702	60.2	308.8	14:19:01.6	1i	30:07					
ME	..do..	2.45	273	233.2	51.8	14:30:00.04		42	35	105	63		

The Pg and Sg phases of the ME are clearly visible. The Pn phase of the ME is discernible at this epicentral distance from the explosion; it persists due to its timing with respect to the teleseism. Traces for the CE are omitted because no suitable records could be found.

The trace is reproduced at a scale factor of 100% from the original drum record which was transcribed by an inked pen. (see Note 3, Table IV).

35 b)

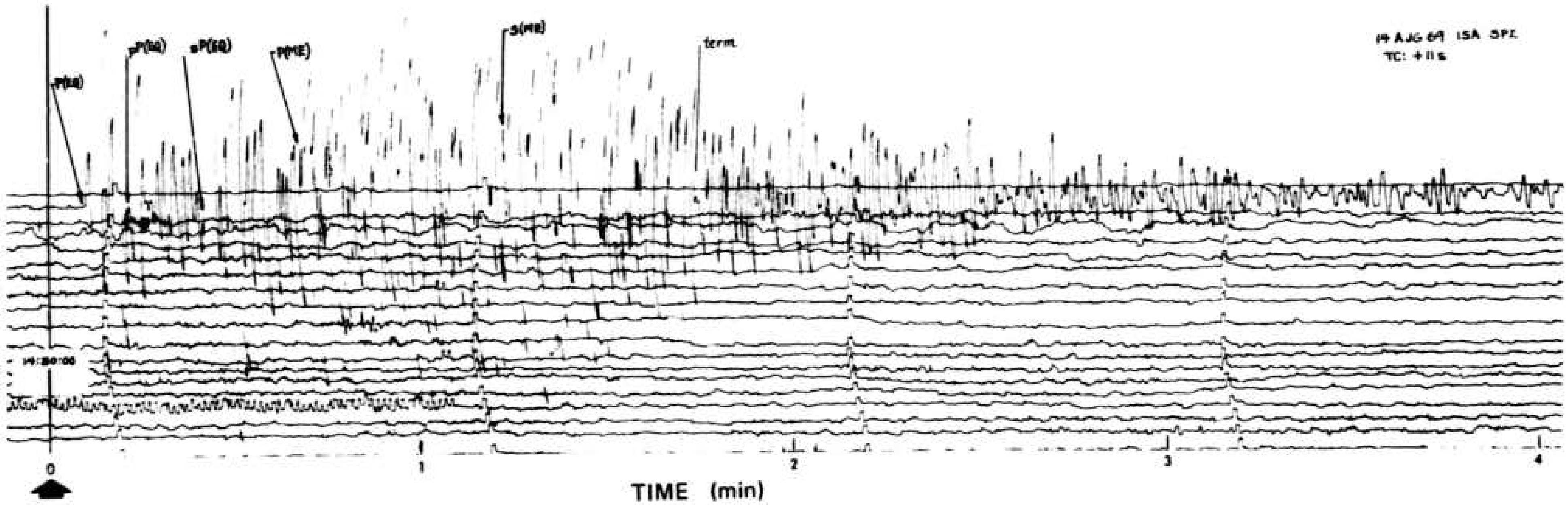
P(EQ)
pP(EQ)
sP(EQ)
P(ME)
S(ME)
term
14 AUG 69 ISA SPZ
TC: +11 s
0
1
2
3
4
TIME (min)

Plate 17

Event	Date (GMT)	Δ (°)	Range (km)	Azm (°)	B Azm (°)	Origin (h m s)	T C (s)	Onset (s)	Dif (s)	Term (s)	Dur (s)	Mask (%)	Mask F (1/M)
Group 36	Kanab, Utah (KN-UT) Short-period vertical (SPZ)												
a) CE	13 SEP 63	2.60	290	92.1	274.1	13:53:00.15	0	42.5		210a 480b	177a 437b		
b) EQ	14 AUG 69	72.0	7996	56.0	310.7	14:19:01.6	0	30:24.5					
ME	..do..	2.59	288	92.1	274.0	14:30:00.04		42.5	18	180	137	22.5a 68.6b	4.43a 1.46b

Of the three phases shown by the CE, only two (the Pg and Sg phases) of the ME are identifiable. The arrival of the sP phase of the teleseism (approximately 20 seconds after the main P-phase) masks the Pn phase from the ME. The portions of the traces beyond 140 seconds show some similarity between the CE and ME.

The data are reproduced from the best archive copies available of the 35 mm film originals at a scale factor of 402%. The gain of the instrument for both traces is assumed to be the same. (see Note 4, Table IV).

a. End of the motion characteristic of the explosion.
b. End of the signal.

36 a)

b)

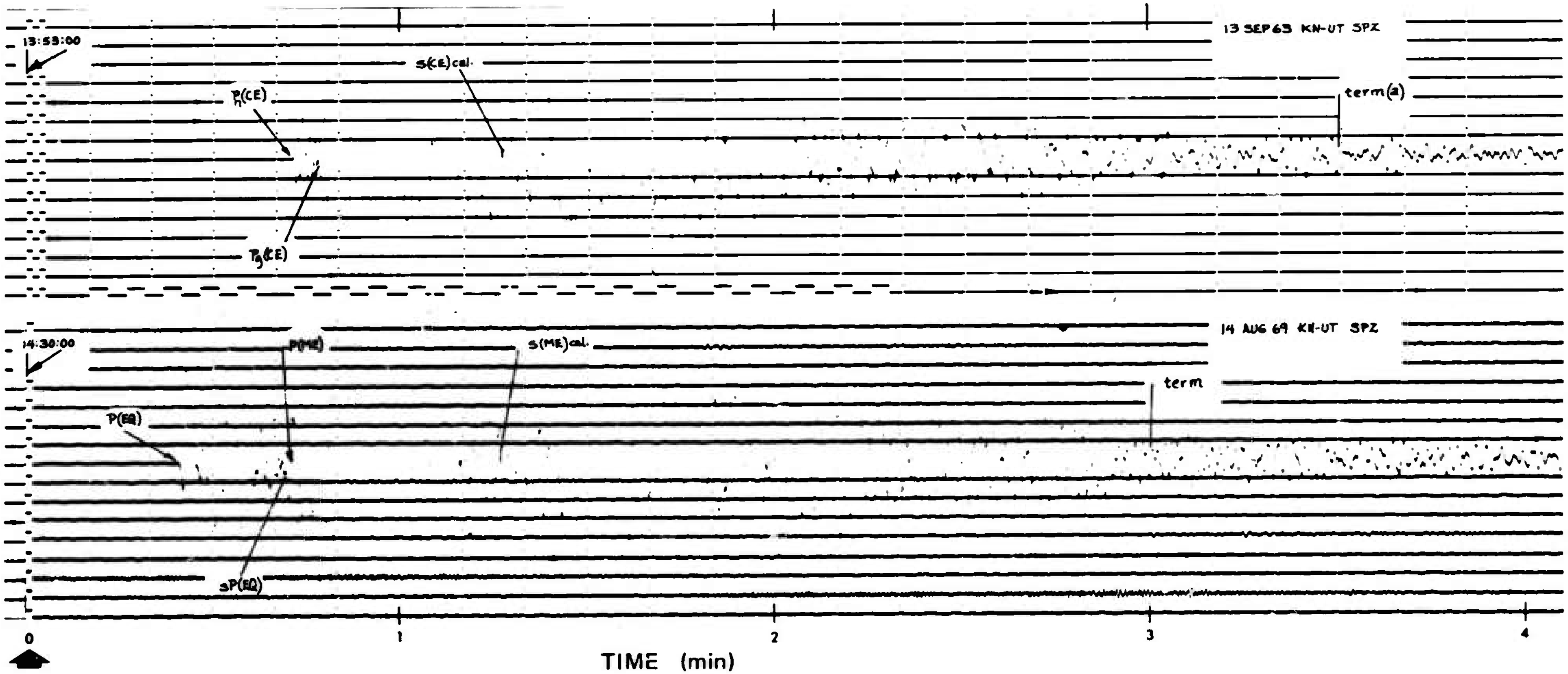

Plate 18

Event	Date (GMT)	Δ (°)	Range (km)	Azm (°)	B Azm (°)	Origin (h m s)	T C (s)	Onset (s)	Dif (s)	Term (s)	Dur (s)	Mask (%)	Mask F (1/M)
Group 37	Woody, California (WDY)			Short-period vertical (SPZ)									
a) CE	13 SEP 63	2.66	296	237.6	55.9	13:53:00.15	22.5	44.5		150a 279b	105a 234b		
b) EQ	14 AUG 69	69.1	7674	60.3	308.6	14:19:01.6	30.0	30:05					
ME	..do..	2.67	297	237.8	56.2	14:30:00.04		45*	40	108*	63*	40a 73.1b	2.5a 1.37b

The only suggestion for the ME is a very weak high-frequency modulation of the teleseism after the table value (49.5 seconds) for the arrival time of the Pg phase. No peak amplitudes for the ME are discernible.

The data are reproduced from the photographic paper originals at a scale factor of 100%. The magnification of the instrument is assumed to be equal for both traces. (see Note 1, Table IV).

---

a. End of the motion characteristic of the explosion.
b. End of the signal.
* Values estimated from the high-frequency signal attributed to the ME.

37 a)

b)

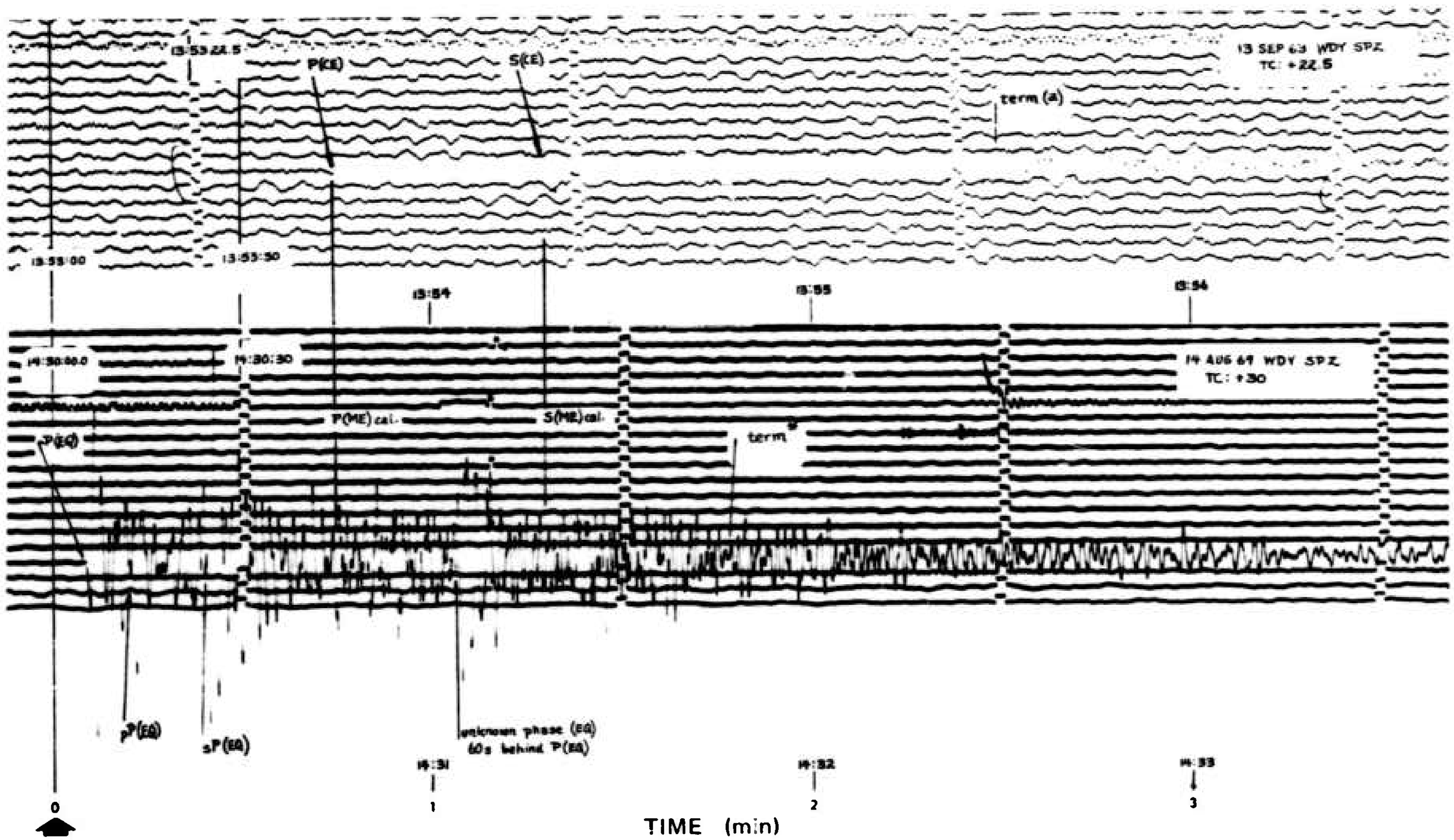

Plate 19

Event	Date (GMT)	Δ (°)	Range (km)	Azm (°)	B Azm (°)	Origin (h m s)	T C (s)	Onset (s)	Dif (s)	Term (s)	Dur (s)	Mask (%)	Mask F (1/M)
Group 38	Fort Tejon, California (FTC) Short-period vertical (SPZ)												
a) CE	13 SEP 63	3.23	360	225.8	44.1	13:53:00.15	0.9	54		180	116		
b) EQ	14 AUG 69	69.5	7728	61.0	308.8	14:19:01.6	-9.5	30:09.5					
ME	..do..	3.24	360	226.0	44.3	14:30:00.04		55*	45	135*	80*	31.0	3.22
Group 39	Riverside, California (RVR) Short-period vertical (SPZ)												
a) CE	13 SEP 63	3.33	371	198.8	18.1	13:53:00.15	-23.6	54.7		170a 221b	115a 166b		
b) EQ	14 AUG 69	71.1	7897	60.9	309.6	14:19:01.6	-26.0	30:19					
ME	..do..	3.34	371	199.1	18.3	14:30:00.04		55*	36	155*	100*	13.0a 39.8b	7.67a 2.52b
Group 40	Mount Wilson, California (MWC) Short-period vertical (SPZ)												
a) CE	13 SEP 63	3.35	372	209.3	28.2	13:53:00.14	14.7	55		215	160		
b) EQ	14 AUG 69	70.5	7833	61.1	309.3	14:19:01.6	-4.0	30:15					
ME	..do..	3.35	373	209.6	28.4	14:30:00.04		55*	40	150*	35*	40.6	2.46

The only suggestion for the ME at all three stations is a very weak high-frequency modulation of the teleseism at the times for the peak amplitudes of the CE. No phases of the ME are identifiable.

The data are reproduced from the photographic paper originals at a scale factor of 100%. The magnification of each instrument is assumed to be equal for each pair of traces. (see Note 1, Table IV).

a. End of the motion characteristic of the explosion.
b. End of the signal.
* Values estimated from the high-frequency signal attributed to the ME.

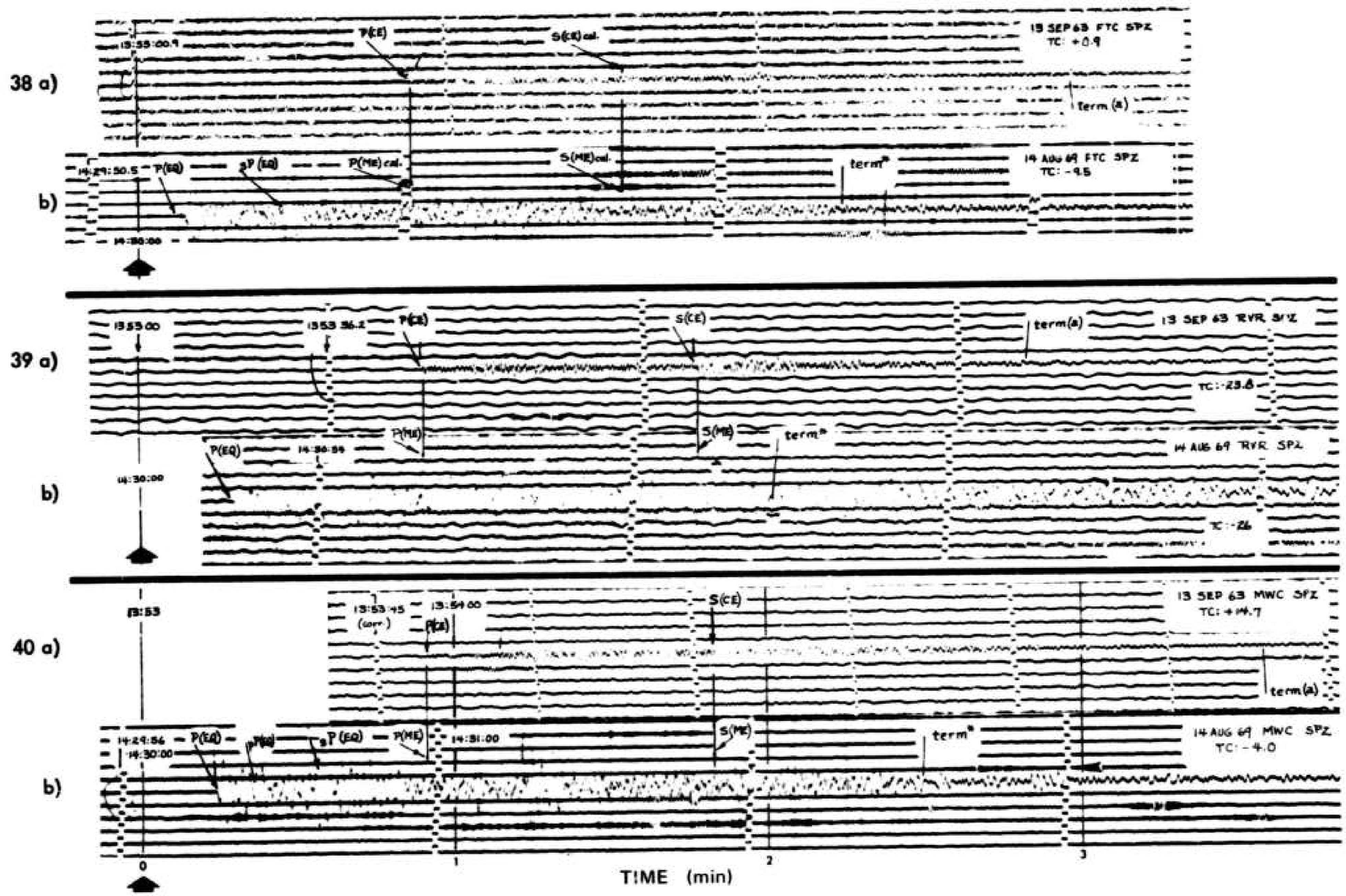

38 a)
b)
13:55:00.9
P(CE)
S(CE) cal.
13 SEP 63 FTC SPZ
TC: +0.9
term (a)
14:29:50.5
P(EQ)
sP (EQ)
P(ME) cal.
S(ME) cal.
term*
14 AUG 69 FTC SPZ
TC: -9.5
14:30:00
39 a)
b)
13:53:00
13:53 36.2
P(CE)
S(CE)
term(a)
13 SEP 63 RVR SPZ
TC: -23.8
P(EQ)
14:30:54
P(ME)
S(ME)
term*
14 AUG 69 RVR SPZ
14:30:00
TC: -26
40 a)
b)
13:53
13:53:45
(corr)
13:54:00
P(CE)
S(CE)
13 SEP 63 MWC SPZ
TC: +14.7
term(a)
14:29:56
14:30:00
P(EQ)
sP (EQ)
P(ME)
14:31:00
S(ME)
term*
14 AUG 69 MWC SPZ
TC: -4.0
0
1
2
3
TIME (min)

Plate 20

Event	Date (GMT)	Δ (°)	Range (km)	Azm (°)	B Azm ( )	Origin (h m s)	T C (s)	Onset (s)	Dif (s)	Term (s)	Dur (s)	Mask (%)	Mask F (1/M)
Group 41	Battle Mountain, Nevada (BMN) Short-period vertical (18-300)												
a) CE	none												
b) EQ	14 AUG 69	67.2	7461	55.5	307.8	14:19:01.6	0	29:54.3					
ME	..do..	3.39	377	344.9	164.2	14:30:00.04		64*		124*	60*		
Group 42	..do.. Wide-band vertical (WBZ)												
a) CE													
b) EQ	..do..						0	29:54.3					
ME								65*		124*	59*		
Group 43	..do.. Wide-band radial (WBR)												
a) CE													
b) EQ	..do..						0	29:54.3					
ME								63*		124*	61*		

This station was installed relatively recently; no traces from suitable CE's are available.

All three records show a high-frequency modulation of the teleseism at the times of the peak amplitudes for the Pg and Sg phases. The most modulation is shown by the short-period component (Trace 41b). Of the wide-band records the vertical component (Trace 42b) shows the least signal attributable to the ME, while the horizontal component (Trace 43b) displays the Sg phase most clearly.

The data are reproduced from Sanborn recorder playouts at a scale factor of 100%. (see Note 6, Table IV).

* Values estimated from the high-frequency modulation attributed to the ME.

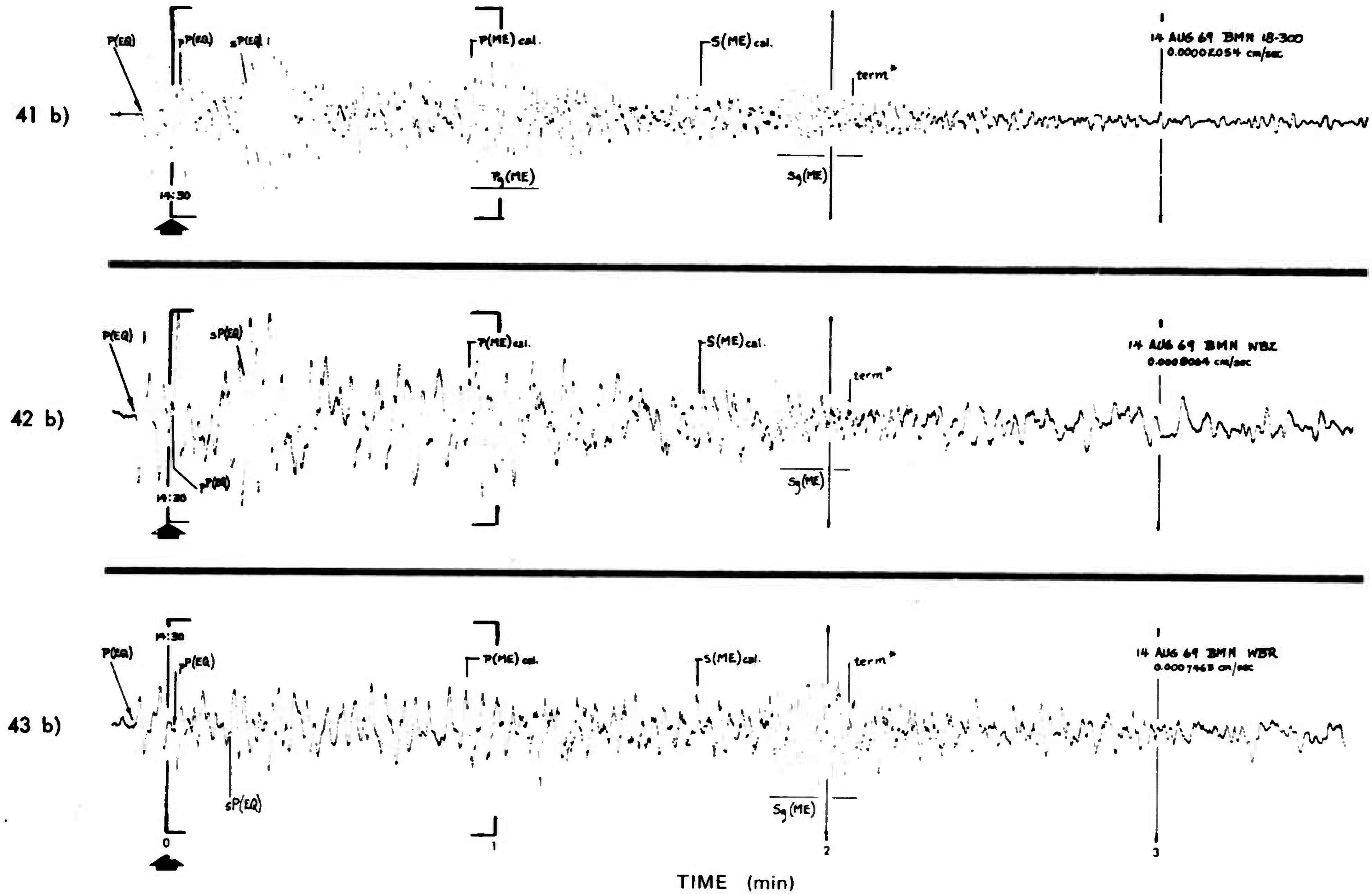
41 b)
P(EQ)
pP(EQ)
sP(EQ)
P(ME) cal.
S(ME) cal.
term*
14 AUG 69 BMN 18-300
0.00002054 cm/sec
14:30
Pg(ME)
Sg(ME)
42 b)
P(EQ)
sP(EQ)
pP(EQ)
P(ME) cal.
S(ME) cal.
term*
14 AUG 69 BMN NBZ
0.0008064 cm/sec
14:30
Sg(ME)
43 b)
P(EQ)
14:30
pP(EQ)
sP(EQ)
P(ME) cal.
S(ME) cal.
term*
14 AUG 69 BMN WBR
0.0007468 cm/sec
Sg(ME)
0
1
2
3
TIME (min)

Plate 21

Event	Date (GMT)	Δ (°)	Range (km)	Azm (°)	B Azm (°)	Origin (h m s)	T C (s)	Onset (s)	Dif (s)	Term (s)	Dur (s)	Mask (%)	Mask F (1/M)
Group 44	Pasadena, California (PAS)				Short-period vertical (SPZ)								
a) CE	13 SEP 63	3.46	384	210.1	28.9	13:53:00.15	23.1	56.1	42	153	97		
b) EQ	14 AUG 69	70.5	7830	61.2	309.3	14:19:01.6	11.0	30:14					
ME	..do..	3.46	385	210.4	29.1	14:30:00.04		c		c	c		
Group 45	..do..				Long-period North-South (LP NS)								
b) EQ	14 AUG 69	70.5	7830	61.2	309.3	14:19:01.6	11.0	30:15					
ME	..do..	3.46	385	210.4	29.1	14:30:00.04		75*		150*	75*		
Group 46	..do..				Long-period East-West (LP EW)								
b) EQ	..do..						11.0	30:15					
ME								68*		140*	72*		
Group 47	Hayfield, California (HAY)				Short-period vertical (SPZ)								
a) CE	13 SEP 63	3.47	386	173.9	354.1	13:53:00.15	10.8	55:3	29	165a 208b	110a 153b		
b) EQ	14 AUG 69	72.4	8041	60.2	310.4	14:19:01.6	-9.0	30:26					
ME	..do..	3.46	385	174.1	354.4	14:30:00.04		111*		149*	38*	65.5a 75.2b	1.53a 1.33b

The only suggestion for the ME at both stations is a very weak high-frequency modulation of the teleseism which appears in the long-period records for Pasadena (Traces 45b and 46b) and the short-period record for Hayfield (Trace 47b). No phases of the ME are identifiable.

The data are reproduced from the photographic paper originals at a scale factor of 100%. The magnifications of the instruments are assumed to be equal for each pair of traces. (see Notes 1 & 2, Table IV).

a. End of the motion characteristic of the explosion.
b. End of the signal.
c. No identifiable explosion waveform present.
* Values estimated from the high-frequency signal attributed to the ME.

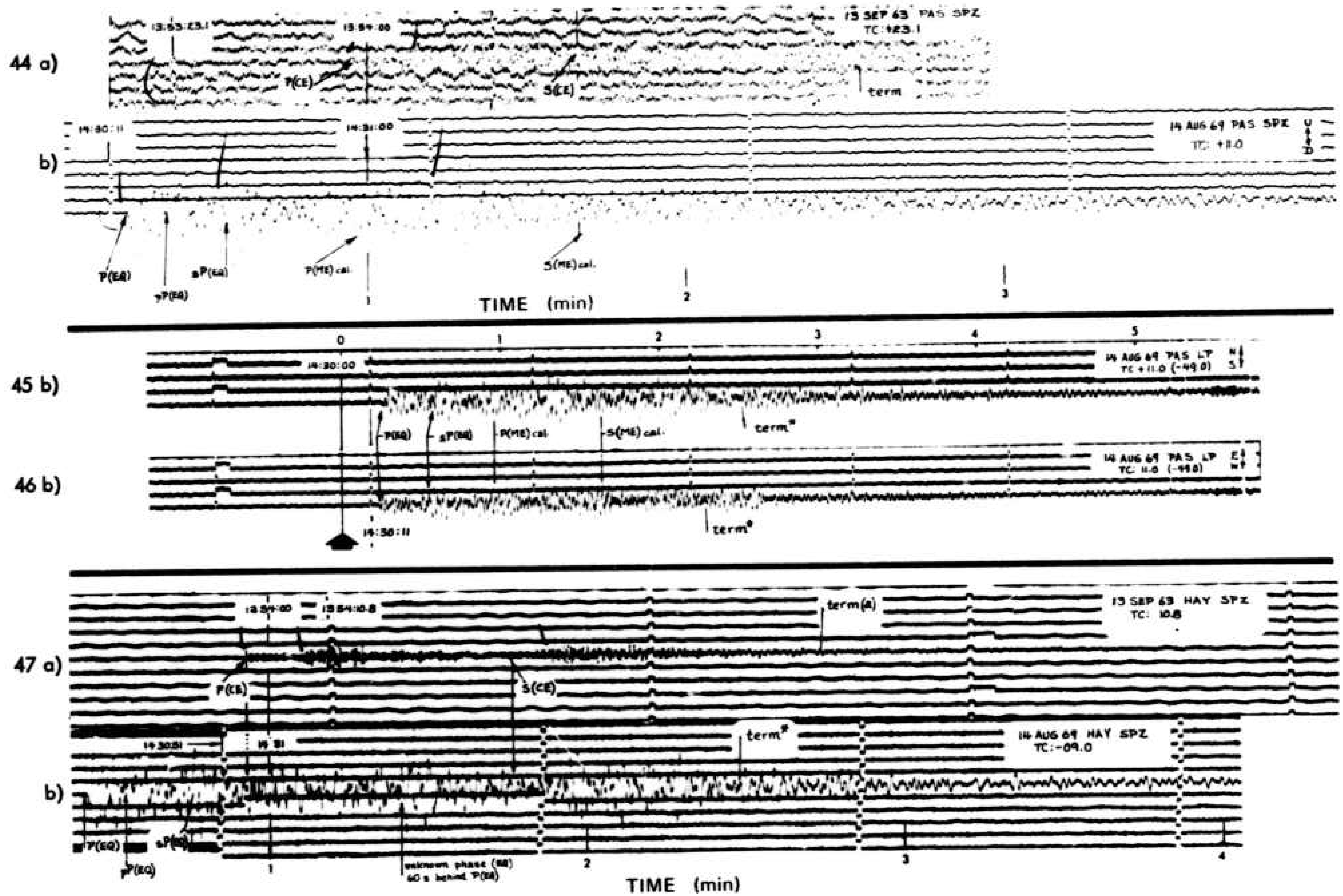
44 a)
13:53:23.1
13:54:00
P(CE)
S(CE)
13 SEP 63 PAS SPZ
TC: +23.1
term
b)
14:30:11
14:31:00
14 AUG 69 PAS SPZ
TC: +11.0
U
D
P(EQ)
pP(EQ)
sP(EQ)
P(ME) cal.
S(ME) cal.
1
2
3
TIME (min)
0
1
2
3
4
5
45 b)
14:30:00
14 AUG 69 PAS LP
TC +11.0 (-49.0)
N
S
P(EQ)
sP(EQ)
P(ME) cal.
S(ME) cal.
term*
46 b)
14 AUG 69 PAS LP
TC: 11.0 (-49.0)
E
W
14:30:11
term*
47 a)
13:54:00
13:54:10.8
term(a)
13 SEP 63 HAY SPZ
TC: 10.8
P(CE)
S(CE)
b)
14:30:51
14:31
term*
14 AUG 69 HAY SPZ
TC: -09.0
P(EQ)
pP(EQ)
sP(EQ)
unknown phase (EQ)
60 s behind P(EQ)
1
2
3
4
TIME (min)

Plate 22

Event	Date (GMT)	Δ (°)	Range (km)	Azm (°)	B Azm (°)	Origin (h m s)	T C (s)	Onset (s)	Dif (s)	Term (s)	Dur (s)	Mask (%)	Mask F (1/M)
Group 48	Jamestown, California (JAS)				Short-period vertical (SPZ)								
a) CE	18 MAR 69	3.60	401	283.3	100.6	14:40:02.7	0	57	66	212a 270b	155a 213b		
b) EQ	14 AUG 69	66.7	7408	59.3	307.2	14:19:01.6	0	29:51.0					
ME	..do..	3.56	396	284.1	101.4	14:30:00.04		68		145	77	50.3a 63.8b	1.99a 1.57b

Jamestown was installed after 13 September 1963, the date of the primary CE. As a substitute the trace from the seismic event in southern Nevada of 18 March 1969 is used.

The Pg phase for the ME is partially visible as a high-frequency signal while the Sg phase shows a pattern of peak amplitudes which corresponds very closely to that of the CE. The Seismographic Station at the University of California, Berkeley[1] assigned the following onsets to the ME:

P 14:31:08.0 denoted by $P(ME)_{UCB}$,
*E 14:31.53 denoted by $S(ME)_{UCB}$.

The traces are reproduced from the original hot-wire stylus records at a scale factor of 100%. The magnification of the instrument is assumed to be equal for both traces. (see Note 7, Table IV).

a. End of the motion characteristic of the explosion.
b. End of the signal.
1. Chandra, Peppin and Adams (1970), p. 137.

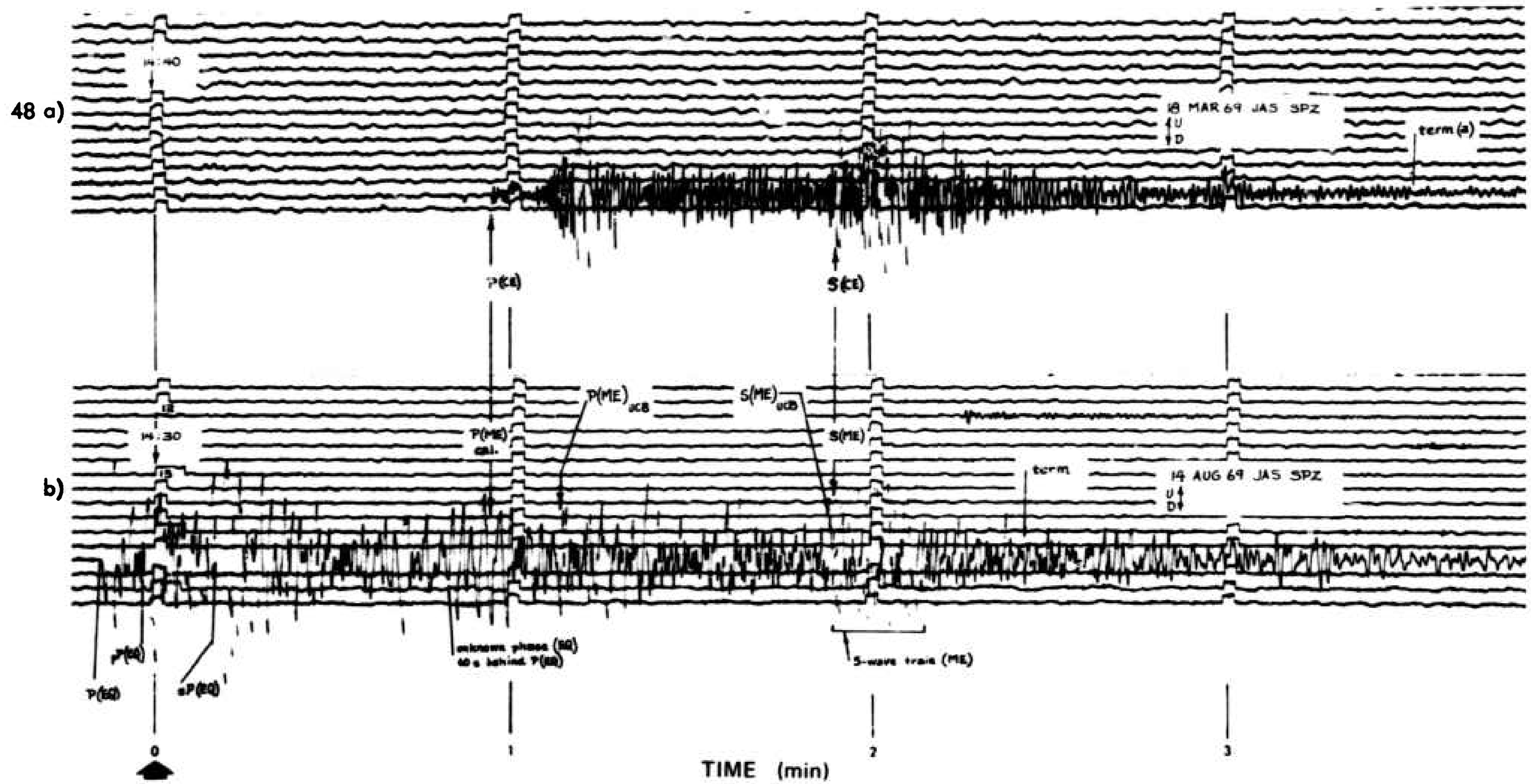
48 a)
b)
14:40
18 MAR 69 JAS SPZ
U
D
term (a)
P(EE)
S(EE)
14:30
P(ME) cal.
P(ME) UCB
S(ME) UCB
S(ME)
term
14 AUG 69 JAS SPZ
P(EQ)
pP(EQ)
sP(EQ)
unknown phase (EQ) 60 s behind P(EQ)
S-wave train (ME)
0
1
2
3
TIME (min)

Plate 23

Event	Date (GMT)	Δ (°)	Range (km)	Azm (°)	B Azm (°)	Origin (h m s)	T C (s)	Onset (s)	Dif (s)	Term (s)	Dur (s)	Mask (%)	Mask F (1/M)
Group 49	Priest, California (PRI) Short-period vertical (SPZ)												
a) CE	13 SEP 63	3.82	425	255.9	73.2	13:53:00.15	0	62	64	174a 245b	112a 18[illegible]		
b) EQ	14 AUG 69	67.6	7514	60.9	307.8	14:19:01.6	0	29:57.5					
ME	..do..	3.84	427	256.0	73.3	14:30:00.04		76*		143*	67*	40.2a 63.4b	2.49a 1.58b
Group 50	Palomar, California (PLM) Short-period vertical (SPZ)												
a) CE	13 SEP 63	3.85	429	189.8	9.3	13:53:00.15	-12.6	61.6	39	187a 268b	125a 206b		
b) EQ	14 AUG 69	71.8	7980	61.1	310.0	14:19:01.6	11.0	30:23					
ME	..do..	3.85	429	190.0	9.5	14:30:00.04		63*		145*	82*	34.4a 60.2b	2.91a 1.66b

The Pg and Sg phases for the ME are partially visible as high-frequency modulations of the teleseism for Priest. In the case of Palomar the modulations are very weak and barely visible, appearing as a darkening of the trace at the times of the Pg and Sg phases for the CE.

The traces for Priest are reproduced from the original hot-wire stylus records. In the case of Palomar the trace for the CE is reproduced from the original photographic paper record, while that for the ME is taken from the original inked-pen paper record. The scale factor in all cases is 100%. The magnification of each instrument is assumed to be equal for each pair of traces. (see Notes 1, 3 & 7, Table IV).

---

a. End of the motion characteristic of the explosion
b. End of the signal.
* Values estimated from the high-frequency modulation attributed to the ME.

49 a)

b)

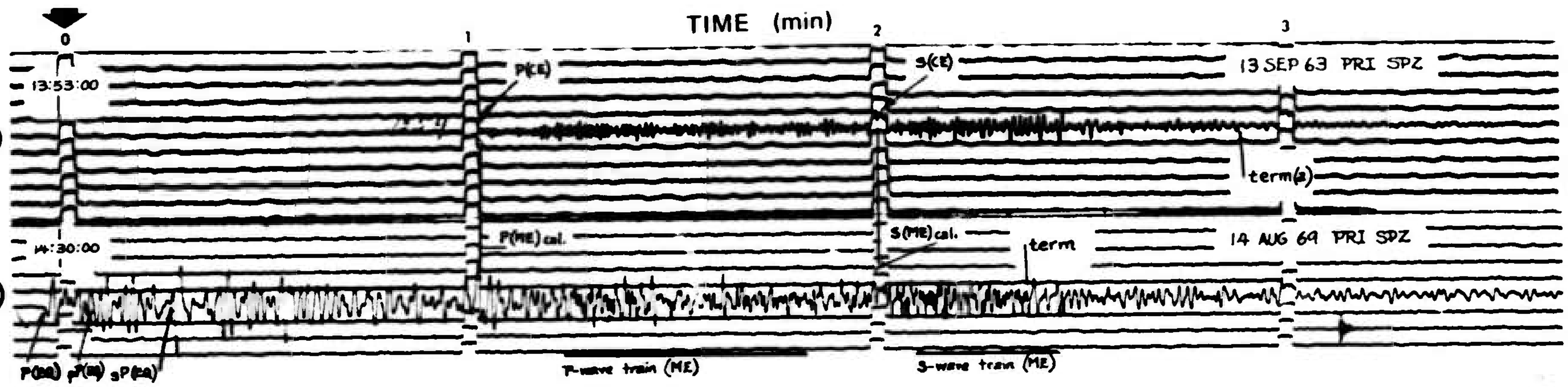

50 a)

b)

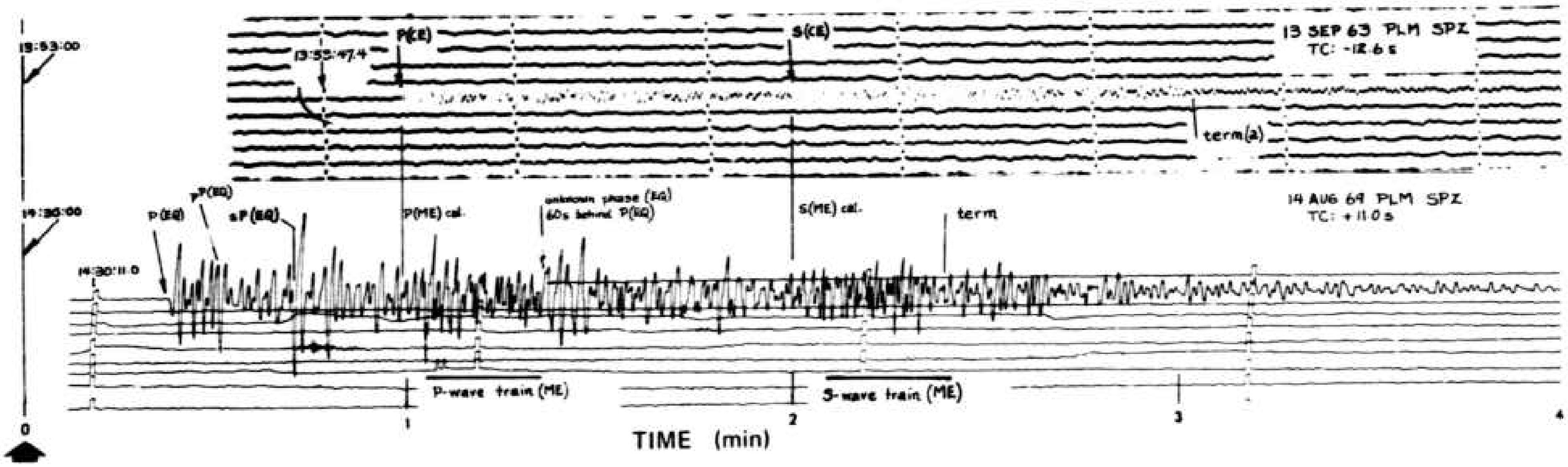

Plate 24

Event	Date (GMT)	Δ (°)	Range (km)	Azm (°)	B Azm (°)	Origin (h m s)	T C (s)	Onset (s)	Dif (s)	Term (s)	Dur (s)	Mask (%)	Mask F (1/M)
Group 51	Dugway, Utah (DUG)			Short-period vertical (SPZ)									
a) CE	13 SEP 63	3.96	440	39.2	221.2	13:53:00.15	0	65.5	54	320	255		
b) EQ	14 AUG 69	69.9	7769	53.4	309.9	14:19:01.6	0	30:12					
ME	..do..	3.95	440	39.0	221.0	14:30:00.04		*		*	*		

For the CE only the onset time and the later portion of the explosion waveform are discernible. The blank portion of the trace beginning at 13:54:18 resulted from the shadows of the drum clamps. The record for 14 August 1969 required a large vertical portion to show the excursions of the teleseism which in turn resulted from the high gain (400K) of the instrument. Only the onset for the teleseism can be read. None of the phases for the CE or the ME are discernible.

The trace for the CE is reproduced from the best copy available from archives of the original photographic paper record. The trace for the ME is reproduced directly from the original photographic paper record. Scale factors for both traces are 100%. The magnification of the instrument is the same for both traces. (see Notes 11 & 12, Table IV).

* No recognizable explosion waveform visible.

51 a)

b)

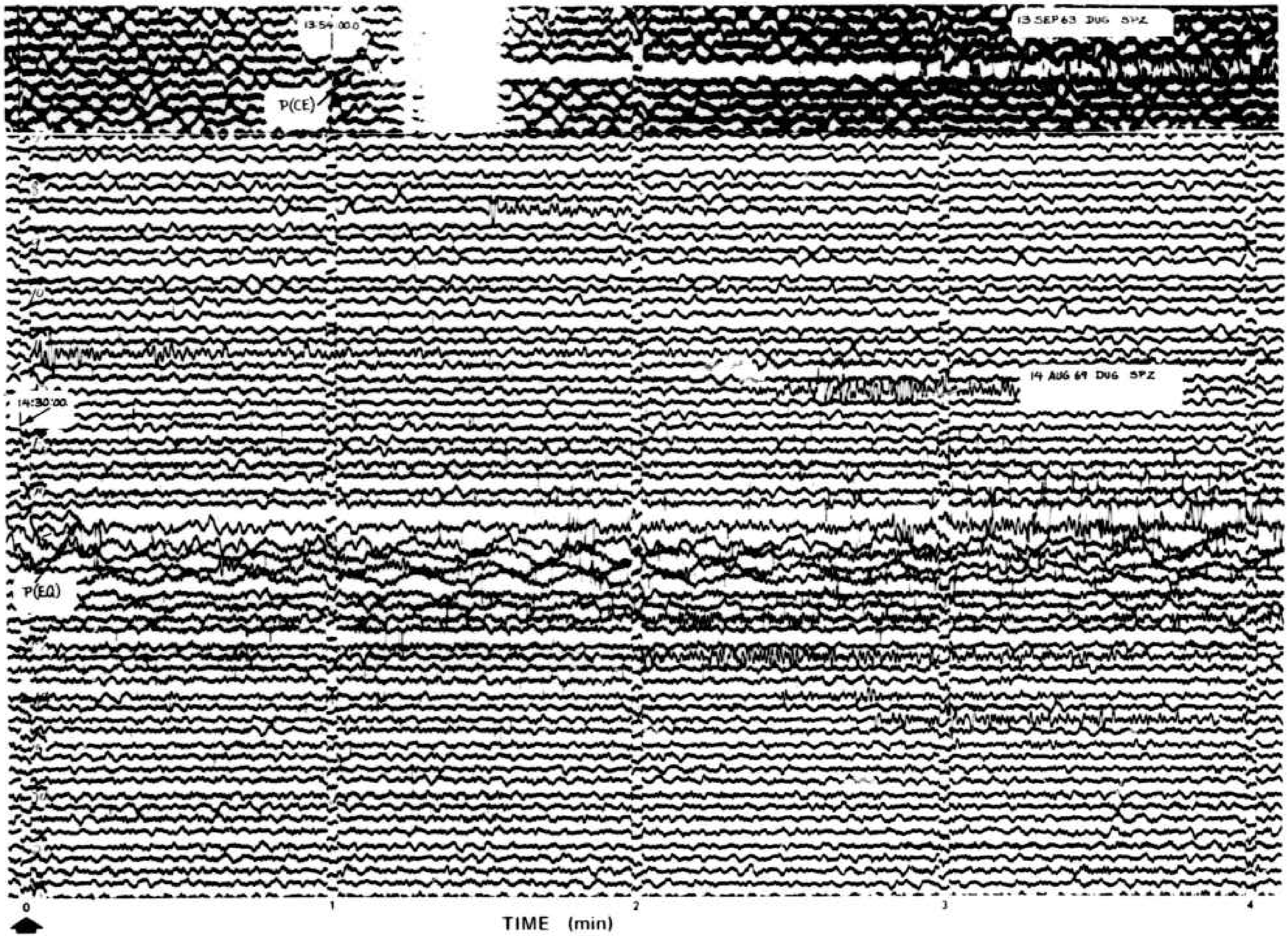

Plate 25

Event	Date (GMT)	Δ (°)	Range (km)	Azm (°)	B Azm (°)	Origin (h m s)	T C (s)	Onset (s)	Dif (s)	Term (s)	Dur (s)	Mask (%)	Mask F (1/M)
Group 52	Santa Barbara, California (SBC) Short-period vertical (SPZ)												
a) CE	none												
b) EQ	14 AUG 69	69.3	7699	61.8	308.6	14:19:01.6	8.1	30:08.1					
ME	..do..	4.02	447	228.6	46.5	14:30:00.04		+	+	+			
Group 53	Santa Ynez Peak, California (SYP) Short-period vertical (SPZ)												
a) CE	none												
b) EQ	14 AUG 69	69.1	7674	61.9	308.5	14:19:01.6	11.0	30:07					
ME	..do..	4.13	459	231.6	49.3	14:30:00.04		79*		138*	59*		
Group 54	Paraiso, California (PRS) Short-period vertical (SPZ)												
a) CE	13 SEP 63	4.33	481	260.5	77.4	13:53:00.15	0	74.5	82	185a 215b	110a 140b		
b) EQ	14 AUG 69	67.1	7451	61.1	307.4	14:19:01.6	0	29:53.1					
ME	..do..	4.34	483	260.6	77.4	14:30:00.04		80*		168*	88*	20.0a 37.1b	5.00a 2.69b

The trace for Santa Barbara shows no evidence of the ME. In the case of Santa Ynez Peak a very weak high-frequency modulation is present in the troughs of the teleseism. Traces for the CE have been omitted for both stations because no suitable records could be found. At Paraiso the ME appears as signals at the times of the phases for the CE, with a reduction in amplitude due to the replacement of the short-period vertical instrument by a horizontal Willmore.

The trace for Santa Barbara is reproduced from the original photographic paper record, while that for Santa Inez Peak is taken from the original inked-pen drum record. In the case of Paraiso the trace for the CE is reproduced directly from the original hot-wire stylus record; the record for the ME is a photoreduction of a hand tracing extracted from the projected image of the 16 mm film original, copies of which are shown on Plate 31. The disparities in amplitude for the last station are due to changes in instrumentation. The scale factors are 100% for the first 3 traces and 10% for the last. (see Notes 1, 3, 7 & 10, Table IV).

a. End of the motion characteristic of the explosion.
b. End of the signal.
\+ No explosion waveform visible.
* Values estimated from the high-frequency modulation attributed to the ME.

52 b)

53 b)

54 a)

b)

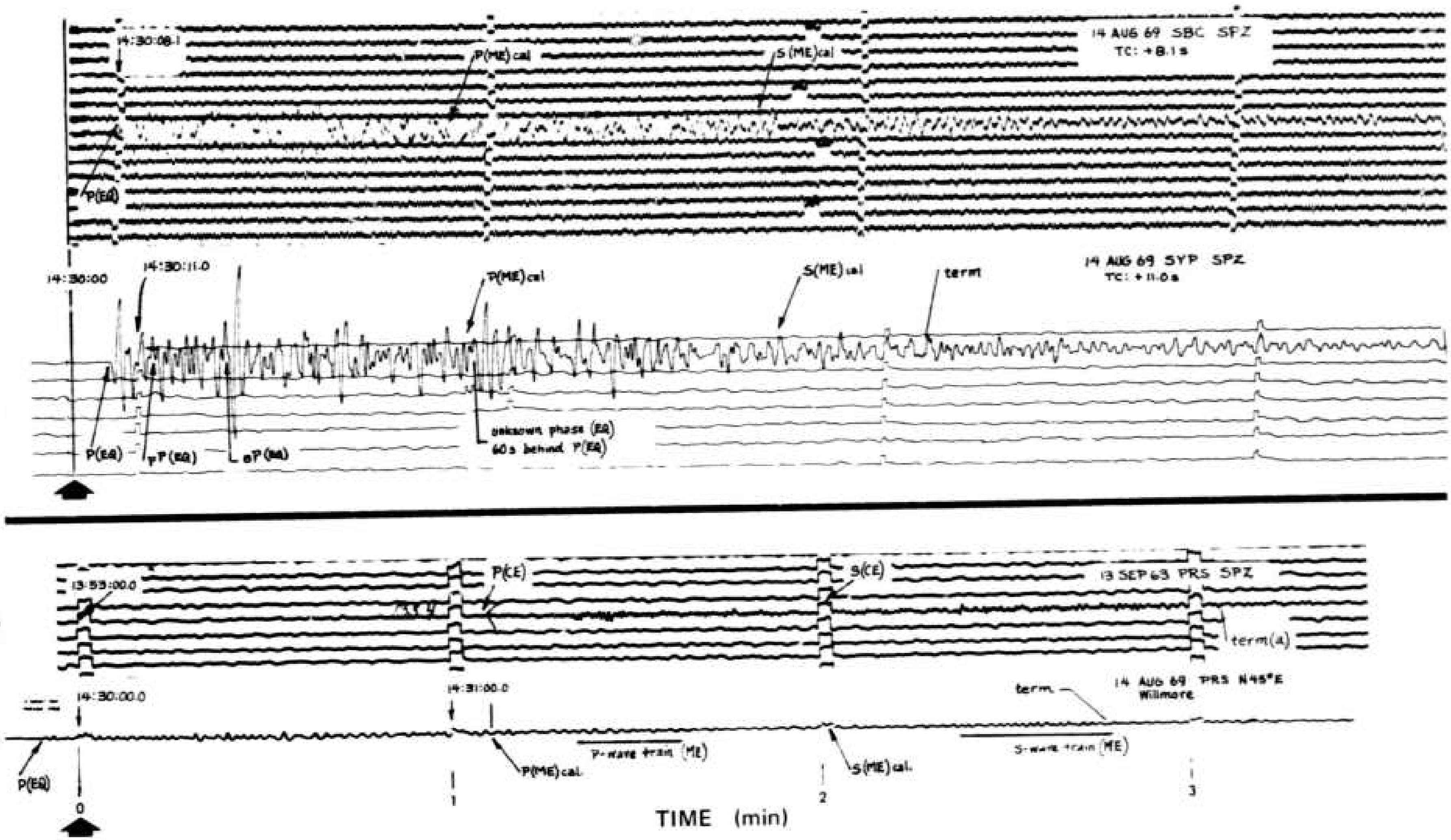
14:30:08.1
P(ME)cal
S(ME)cal
14 AUG 69 SBC SPZ
TC: +8.1 s
P(EQ)
14:30:00
14:30:11.0
P(ME)cal
S(ME)cal
term
14 AUG 69 SYP SPZ
TC: +11.0 s
P(EQ)
pP(EQ)
sP(EQ)
unknown phase (EQ)
60 s behind P(EQ)
13:53:00.0
P(CE)
S(CE)
13 SEP 63 PRS SPZ
term(a)
14:30:00.0
14:31:00.0
term
14 AUG 69 PRS N45°E
Willmore
P-wave train (ME)
S-wave train (ME)
P(EQ)
P(ME)cal.
S(ME)cal.
0
1
2
3
TIME (min)

Event	Date (GMT)	Δ (°)	Range (km)	Azm (°)	B Azm (°)	Origin (h m s)	T C (s)	Onset (s)	Dif (s)	Term (s)	Dur (s)	Mask (%)	Mask F (1/M)
Group 55	Mount Hamilton, California (MHC) Short-period vertical (SPZ)									190a	110a		
a) CE	13 SEP 63	4.44	494	273.9	90.6	13:53:00.15	0	79.5	91	245b	165b		
b) EQ	14 AUG 69	66.3	7364	60.4	307.0	14:19:01.6	0	29:48.4					
ME	..do..	4.45	495	274.0	90.6	14:30:00.04		78c		159	81	26.4a 50.9b	3.79a 1.96b
Group 56	Barrett, California (BAR) Short-period vertical (SPZ)												
a) CE	13 SEP 63	4.50	500	186.4	6.0	13:53:00.15	2.6	69	43	218	149		
b) EQ	14 SEP 69	72.4	80[illegible]1	61.6	310.2	14:19:01.6	-13.5	30:26					
ME	..do..	4.50	500	186.6	6.2	14:30:00.04		73+		81+	12+	91.9	1.09
Group 57	Berkeley, California (BKS) Short-period vertical (SPZ)												
a) CE	13 SEP 63	4.94	550	280.2	96.4	13:53:00.15	0	79	95	200	121		
b) EQ	14 AUG 69	65.6	7287	60.3	306	14:19:01.6	0	29:43.5					
ME	..do..	4.96	55[illegible]	280.2	96.4	14:30:00.04		107*		111*	4*	96.7	1.03

For Mount Hamilton both the Pg and Sg phases of the ME are clearly visible as high-frequency signals superimposed on the teleseism. The onset for the ME nearly coincides with that for the CE, while the later portions after the Sg wave-train appear in a segmented manner. For the remaining two stations the only suggestion of the ME is a high-frequency modulation in the troughs of the teleseism which again appears segmented. At this distance from NTS the masking of the ME is nearly complete.

The data for Mount Hamilton are reproduced from the original hot-wire stylus records. The remaining traces are taken from photographic paper records. For Barrett the records are copied directly from the originals, while those for Berkeley are made from the best copies available from archives. The scale factor in all cases is 100%. The magnification for each instrument is assumed to be the same for each pair of traces. (see Notes 1, 7 & 11, Table IV).

a. End of the motion characteristic of the explosion.
b. End of the signal.
c. Value assigned by the University of California, Berkeley (Chandra et al, 1970, p. 137).
\+ Values for first segment. Second segment extends for 4 sec beginning at 147 sec.
* Only clearly identifiable segment of explosion waveform.

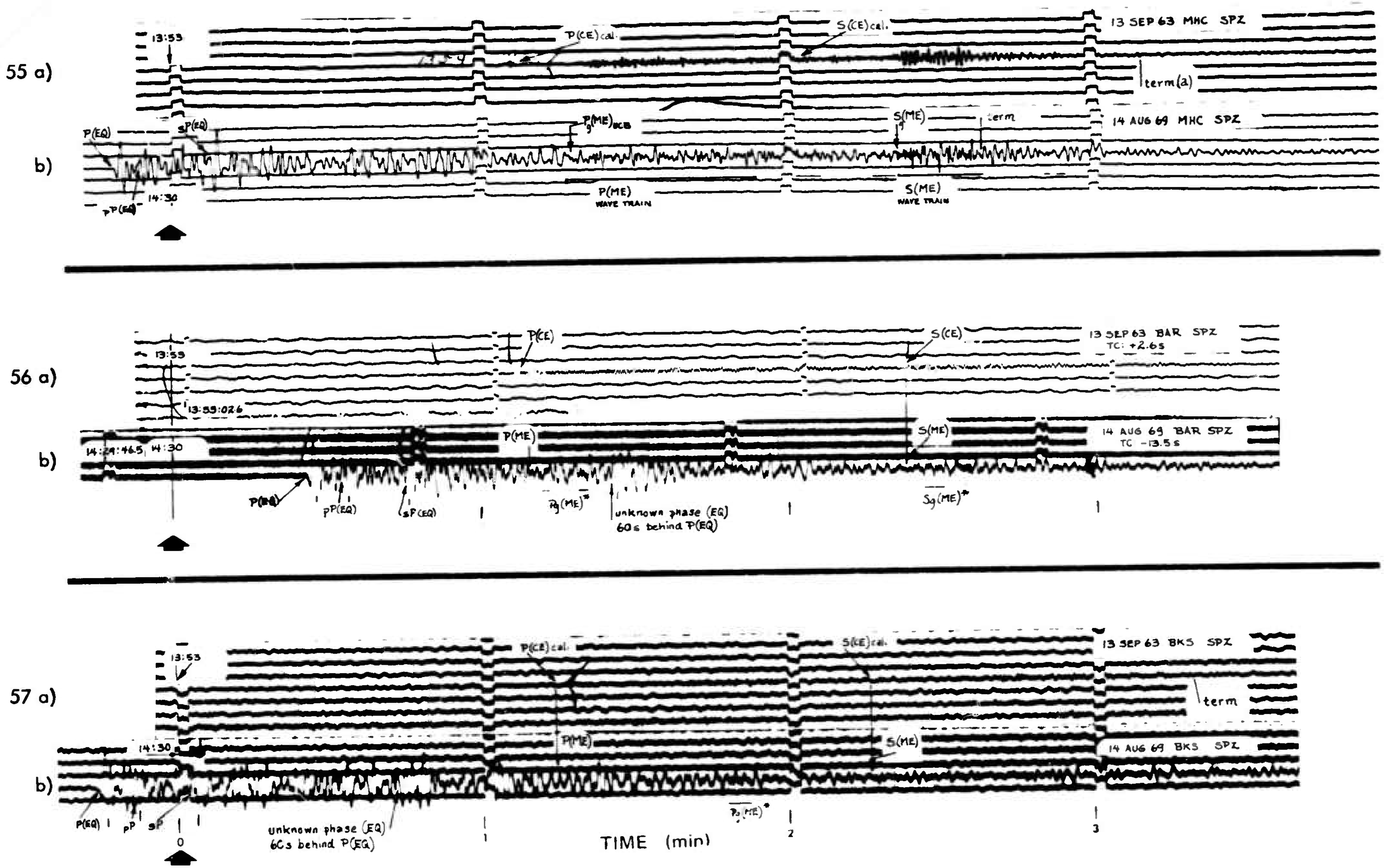
55 a)
13:53
P(CE) cal.
S(CE) cal.
13 SEP 63 MHC SPZ
term(a)
b)
P(EQ)
sP(EQ)
pP(EQ)
14:30
P_g(ME) BCB
S(ME)
term
14 AUG 69 MHC SPZ
P(ME) WAVE TRAIN
S(ME) WAVE TRAIN
56 a)
13:53
13:53:02.6
P(CE)
S(CE)
13 SEP 63 BAR SPZ
TC: +2.6 s
b)
14:29:46.5
14:30
P(ME)
S(ME)
14 AUG 69 BAR SPZ
TC -13.5 s
P(EQ)
pP(EQ)
sP(EQ)
P_g(ME)*
unknown phase (EQ)
60 s behind P(EQ)
Sg(ME)*
57 a)
13:53
P(CE) cal.
S(CE) cal.
13 SEP 63 BKS SPZ
term
b)
14:30
P(ME)
S(ME)
14 AUG 69 BKS SPZ
P(EQ)
pP
sP
0
unknown phase (EQ)
60 s behind P(EQ)
P_g(ME)*
1
2
3
TIME (min)

Plate 27

Event	Date (GMT)	Δ (°)	Range (km)	Azm (°)	B Azm (°)	Origin (h m s)	T C (s)	Onset (s)	Dif (s)	Term (s)	Dur (s)	Mask (%)	Mask F (1/M)
Group 58	Tucson, Arizona (TUC) Short-period vertical (SPZ)												
a) CE	13 SEP 63	6.52	725	136.4	319.5	13:53:00.15	0	121	71	353	232		
b) EQ	14 AUG 69	76.3	8484	58.4	312.5	14:19:01.6	0	30:50					
ME	..do..	6.50	723	136.5	319.5	14:30:00.04		240+		242+	2+	99.1	1.009
Group 59	Albuquerque, New Mexico (ALQ) Short-period vertical (SPZ)												
a) CE	13 SEP 63	8.10	901	103.0	288.7	13:53:00.15	0	135	81	385	250		
b) EQ	14 AUG 69	77.2	8576	54.0	313.9	14:19:01.6	0	30:54					
ME	..do..	8.09	899	103.0	288.7	14:30:00.04		*		*	*		

At this range from NTS the dispersion of the explosion waveform becomes more pronounced. For Tucson the only suggestion of the ME is a high-frequency signal of 2-second duration beginning at 240 seconds. In the case of Albuquerque the detailed structure of the waveform for 14 August 1969 is not discernible due to the poor quality of the copy available. No phases of ME are identifiable at either station.

The data are reproduced from the best copies available from archives at a scale factor of 100%. The magnification of each instrument is assumed to be the same for each pair of traces. (see Note 11, Table IV).

+ Value estimated from the high-frequency signal attributed to the ME.
* No explosion waveform visible.

58 a)

b)

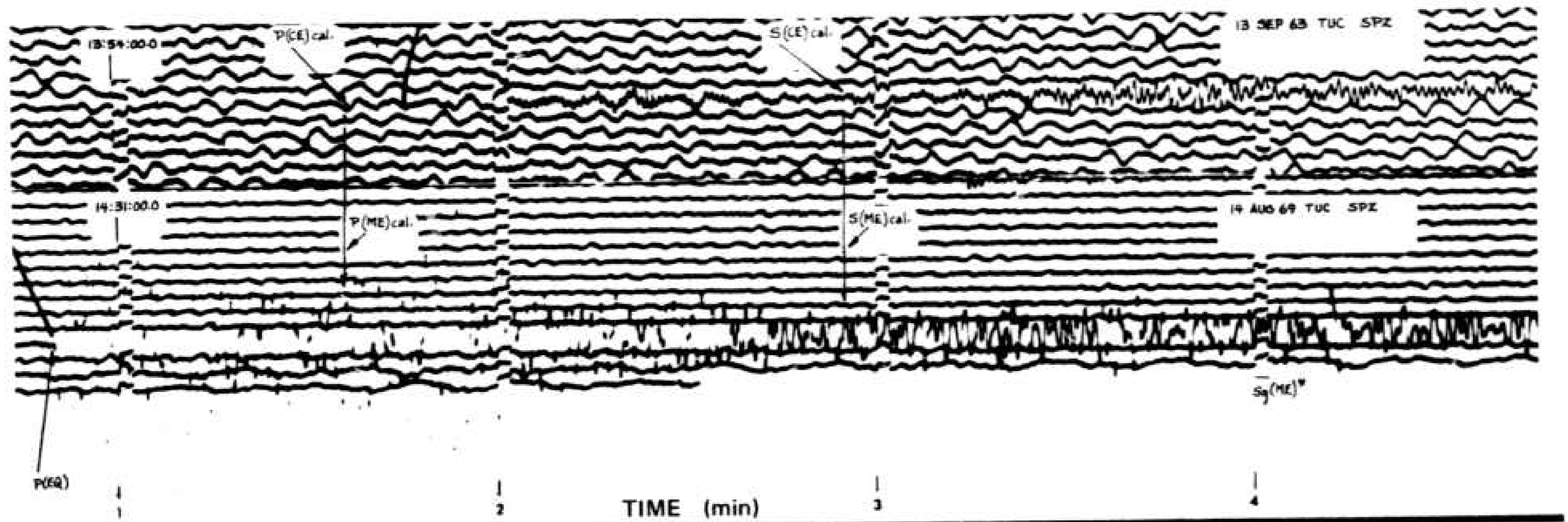

59 a)

b)

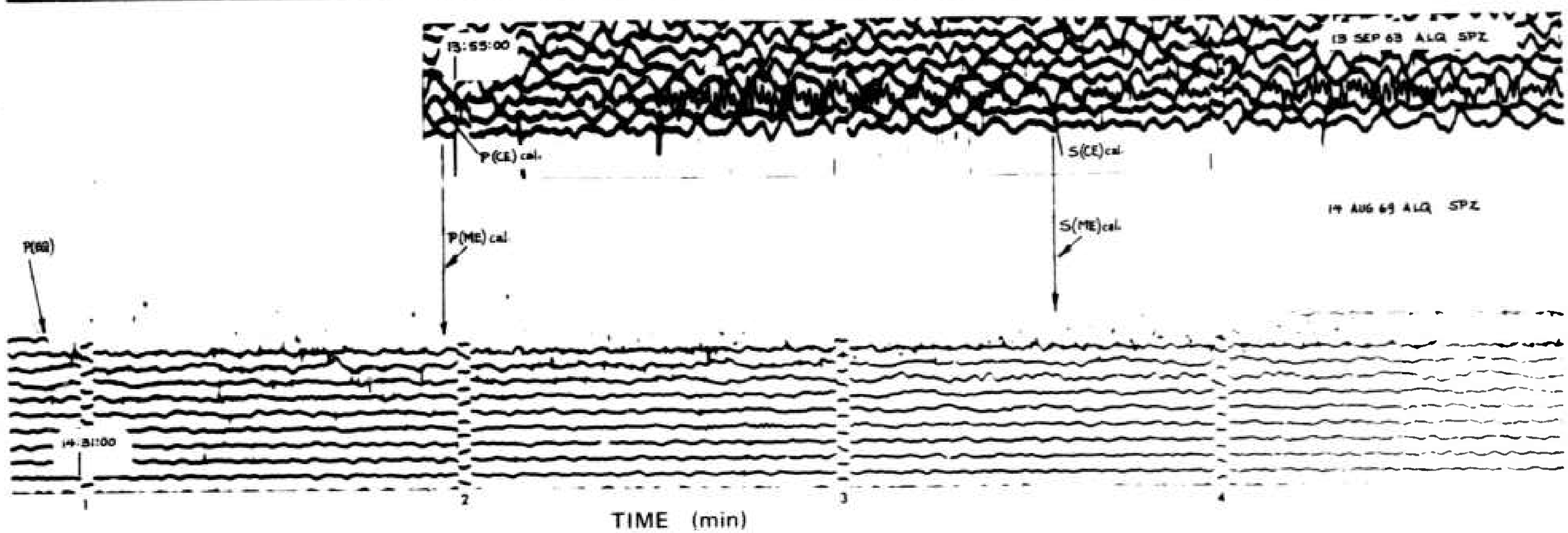

Plate 28

Event		Date (GMT)	Δ (°)	Range (km)	Azm (°)	B Azm (°)	Origin (h m s)	T C (s)	Onset (s)	Dif (s)	Term (s)	Dur (s)	Mask (%)	Mask F (1/M)
Group	60	Golden, Colorado (GOL)			Short-period vertical (SPZ)									
a) CE		13 SEP 63	8.78	976	70.0	256.6	13:53:00.15	0	135	95	330	195		
a') CE		18 MAR 69	8.70	968	70.1	256.7	14:40:02.7	0	136	96	357	221		
b) EQ		14 AUG 69	74.5	8280	49.8	313.5	14:19:01.6	0	30:39.5					
ME		..do..	8.77	975	69.9	256.6	14:30:00.04		+		+	+		
Group	61	..do..			Short-period North-South (SP NS)									
a') CE		18 MAR 69	8.70	968	70.1	256.7	14:40:02.7	0	134	94	354	220		
b) EQ		14 AUG 69	74.5	8280	49.8	313.5	14:19:01.6	0	30:39.5					
ME		..do..	8.77	975	69.9	256.6	14:30:00.04		291*		309*	5*	97.7	1.02
Group	62	..do..			Short-period East-West (SP EW)									
a') CE								0	132	92	344	212		
b) EQ		..do..						0	30:39.5					
ME									+		+	+		

At this range (975 km) the explosion waveforms are much more dispersed than those shown on Plate 28. The trace for the primary CE of 13 September 1963 is too heavily embedded in the noise to be useful for comparison. As substitutes traces from the seismic event in southern Nevada of 18 March 1969† are used. Even though the gain (400K) on 14 August 1969 is twice that of the substitute CE, no phases for the ME are discernible. Only the North-South component shows any suggestion for the ME which appears as a high-frequency signal of approximately 5 seconds duration and segmented structure for the interval 290-309 seconds. This heavily masked signal corresponds to the Sg phase as shown by the CE. The onsets of the teleseism are shown on Plate 30.

The data from 18 March and 14 August 1969 are reproduced directly from the original photographic paper records. The trace for 13 September 1963 is taken from the best copy available from archives. The scale factor for all traces is 100%. The magnification of the instruments for 13 September 1963 and 14 August 1969 is 400K. For 18 March 1969 it is 200K. (see Notes 11 & 12, Table IV).

+ No explosion waveform visible.
* Values estimated from the high-frequency signal attributed to the ME.
† The arrival times compare directly to those given by Simon (1972, pp. 32-35).

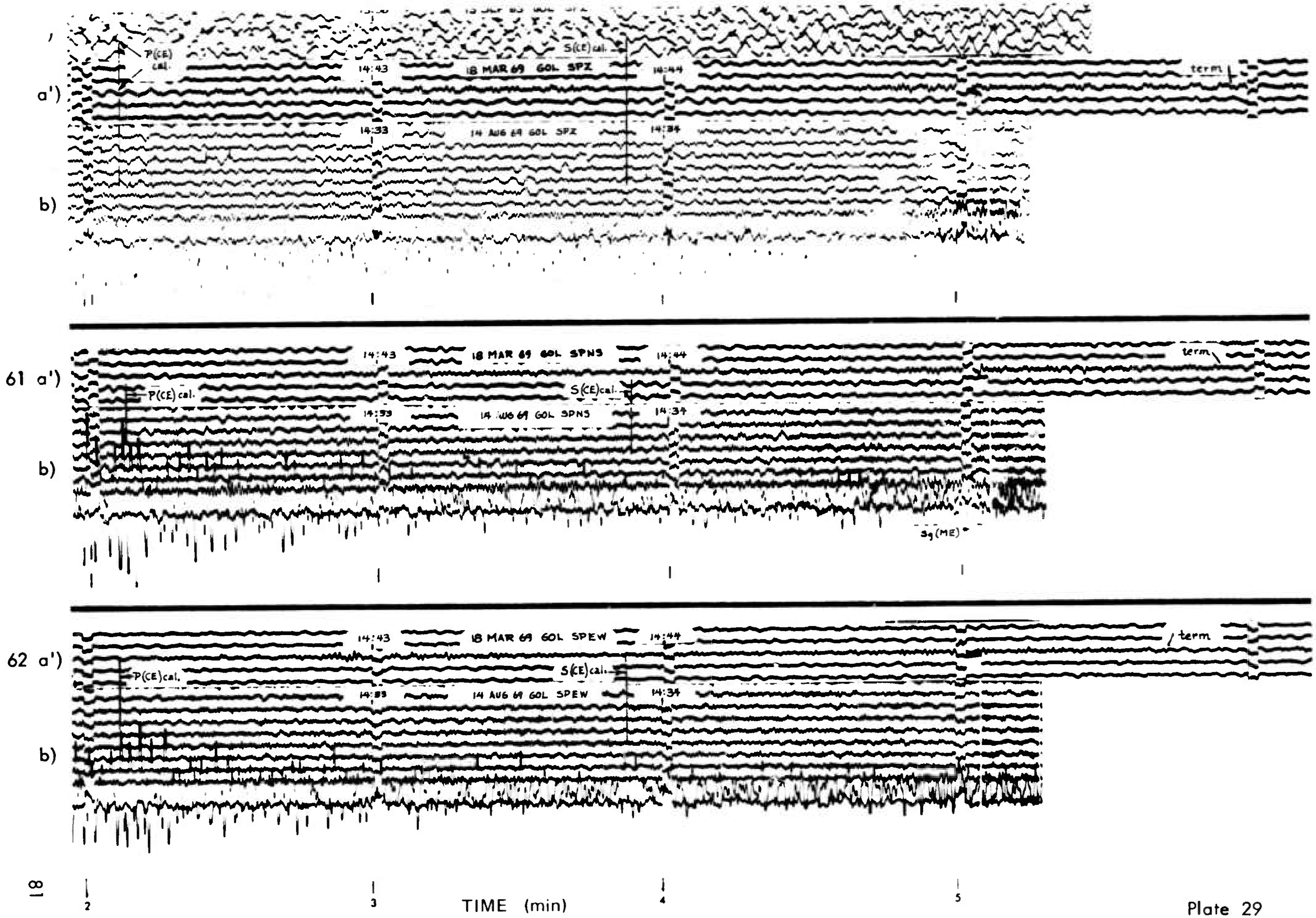
a')
b)
P(CE) cal.
S(CE) cal.
14:43
18 MAR 69 GOL SPZ
14:44
term
14:33
14 AUG 69 GOL SPZ
14:34
61 a')
b)
18 MAR 69 GOL SPNS
14 AUG 69 GOL SPNS
Sg(ME)
62 a')
b)
18 MAR 69 GOL SPEW
14 AUG 69 GOL SPEW
2
3
4
5
TIME (min)

Plate 29

Event	Date (GMT)	Δ (°)	Range (km)	Azm (°)	B Azm (°)	Origin (h m s)	T C (s)	Onset (s)	Dif (s)	Term (s)	Dur (s)	Mask (%)	Mask F (1/M)
Group 63	Golden, Colorado (GOL)			Short-period vertical (SPZ), scale factor of 75%									
a) CE	none												
b) EQ	14 AUG 69	74.5	8280	49.8	313.5	14:19:01.6	0	30:39.5					
ME	..do..	8.77	975	69.9	256.6	14:30:00.04							
Group 64	..do..			Short-period North-South (SP NS), scale factor of 75%									
a) CE													
b) EQ	..do..						0	30:39.5					
ME													
Group 65	..do..			Short-period East-West (SP EW), scale factor of 75%									
a) CE													
b) EQ	..do..						0	30:39.5					
ME													

Copies of the three components given on Plate 29 are displayed here in reduced scale to show the onsets of the teleseism for 14 August 1969.

The data reproduced from PMT copies of the original photographic paper records at a scale factor of 75%. (see Note 12, Table IV).

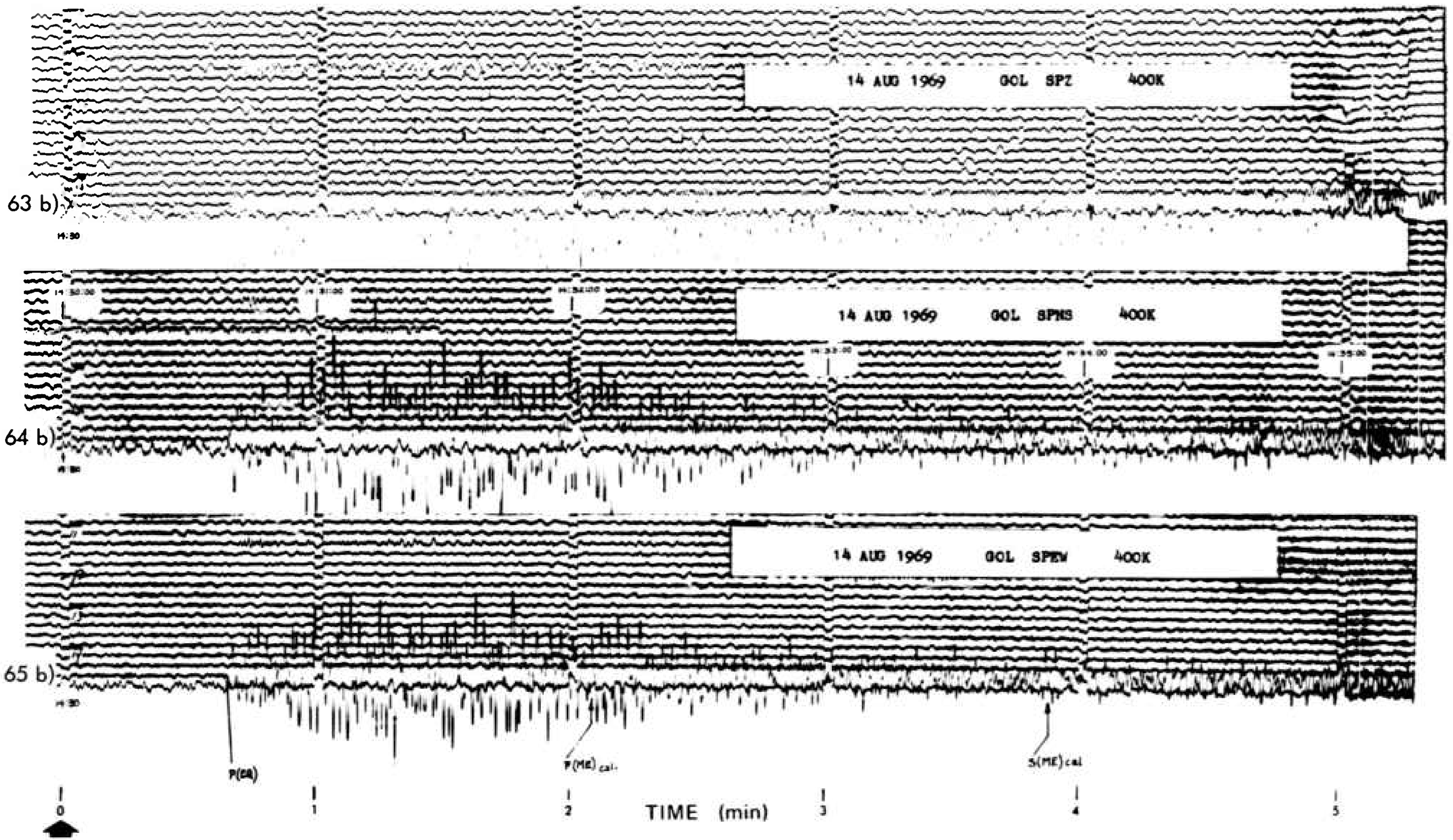
14 AUG 1969 GOL SPZ 400K
63 b)
14 AUG 1969 GOL SPNS 400K
64 b)
14 AUG 1969 GOL SPEW 400K
65 b)
P(CR)
P(ME)cal.
S(ME)cal
0
1
2
3
4
5
TIME (min)

Plate 30

Group 66 Berkeley Develocorder
(16 mm film)

a) CE of 13 September 1963
scale factor of 218%

b) ME of 14 August 1969
scale factor of 218%

b*) ..do.. scale factor of 707%

(see Notes 8 & 9, Table IV).

Trace motion down is compression

KEY TO TRACES

Channel	a) CE of 13 September 1963	b) ME of 14 August 1969
1.	Time Code (radio)	Time Code (radio)
2.	Point Reyes (PR)	Pilarcitos Creek (PCC)
3.	Vinyard (VIT)	Mina (MINA)[1]
4.	Priest (PRI)	same
5.	Priest Strong-Motion (PSM)	same
6.	Calistoga (CL)	Jamestown (JAS)
7.	Concord (CNC)	SAO[3] N45E (UP)[2]
8.	Berkeley (BRK)	same
9.	.do. Strong-Motion (BSM)	SAO[3] High Frequency
10.	Mount Hamilton (MHC)	Mineral (MIN)
11.	Santa Cruz (SC)	Mount Hamilton (MHC)
12.	Paraiso (PRS)	Granite Creek (GCC) NE (UP)
13.	Llanada (LLA)	Paraiso (PRS) NE (UP)
14.		Llanada (LLA)
15.		Fickle Hill (FHC)

1. Polarity is reversed.
2. Willmore.
3. San Andreas Geophysical Observatory.

66 a)

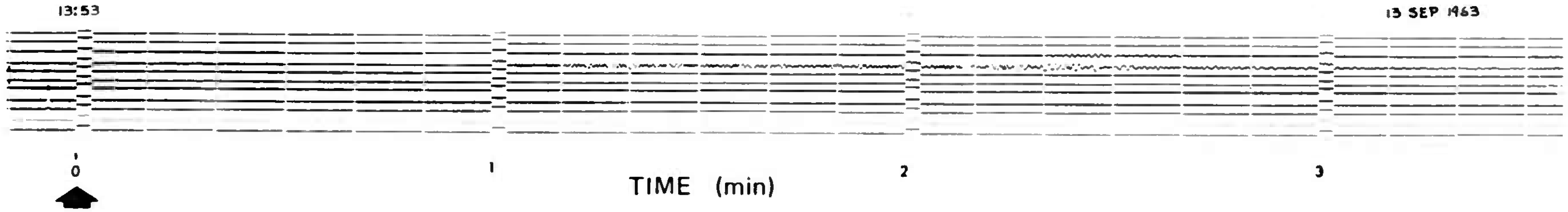

b)

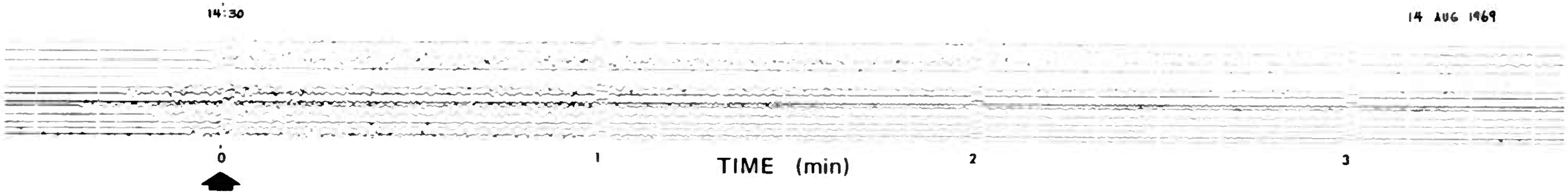

b*)

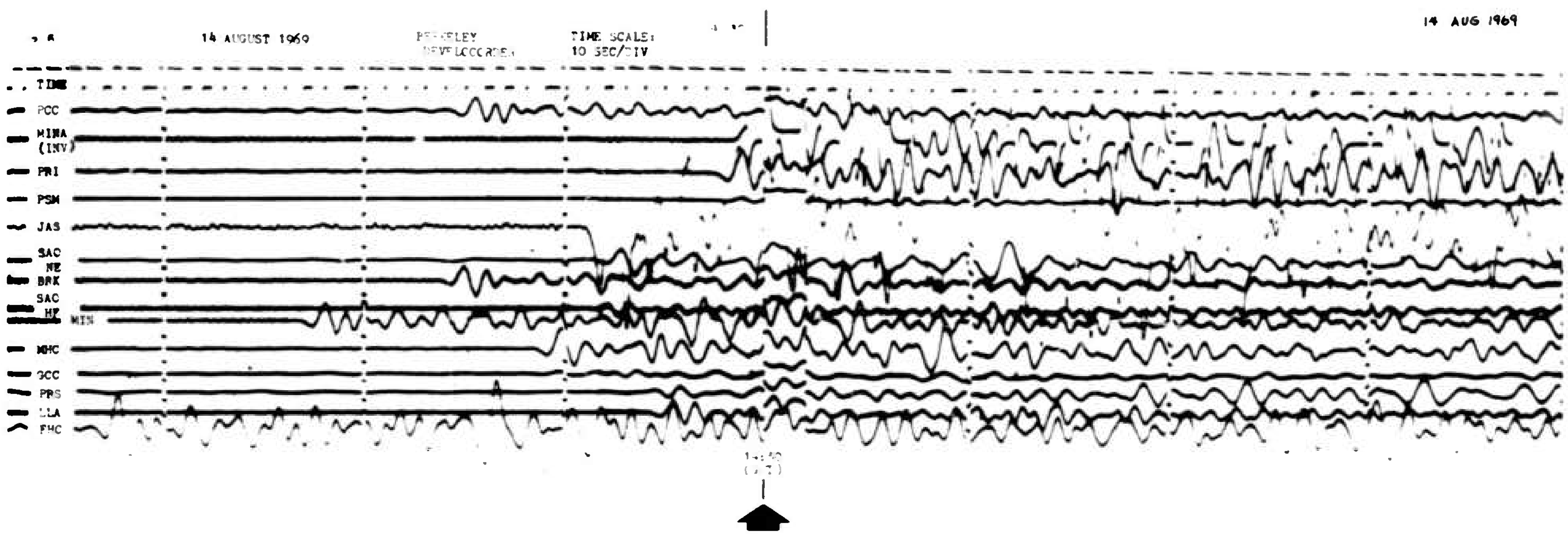

Plate 31

III. CONCLUSIONS

To aid the discussion the measurements from the seismograms are condensed into a single tabulation (Table V). In addition, the general appearances of the records are summarized in a qualitative characterization of the masking effects (Table VI), listing the dominant wave, its level of domination and the visibility of the masked explosion at each station. The records of particular significance are also identified. Furthermore, we recall the results of the preliminary analysis: 1) the masked explosion has a yield of approximately 3 kt (determined seismically) and a depth of burial of 784 feet in alluvium. 2) the duration of its waveform at 27 of the 32 stations is calibrated with the aid of the waveforms from comparison events of similar source characteristics. 3) the interfering earthquake is the most well-recorded shock of the major earthquake sequence in the Kurile Islands of August 1969 with 400 observations worldwide, a magnitude of 6.2, a depth of 46 km (all values from the ISC Bulletin), and an epicentral distance from NTS of 70°.

The findings of this investigation of seismic masking can be summarized as follows:

1) the waveform characteristic of this particular explosion recorded in the teleseism of this strong earthquake remains clearly visible out to 288 km (Kanab, Utah). Beyond this range the role of the dominant wave is taken over by the teleseism, although instances of partial visibility occur at further distances. Because of the importance of this result we shall define this distance as the maximum range of domination for the waveforms from the masked explosion.

2) In terms of the general appearance of the explosion waveform the interference first degrades and then eliminates the fine structure from the tail of the waveform as the amplitudes of this portion of the signal become smaller and more heavily modulated by the teleseism. The identification of the exact point of termination for an explosion waveforem with a slowly decaying amplitude profile proves to be an extremely difficult task, even without interference. As an accommodation to the complexity of this decision, we are forced to introduce two different criteria for termination, since most of these explosion waveforms exhibit very weak signals with no apparent information content for a considerable time after the end of amplitude pattern characteristic of the explosion. In this context we can restate the criteria defined in Section 2.4 by noting that the first termination (end of the motion characteristic of the explosion) is independent of gain, while the second (end of the signal) is a function of the noise level and hence depends on the magnification of the system. Thirty out of the forty-two traces presented for the comparison events are analyzed in this manner.

3) The usefulness of placing the seismograms from the comparison events and the masked explosion in juxtaposition cannot be overemphasized. As the level of interference is increased from the relatively simple background noise of the system to that of the complex teleseism, it becomes virtually impossible in many cases to decide even an approximate point of termination for the explosion waveform without the use of this technique of pattern comparison.

4) The next effect of the interference is to degrade and then suppress the pattern characteristic of the onset of the waveform. The delay in onsets between the comparison and masked waveforms increases slowly out to 495 km (Mount Hamilton, California) and then abruptly for greater distances. The weaker phases, such as Pn and Sn, are seen only at the closer stations and primarily those with

higher gain.

5) As the distance from the masked explosion increases, the degradation of its waveform continues until the interference begins to destroy the basic pattern of the Pg and Sg phases. Because its amplitude is frequently larger the Sg phase is generally more persistent than the Pg phase. As an example of this type of selective degradation we mention the record for Jamestown, California, (Plate 23). Although the Pg phase is severely obliterated by the teleseism, it is still identifiable as a separate arrival, while the Sg phase can be recognized easily from the pattern of its peak amplitudes.

6) The quantitative estimates of masking (Table V) are based on the reduction of the relative duration of the explosion waveform. By use of durations which are independent of gain (based on the end of the motion characteristic of the explosion) it is possible to circumvent possible changes in instrumentation and gain which may have occurred during the time interval between the comparison events and the masked explosion. Plots (Porter, 1973) of the masking factor show an irregular correlation with distance from the explosion and secondary dependences on back azimuth and the difference between the onsets of the teleseism and the explosion. Some of the variations may also be due to regional effects.

7) Although the difference between the onset times for the teleseism and the explosion waveform appears to be only a secondary controlling factor in the masking, the difference in the origin times for the earthquake and the explosion is a parameter paramount to the generation of this data set. To illustrate this point we note that if the origin time of the explosion were advanced by a few seconds its waveforms would no longer be fully engulfed by the teleseism. On the other hand, if the origin time were delayed by more than a few seconds its waveforms would not be superimposed on the portions of intense signal activity of the teleseism. Furthermore, we see that if the origin time were delayed to any considerable extent it would be impossible to display the data in the compact fashion used in this report. A wider separation in the origin times would require more prints at reduced scale factors (such as those in Plate 30) or a larger format.

8) The two most striking regional effects are the absence of any appreciable evidence for the masked explosion in southern California beyond the range of Isabella (273 km) and the appearance of the partial waveforms at four northern California stations (Jamestown, Mount Hamilton, Paraiso and Priest). In this regard, the difference between the onsets may be the controlling factor because the explosion waveform at the closest northern California station (Jamestown) appears at least 66 seconds behind the arrival of the teleseism, well after the period of intense signal activity of the latter. In contrast, the difference in onset times for stations in southern California at the range of Woody (297 km) or greater does not exceed 45 seconds and the traces show at most only an extremely weak high-frequency signal superimposed on the teleseism. Woody deserves special attention because this station shows almost no signal for the masked explosion while Isabella at a range of 24 km less and along nearly the same azimuth has equal amplitudes for the teleseism and the explosion. This abrupt decrease may be a consequence of Woody's location west of the Sierra Nevada.

9) The great variety of recording techniques utilized in this study shows that the machine-readibility of magnetic tape makes it the most desirable technique. The best paper records are produced by either an inked pen or a hot-wire stylus. The oscillograph playouts also have high contrast and photograph relatively easily, but they suffer from the disadvantage that they are light sensitive.

TABLE V

SUMMARY OF MASKING EFFECTS FOR THE EXPLOSION OF 14 AUGUST 1969
(arranged in the order of increasing epicentral distance from the explosion)

						Comparison Event			Earthquake & Masked Explosion						
Plate	Group	Stn & Inst		Range (°)	& Azm (°)	Onset (s)	Term (s)	Dur (s)	P(EQ) (GMT)	Dif (s)	Onset (s)	Term (s)	Dur (s)	Mask (%)	Mask F
1	1	TPH	SPZ	1.30	315.1	25.2	145a	120a	30:03.7	21.6	25.3	75	50	58.3a	1.72a
							352b	327b						84.7b	1.18b
	2		SPR			25.2	175a	150a	30:03.7	21.8	25.5	90	65	56.7a	1.75a
							350b	325b						80.0b	1.25b
	3		SPT			26.2	125a	100a	30:04.9	21.6	26.5	80	54	46.0a	2.28a
							308b	282b						80.9b	1.24b
2	4	TPH	WBZ	1.30	315.1	NYI			30:03.0	22	25	82	57	60*	1.67*
	5		WBR			NYI			30:03.4	21.6	25	80	55	60*	1.67*
	6		LPZ			NYI			30:03.5	22.1	25.6	94	68	55*	1.83*
3	7	DAC	SPZ	1.51	234.8	28	115a	87a	30:08	21	29	91	62	28.7a	3.48a
							183b	155b						60.0b	1.67b
	8		SPR			28	131a	103a	30:08	20	28	94	66	35.9a	2.73a
							177b	149b						55.7b	1.80b
	9		SPT			28	138a	110a	30:09	22	31	87	56	49.1a	2.04a
							335b	307b						81.8b	1.22b
4	10	DAC	WBZ	1.51	234.8	NYI			30:09	20	29	92	63	30*	3.33*
	11		WBR			NYI			30:09	20	29	96	67	35*	2.86*
5	12	TIN	SPZ	1.73	267.2	32	147a	115a	30:04	28	33	148	115	0a	∞ a
							269b	237b						51.5b	1.94b
6	13	TIN	WANS	1.73	267.2	33	128a	95a	30:06	28	34	117	83	12.6a	7.92a
							208b	175b						52.6b	1.90b
	14		WAEW			33	131a	98a	30:06	28	34	118	84	14.3a	7.00a
							225b	192b						56.3b	1.78b
7	15	TIN	LPZ	1.73	267.2	32	142a	110a	30:05	28	33	96	63	42.7a	2.34a
							218b	186b						66.1b	1.51b
	16		LPNS			34	118a	84a	30:05	32	37	73	44	47.6a	2.10a
							230b	196b						77.6b	1.29b
	17		LPEW			34	128a	94a	30:05	32	37	77	48	48.9a	2.04a
							226b	192b						75.0b	1.33b

Plate	Group	Stn & Inst		Range (°)	& Azm (°)	Comparison Event Onset (s)	Term (s)	Dur (s)	Earthquake & Masked Explosion P(EQ) (GMT)	Dif (s)	Onset (s)	Term (s)	Dur (s)	Mask (%)	Mask F
8	18	NEL	18-300	1.75	145.4	NYI			30:21.5	13	34	93	59	34*	2.90*
	19		SPZ			34	122a	88a	30:21.5	12	33.5	90	56	36.3a	2.75a
							202b	168b						66.7b	1.50b
	19A		SPR			34	125a	91a	WFS						
							234b	200b							
	20		SPT			34	130a	96a	30:23.5	12	35	90	55	42.7a	2.34a
							203b	109b						67.5b	1.48b
9	21	NEL	WBZ	1.75	145.4	NYI			30:21.5	12	33.5	87	55	40*	2.50*
	22		WBR			NYI			30:21.5	12	33.5	90	56	40*	2.50*
10	23	CLC	SPZ	1.82	223.1	32.4	129a	96a	30:11	22	33	123	90	6.3a	16a
							275b	242b						62.8b	1.59b
11	24	GSC	SPZ	1.95	198.1	35	205a	170a	30:16	19	35	160	125	26.5a	3.77a
							287b	252b						50.4b	1.98b
12	25	MN-NV	SPZ	2.09	308.1	37	177a	140a	29:58.4	38.6	37	137	100	28.6a	3.50a
							440b	403b						75.2b	1.33b
13	26	LEE	SPZ	2.15	87.0	37.2	170a	133a	30:21.5	16	37.6	138	100	24.8a	4.03a
							257b	220b						54.5b	1.83b
	27		SPR			37.2	170a	133a	WFS						
							250b	213b							
	28		SPT			37.2	170a	133a	30:22.0	16	38	128	90	32.3a	3.09a
							314b	277b						67.5b	1.48b
14	29	LEE	18-300	2.15	87.0	NYI			30:21	17	38	130	92	30*	3.33*
	30		WBR			NYI			30:21	17	38	130	92		
15	31	ELY	18-300	2.17	24.8	NYI			30:08	32	40.5	93	52		
	32		WBZ			NYI				33	41	.23	82		
	33		WBR			NYI				33	41	128	87		
16	34	EUR	SPZ	2.32	1.8	40	277	237	30:03	37	c	c	c		
17	35	ISA	SPZ	2.45	233.2	NSR			30:07	35	42	105	63		
18	36	KN-UT	SPZ	2.59	92.1	42.5	210a	177a	30:24.5	18	42.5	180	137	22.5a	4.43a
							480b	437b						68.6b	1.46b
19	37	WDY	SPZ	2.67	237.8	44.5	150a	105a	30:05	40	45*	108*	63*	40.0a	2.50a
							279b	234b						73.1b	1.37b

Plate	Group	Stn	& Inst	Range (°)	& Azm (°)	Comparison Event Onset (s)	Comparison Event Term (s)	Comparison Event Dur (s)	Earthquake & Masked Explosion P(EQ) (GMT)	Dif (s)	Onset (s)	Term (s)	Dur (s)	Mask (%)	Mask F
20	38	FTC	SPZ	3.24	226.0	54	180	116	30:09.5	45	55*	135*	80*	31.0	3.22
	39	RVR	SPZ	3.34	199.1	54.7	170a	115a	30:19	36	55*	155*	100*	13.0a	7.67a
							221b	166b						39.8b	2.52b
	40	MWC	SPZ	3.35	209.6	55	215	160	30:15	40	55*	150*	95*	40.6	2.46
21	41	BMN	18-300	3.39	344.9	NYI			29:54.3		64*	124*	60*		
	42		WBZ			NYI			29:54.3		65*	124*	59*		
	43		WBR			NYI			29:54.3		63*	124*	61*		
22	44	PAS	SPZ	3.46	210.4	56.1	153	97	30:14	42	c	c	c		
	45		LPNS			NSR			30:15		75*	150*	75*		
	46		LPEW			NSR			30:15		68*	140*	72*		
	47	HAY	SPZ	3.46	174.1	55.3	165a	110a	30:26	29	111*	149*	38*	65.5a	1.53a
							208b	153b						75.2b	1.33b
23	48	JAS	SPZ	3.56	284.1	57	212a	155a	29:51	66	68	145	77	50.3a	1.99a
							270b	213b						63.8b	1.57b
24	49	PRI	SPZ	3.84	256.0	62	174a	112a	29:57.5	64	76*	143*	67*	40.2a	2.49a
							245b	183b						63.4b	1.58b
	50	PLM	SPZ	3.85	190.0	61.6	187a	125a	30:23	39	63*	145*	82*	34.4a	2.91a
							268b	206b						60.2b	1.66b
25	51	DUG	SPZ	3.95	39.0	65.5	320	255	30:12	54	c	c	c		
26	52	SBC	SPZ	4.02	228.6	NSR			30:08.1		c	c	c		
	53	SYP	SPZ	4.13	231.6	NSR			30:07		79*	138*	59*		
	54	PRS	SPZ	4.34	260.6	74.5	185a	110a	29:53.1	82	80*	168*	88*	20.0a	5.00a
							215b	140b						37.1b	2.69b
27	55	MHC	SPZ	4.45	274.0	79.5	190a	110a	29:48.4	91	78	159	81	26.4a	3.79a
							245b	165b						50.9b	1.96b
	56	BAR	SPZ	4.50	186.6	69	218	149	30:26	43	73+	81+	12+	91.9	1.09
	57	BKS	SPZ	4.96	280.2	79	200	121	29:43.5	95	107+	111+	4+	96.7	1.03
28	58	TUC	SPZ	6.50	136.5	121	353	232	30:50	71	240+	242+	2+	99.1	1.01
	59	ALQ	SPZ	8.09	103.0	135	385	250	30:54	81	c	c	c		
29	60	GOL	SPZ	8.77	69.9	136	357	221	30:39.5	96	c	c	c		
	61		SPNS			134	354	220	30:39.5	94	291+	309+	5+	97.7	1.02
	62		SPEW			132	344	212	30:39.5	92	c	c	c		

a. End of the motion characteristic of the explosion.
b. End of the signal.
c. No identifiable explosion waveform present.
* Values estimated from the high-frequency signal attributed to the ME.
\+ Values estimated for the total duration of the segmented waveform attributed to the ME.

NYI Not yet installed
WFS Withdrawn from service
NSR No suitable record

KEY TO ABBREVIATIONS FOR INSTRUMENTS
(arranged alphabetically)

LPEW	Long-period East-West
LPNS	Long-period North-South
LPZ	Long-period vertical
SPEW	Short-period East-West
SPNS	Short-period North-South
SPR	Short-period radial
SPT	Short-period transverse
SPZ	Short-period vertical
WAEW	Wood-Anderson East-West
WANS	Wood-Anderson North-South
WBR	Wide-band radial
WBZ	Wide-band vertical
18-300	Short-period vertical, with response similar to that of the Benioff.

TABLE VI

QUALITATIVE CHARACTERIZATION OF THE MASKING EFFECTS OBSERVED FOR THE EXPLOSION OF 14 AUGUST 1969
(listed in the order of increasing epicentral distance from the explosion)

Key to abbreviations

ME masked explosion
EQ earthquake

Pg granitic phase for the compressional wave from the ME
Sg granitic phase for the shear wave from the ME

No.	Station Symbol	Range (km)	Dominant wave (phase)	Level of Domination	Visibility of the ME	Plate	Particularly significant records
1	TPH	144	ME (Pg & Sg)	high	good	1,2	*
2	DAC	168	ME (Sg only)	do	do	3,4	*
3	TIN	193	ME (Pg & Sg)	do	do	5,6,7	*
4	NEL	194	ME (Sg only)	do	do	8,9	*
5	CLC	203	None (all amplitudes equal)		do	10	*
6	GSC	217	ME (Pg & Sg)	slight	do	11	*
7	MN-NV	232	None (all amplitudes equal)		do	12	*
8	LEE	239	ME (Pg & Sg)	slight	do	13,14	*
9	ELY	242	ME (Sg only)	very slight	poor[1]	15	*
10	EUR	258	Indeterminate (poor copy)			16	
11	ISA	273	None (all amplitudes equal)		good	17	*
12	KN-UT	288	do		poor[2]	18	
13	WDY	297	EQ	very high	negligible[3]	19	
14	FTC	360	do	do	do	20	
15	RVR	371	do	do	do	20	
16	MWC	373	do	do	do	20	
17	BMN	377	do	high	poor[4]	21	*
18	PAS	385	do	very high	negligible[3]	22	
19	HAY	387	do	do	do	22	
20	JAS	396	do	slight	fair[5]	23	*
21	PRI	427	do	high	do[6]	24	*
22	PLM	429	do	very high	negligible[3]	24	
23	DUG	440	Indeterminate (excessive gain)			25	
24	SBC	447	EQ	very high	negligible[3]	26	
25	SYP	459	do	do	do	26	
26	PRS	483	do	high	fair[6]	26	*
27	MHC	495	do	do	fair[6]	27	*
28	BAR	500	do	very high	negligible[3]	27	
29	BKS	551	do	do	do	27	
30	TUC	723	do	do	do	28	
31	ALQ	899	Indeterminate (poor copy)			28	
32	GOL	975	EQ	very high	negligible[3]	29,30	

1. only a short portion of the Sg phase is present.
2. waveforms are barely discernible due to the low contrast of the trace.
3. only an extremely weak high-frequency signal is present.
4. only a weak high-frequency signal is present.
5. the Pg phase is only partially visible as a high-frequency signal; the peak amplitudes for the Sg phase are clearly recognizable.
6. the Pg and Sg phases are partially visible as high-frequency signals.

ACKNOWLEDGMENTS

During the course of this investigation several organizations were visited to examine the original records from their respective seismographic stations which might prove useful in illustrating the masking effects being studied under this grant. I am particularly grateful to the individuals named below for their assistance and also permission to photograph original records so that the best available copies for this report could be obtained:

1. Seismological Laboratory, California Institute of Technology, Pasadena, California; Don L. Anderson, Donald V. Helmberger, and Violet Taylor.
2. Department of Geophysics, Colorado School of Mines, Golden, Colorado; Ruth B. Simon.
3. Seismographic Station, University of California, Berkeley, California; Bruce A. Bolt, Thomas V. McEvilly, and Roy D. Miller.
4. Department of Geological and Geophysical Sciences, University of Utah, Salt Lake City, Utah; Kenneth L. Cook.

In addition, thanks are due the following for providing data for use in this report: Thomas A. Modgling of the Environmental Data Service, National Oceanic and Atmospheric Administration, Asheville, North Carolina; John R. Banister, Leo Brady, and Dorris M. Tendall of Sandia Laboratories, Albuquerque, New Mexico; John R. Woolson of Teledyne-Geotech, Alexandria, Virginia; and James F. Lander of the U. S. Geological Survey, Boulder, Colorado.

REFERENCES

Anderson, J. A. and H. O. Wood (1925). Description and theory of the torsion seismometer, Bull. Seism. Soc. Am. 15, 1-72.

Anonymous (1964). Composite record discussion, KAWEAH, Long Range Seismic Measurements Program, The Geotechnical Corporation, Technical Report No. 64-38, 6 April.

_______ (1969). U. S. Dept. of Commerce, Environmental Science Services Administration, Coast and Geodetic Survey, Preliminary Determination of Epicenters, Monthly listings, March and August.

_______ (1973). U. S. Dept. of Commerce, Environmental Science Services Administration, Coast and Geodetic Survey, Preliminary Determination of Epicenters, Monthly listings, June.

Bomford, G. (1962). Geodesy, Oxford University Press, 2nd Edition.

Bullen, K. E. (1963). An introduction to the theory of seismology, Cambridge University Press, 3rd edition.

Chandra, U., W. A. Peppin, and R. D. Adams (1970). Bulletin of the seismographic stations, Earthquakes and the registration of earthquakes, from July 1, 1969 to December 31, 1969, University of California, Berkeley, 39, No. 2, 91-203.

Chandra, U. and A. Qamar (1970). Bulletin of the seismographic stations, Earthquakes and the registration of earthquakes from January 1, 1969 to June 30, 1969, University of California, Berkeley, 39, No. 1, 1-89.

Eckel, E. B. (Editor) (1968). Nevada Test Site, Geol. Soc. Am., Memoir 110.

Glasstone, S. (Editor) (1964). The effects of nuclear weapons, U. S. Atomic Energy Commission, Revised Edition.

Hinrichs, E. N. (1968). Geologic structure of Yucca Flat area, Nevada, Nevada Test Site, Geol. Soc. Am. Memoir 110, 239-246, E. B. Eckel (Editor).

Jeffreys, H. and K. E. Bullen (1940). Seismological Tables, British Association, Gray Milne Trust. Reprinted 1958.

Krivoy, H. L. and C. E. Mears (1969). Seismic events originating at the Atomic Energy Commission's Nevada Test Site, U. S. Geol. Survey Prof. Paper 650-B, B117-B121.

Porter, L. D. (1970). Distance-amplitude relations for large underground nuclear explosions, Abstract, Trans. Am. Geophys, Union 51, 778.

_______ (1971). Use of station corrections in predicting seismic response variations from large underground nuclear explosions, Abstract, Geol. Soc. Am. Abstracts with Programs 3, 180.

_______ (1972). Source region dependence of Lg phases amplitudes from underground nuclear explosions, Abstract, Trans. Am. Geophys, Union 53, 1049.

_______ (1973). Seismic masking of an underground nuclear explosion. Perspective, theory and analysis, Department of Geology, Northern Illinois University, Report No. 73-12-3 (in preparation).

_______ (1974a). The Kurile Island earthquake sequence of August 1969, Abstract, Geol. Soc. Am. Abstracts with Programs 6, 307.

_______ (1974b). Magnitude determination for closely-spaced seismic sources, (in preparation).

Richter, C.F. (1958). Elementary seismology, W. H. Freeman and Co., San Francisco.

Simon, R. B. (1972). Earthquake interpretations, Colorado School of Mines, Golden, Colorado, 3rd Printing (revised), March.

Springer, D. L. and R. L. Kinnaman (1971). Seismic source summary for U. S. underground nuclear explosions, 1961-1970, Bull. Seism. Soc. Am. 61, 1073-1098.

ADDITIONAL REFERENCES

Anonymous (1972). Bulletin, August 1969, Internationl Seismological Center, Edinburgh, Scotland.

Baker, R. G. (1970). Determining magnitude from Lg, Bull. Seism. Soc. Am. 60, 1907-1919.

Båth, M (1973). Introduction to seismology, Halsted Press, John Wiley & Sons, New York.

Ewing, W. M., W. S. Jardetzky and F. Press (1957). Elastic waves in layered media, McGraw-Hill Book Co., New York.

Hays, W. W. and J. R. Murphy (1971). The effect of the Yucca Fault on seismic wave propagation, Bull. Seism. Soc. Am. 61, 697-706.

McEvilly, T. V. and W. A. Peppin (1972). Source characteristics of earthquakes, explosions and afterevents, Geophys. J. R. astr. Soc. 31, 67-82.

APPENDIX A

LOCATIONS AND ELEVATIONS OF SEISMIC STATIONS
(listed alphabetically by station symbol)

No.	Symbol	Station Name	Reporting Network ≠	N. Latitude (d)	(m)	(s)	W. Longitude (d)	(m)	(s)	Elevation (m)
1	ALQ	Albuquerque,New Mexico	WWSSN	34	56	30	106	27	30	1853
2	ARC	Arcata, California	UCB	40	52	36	124	04	30	59
3	BAR	Barrett, California	CIT	32	40	48	116	40	18	510
4	BKS	Berkeley(Strawberry),Ca.	WWSSN	37	52	36	122	14	06	276
5	BMN	Battle Mountain,Nevada	SL	40	25	53	117	13	18	N/A
6	BRK	Berkeley, California	UCB	37	52	24	122	15	36	81
7	CLC	China Lake, California	CIT	35	49	0	117	35	48	766
8	CNC	Concord, California	UCB	37	58	06	122	04	18	36
9	CWC	Cottonwood, California	CIT	36	26	18	118	04	42	1620
10	DAC	Darwin, California	SL	36	16	37	117	35	37	N/A
11	DUG	Dugway, Utah	WWSSN	40	11	42	112	49	0	1481
12	ECC	El Centro, California	CIT	32	47	54	115	32	54	-15
13	ELKO	Elko, Nevada	LLL	40	44	41	115	14	20	2210
14	ELY	Ely, Nevada	SL	39	07	53	114	53	31	N/A
15	EUR	Eureka, Nevada	NOAA	39	29	0	115	58	12	2178
16	FHC	Fickle Hill, California	UCB	40	48	06	123	59	06	610
17	FRE	Fresno, California	UCB	36	46	00	119	47	48	88
18	FTC	Fort Tejon,California	CIT	34	52	24	118	53	36	990
19	GCC	Granite Creek,California	UCB	37	01	48	121	59	48	122
20	GLA	Glamis, California	CIT	33	03	06	114	49	36	627
21	GOL	Golden, Colorado	WWSSN	39	42	01	105	22	16	2359
22	GSC	Goldstone,California	WWSSN	35	18	06	116	48	18	990
23	HAY	Hayfield, California	CIT	33	42	24	115	38	12	439
24	ISA	Isabella, California	CIT	35	39	45	118	28	24	835
25	JAS	Jamestown, California	UCB	37	56	48	120	26	18	457
26	KN-UT	Kanab, Utah 1)	LRSM	37	01	22	112	49	39	1737
27	LAN	Landers,California	LLL	34	23	23	116	24	41	793
28	LEE	Leeds, Utah	SL	37	14	35	113	22	36	N/A
29	LLA	Llanada, California	UCB	36	37	00	120	56	36	475
30	MHC	Mount Hamilton,California	UCB	37	20	30	121	38	30	1282
31	MIN	Mineral, California	UCB	40	20	42	121	36	18	1495
32	MLC	Manzanita Lake,California	UCB	40	32	12	121	33	42	1800
33	MN-NV	Mina, Nevada 2)	LRSM	38	26	10	118	08	53	1524
34	MWC	Mount Wilson, California	CIT	34	13	24	118	03	30	1730
35	NEL	Nelson, Nevada 3)	SL	35	42	44	114	50	36	N/A
36	ORV	Oroville, California	UCB	39	33	18	121	30	00	360
37	PAS	Pasadena, California	WWSSN	34	08	54	118	10	18	295
38	PCC	Pilarcitos Creek,Calif.	UCB	37	30	00	122	22	54	91
39	PLM	Palomar, California	CIT	33	21	12	116	51	42	1692
40	PRI	Priest, California	UCB	36	08	30	120	39	54	1187
41	PRS	Paraiso, California	UCB	36	19	54	121	22	12	363
42	RVR	Riverside, California	CIT	33	59	36	117	22	30	260
43	SAO	San Andreas Geophysical Observatory,California	UCB	36	45	54	121	26	42	350
44	SBC	Santa Barbara,California	CIT	34	26	30	119	42	48	90
45	SCI	San Clemente Island,Ca.	CIT	33	58	48	118	32	48	219

46	SWM	Sawmill, California	CIT	34	43	06	118	34	54	1220
47	SYP	Santa Ynez Peak,California	CIT	34	31	36	119	58	42	1305
48	TIN	Tinemaha, California	CIT	37	03	18	118	13	42	1195
49	TPH	Tonopah,Nevada	SL	38	04	29	117	13	21	N/A
50	TUC	Tucson,Arizona	WWSSN	32	18	35	110	46	56	985
51	UKI	Ukiah, California	NOAA	39	08	14	123	12	38	199
52	WDY	Woody, California	CIT	35	42	0	118	50	36	500

/ Identification of Reporting Network Abbreviations:

CIT	California Institute of Technology, Pasadena, California
LLL	Lawrence Livermore Laboratory, Livermore, California
LRSM	Long-Range Seismic Measurements Program,U.S. Air Force
NOAA	National Oceanic and Atmospheric Administration
SL	Sandia Laboratories, Albuquerque, New Mexico
UCB	University of California, Berkeley, California
WWSSN	World-Wide Standard Seismograph Network

[1] KANAB	Kanab, Utah	LLL	37	01	00	112	49	21	1715
[2] MINA	Mina, Nevada	LLL	38	25	56	118	09	16	1510
[3] BCN	Boulder City, Nevada	SL	35	58	51	114	50	02	776

APPENDIX B

UNDERGROUND NUCLEAR EXPLOSIONS LOCATED IN THE VICINITY OF THE MASKED EXPLOSION OF 14 AUGUST 1969 [1]

	Date (GMT)	Shot time (GMT)	Name	Yield (kt)	Device depth (ft)	Interval until surface collapse (h)	(m)	(s)	Dimensions of surface collapse Diameter xdepth(ft)	Volume (yd^3)
1.	21 Feb. 1963	19:47:08.23	CARMEL	0-20	536					
2.	15 Aug. 1963	13:00:00.15	SATSOP	0-20	738		16		300x40	4×10^{4}
3.	13 Sept.1963	13:53:00.15	AHTANUM	0-20	740	~ 2-1/2 yr			30x50	.
4.	11 June 1964	16:45:00.15	ACE	0-20	862					
5.	19 Aug. 1964	16:00:00.14	ALVA	0-20	545		7	5	250x27	
6.	9 Oct. 1964	14:00:00.12	PAR	38	1325	3	54		475x72	3.89×10^{4}
7.	12 Feb. 1965	15:10:29.49	ALPACA	0-20	737					
8.	25 June 1966	17:13:00.07	VULCAN	25	1057		58	23	526x77	2.44×10^{5}
9.	10 Aug. 1966	13:16:00.07	ROVENA[b]	0-20	635		19	45	116x8	1.52×10^{3}
10.	29 Sept.1966	14:45:30.09	NEWARK[b]	0-20	750		11	35	264x10	8.54×10^{4}
11.	5 Nov. 1966	14:45:00.00[a]	SIMMS[b]	0-20	650		16	15	190x15	1.36×10^{4}
12.	27 Apr. 1967	14:45:00.0[a]	EFFENDI	0-20	719		18	50	114x12	1.84×10^{4}
13.	18 Jan. 1968	16:30:00.0[a]	HUPMOBILE	0-20	810		21	21	252x32	
14.	10 Apr. 1968	14:00:00.0[a]	NOOR	20-200	1250	9	31		400-600x36	
15.	15 Jan. 1969	19:00:00.07	PACKARD	0-20	810		16	45	350x49	5.64×10^{4}
16.	14 Aug. 1969	14:30:00.04	SPIDER	0-20	784	7			16-30x40	4.98×10^{2}

---

a Actual detonation time was delayed ~ 0.1±0.06 sec due to signal transit time, relay closures, etc., for these events with shot times listed on an exact second.

b These events lie outside of the microzone for the Masked Explosion (SPIDER), but are included as comparison events for the Jamestown (JAS) and Golden (GOL) stations.

1 Springer, D.L. and R.L. Kinnaman (1971).

APPENDIX C

GEOLOGICAL FEATURES FOR THE UNDERGROUND NUCLEAR EXPLOSIONS LOCATED IN THE VICINITY OF THE MASKED EXPLOSION OF 14 AUGUST 1969 [1]

No.	Date	Name	Surface Elevation (ft)	Water Table		Paleozoic Interface	
				Depth (ft)	Elevation (ft)	Depth (ft)	Elevation (ft)
1.	21 Feb. 1963	CARMEL	4390	1980	2410	2450	1940
2.	15 Aug. 1963	SATSOP	4373	1950	2423	2400	1973
3.	13 Sept. 1963	AHTANUM	4419	2010	2409	2400	2019
4.	11 June 1964	ACE	4354	1940	2414	2570	1784
5.	19 Aug. 1964	ALVA	4420	2016	2404	2550	1870
6.	9 Oct. 1964	PAR	4368	1950	2418	2650	1950
7.	12 Feb. 1965	ALPACA	4402	1990	2412	1800	2602
8.	25 June 1966	VULCAN	4354	1940	2414	2050	2304
9.	10 Aug. 1966	ROVENA[a]	4281	1870	2411	1700	2581
10.	29 Sept. 1966	NEWARK[a]	4285	1870	2415	1750	2535
11.	5 Nov. 1966	SIMMS[a]	4286	1875	2411	1450	2836
12.	27 April 1967	EFFENDI	4284	1885	2399	2750	1534
13.	18 Jan. 1968	HUPMOBILE	4266	1910	2356	2400	1866
14.	10 Apr. 1968	NOOR	4385	1980	2405	2450	1935
15.	15 Jan. 1969	PACKARD	4250	1910	2340	2300	1950
16.	14 Aug. 1969	SPIDER	4326	1925	2401	1700	2626

---

[a] These events lie outside of the microzone for the Masked Explosion (SPIDER), but are included as candidate comparison events for the Jamestown (JAS) and Golden (GOL) stations.

[1] Springer, D.L. and R.L. Kinnaman (1971).

APPENDIX D

COORDINATE LOCATIONS FOR THE UNDERGROUND NUCLEAR EXPLOSIONS LOCATED IN THE VICINITY OF THE MASKED EXPLOSION OF 14 AUGUST 1969[1]

	Date	Name	N. Latitude (d)	(m)	(s)	W. Longitude (d)	(m)	(s)	Nevada State Coordinates North (ft)	East (ft)	Distance from ME (SPIDER) (ft)
1.	21 Feb.1963	CARMEL	37	9	17.3	116	4	47.6	875 850	671 000	5140
2.	15 Aug.1963	SATSOP	37	9	14.7	116	4	35.9	875 600	671 950	4407
3.	13 Sept.1963	AHTANUM	37	9	48.1	116	4	50.3	878 970	670 760	5090
4.	11 June1964	ACE	37	8	55.0	116	4	33.6	873 585	672 145	5580
5.	19 Aug.1964	ALVA	37	9	32.4	116	4	59.1	877 380	670 055	5695
6.	9 Oct.1964	PAR	37	9	4.8	116	4	37.2	874 600	671 850	5070
7.	12 Feb.1965	ALPACA	37	9	52.3	116	4	35.6	879 400	671 950	4080
8.	25 June1966	VULCAN	37	9	19.1	116	4	19.8	876 050	673 250	3145
9.	10 Aug.1966	ROVENA[a]	37	10	7.2	116	2	51.8	880 960	680 330	5542
10.	29 Sept.1966	NEWARK[a]	37	10	7.2	116	2	45.8	880 960	680 825	5960
11.	5 Nov.1966	SIMMS[a]	37	10	11.8	116	2	50.0	881 430	680 485	5940
12.	27 Apr.1967	EFFENDI	37	8	19.6	116	3	47.5	870 050	675 900	7820
13.	18 Jan.1968	HUPMOBILE	37	8	44.1	116	3	56.4	872 520	675 160	5375
14.	10 Apr.1968	NOOR	37	9	15.8	116	4	43.9	875 700	671 300	4930
15.	15 Jan.1969	PACKARD	37	8	52.5	116	3	56.4	873 370	675 160	4530
16.	14 Aug.1969	SPIDER	37	9	36.9	116	3	49.0	877 863	675 730	-

[a] These events lie outside of the microzone for the Masked Explosion (SPIDER), but are included as candidate comparison events for the Jamestown (JAS) and Golden (GOL) stations.

[1] Springer, D.L. and R.L. Kinnaman (1971).

APPENDIX E

SEISMIC EVENTS OF SOUTHERN NEVADA LOCATED IN THE VICINITY OF THE MASKED EXPLOSION OF 14 AUGUST 1969[1]

No.	Date (GMT)	Time (GMT)	North Latitude (deg)	West Longitude (deg)	Depth (km)	Magnitude (local)	Standard deviation	No. of Stations Reporting
1.	18 March 1969	14:40:02.7	37.2	116.0	n	4.4	0.5	7
2.	10 June 1973	22:22:07.7	37.2	116.3	5	4.0	0.8	12
3.	11 June 1973	07:56:21.9	37.2	116.3	10		0.8	8
4.	12 June 1973	06:48:51.8	37.2	116.3	10		0.6	6
5.	12 June 1973	08:15:49.9	37.2	116.3	5	4.8	0.9	18

---

1 U.S. Department of Commerce, Environmental Science Services Administration, Coast and Geodetic Survey, Preliminary Determination of Epicenters, Monthly Listings, March 1969 and June 1973.

n Nominal

APPENDIX F

STATIONS OMITTED FROM THE COMPILATION OF RECORDS AND COMPARISON DATA FOR THE MASKED EXPLOSION OF 14 AUGUST 1969

(listed alphabetically by station symbol)

No.	Symbol	Reason for omission
1.	ARC	Unsuitable record (gain too low)
2.	BRK	do
3.	CNC	Withdrawn from service
4.	CWC	Out of service due to flood
5.	ECC	Unsuitable record (gain too low)
6.	ELKO	Not yet installed
7.	FHC	Unsuitable record (gain too low)
8.	FRE	No time correction available
9.	GCC	Unsuitable record (gain too low)
10.	GLA	do
11.	LLA	do
12.	MIN	do
13.	MLC	do
14.	ORV	do
15.	PCC	do
16.	SAO	do
17.	SCI	Withdrawn from service
18.	SWM	Out of service
19.	UKI	Withdrawn from service

"Unsuitable Record" implies that the station in question did not record well explosions similar to the masked explosion [see Plate 31 for the case of the primary comparison event, the explosion of 13 September 1963 (AHTANUM)].

Seismic Distribution List/AFOSR/NPG
(1 December 1972)

Director, ARPA/NMR — 2
1400 Wilson Boulevard
Arlington, VA 22209

AFCRL (LWW and LWH) — 1 each
L. G. Hanscom Field
Bedford, MA 01730

AFOSR/NPG — 15
1400 Wilson Boulevard
Arlington, VA 22209

AFTAC/VSC/Dr. Pilotte — 2
312 Montgomery Street
Alexandria, VA 22314

Dr. T. V. McEvilly
Dept. of Geology and
Geophysics
Berkeley, CA 94920

Dr. James T. Wilson
Institute of Science and
Technology
University of Michigan
Ann Arbor, MI 48107

Fr. W. J. Stauder, S. J.
St. Louis University
3507 Laclede Avenue
St. Louis, MO 63103

Dr. Jack E. Oliver
Cornell University
Department of Geology
Ithaca, NY 14850

Office of Effects Evaluation
AEC Nevada Operations Office
PO Box 1676
Las Vegas, NV 89101

Dr. Don L. Anderson
Seismological Laboratory
California Institute of Technology
220 N. San Rafael Avenue
Pasadena, CA 99109

Dr. Frank Press
Department of Earth and Planetary
Sciences
Massachusetts Institute of Technology
Cambridge, MA 02139

Dr. D. Davies
Massachusetts Institute of Technology
Lexington, MA 02173

Earth Sciences Division
1800 G Street, NW
Washington, DC 20552

Librarian
Naval Research Laboratory
Code 2027
Washington, DC 20390

Department of Navy, Code 410
Washington, DC 20360

Dr. Stewart W. Smith
Geophysics Department
University of Washington
Seattle, WA 98105

Dr. Sidney Kaufman
PO Box 481
Houston, TX 77001

USACDA/Attn: Dr. J. Evernden
State Department
Sciences & Technology Division
Washington, DC 20451

US Geological Survey
Rm 5233, Gen Services Bldg
Washington, DC 20242

Dr. Thomas O'Donnell
4625 5th Avenue
Pittsburgh, PA 15213

Mr. Jon Peterson
NOAA Seismological Center
Sandia Base
Albuquerque, NM 87115

Chief, Office of Research
and Development, US Army
3045 Columbia Pike
Arlington, VA 22204

National Earthquake Research
Center
US Geological Survey
345 Middlefield Road
Menlo Park, CA 94025

National Academy of Sciences
Division of Earth Sciences
2101 Constitution Ave, NW
Washington, DC 20418

AF Weapons Laboratory/WLRU
Kirtland AFB, NM 87117

DASA, Deputy Director
Science and Technology
Washington, DC 20305

Dr. Alan Ryall
University of Nevada
Mackay School of Mines
Reno, NV 89507

University of Alaska
Geophysical Institute
College, AK 99701

Dr. George Kolstad
Research for Physics and
Mathematics, USAEC
Washington, DC 20545

Dr. Eugene Herrin
Southern Methodist University
Dallas Seismological Observ.
Dallas, TX 75222

Dr. John H. Pfluke
U.S. Department of Commerce
NOAA/ERL/EML
390 Main Street
San Francisco, CA 94105

Dr. M. D. Trifunac
California Institute of Technology
Department of Engineering and
Applied Science
Pasadena, CA 91109

Dr. C. B. Archambeau
California Institute of Technology
Seismological Laboratory
PO Bin 2, Arroyo Annex
Pasadena, CA 91109

Mr. Rowland McLaughlin
Environmental Research Institute
of Michigan
PO Box 618
Ann Arbor, MI 48107

Dr. T. Cherry
Systems, Science and Software
PO Box 1620
La Jolla, CA 92037

Dr. Ben Tsai
Texas Instruments, Inc.
314 Montgomery Street
Alexandria, VA 22314

Dr. Keiiti Aki
Massachusetts Institute of
Technology
Earth and Planetary Sciences
Cambridge, MA 02139